

Mechanical Properties of Porous Asphalt, Recommendations for Standardization

**Mechanische Eigenschaften von offenporigem Asphalt,
Empfehlungen für die Normierung**

**Propriétés mécaniques des asphalte poreux,
recommandations pour la normalisation**

**Swiss Federal Laboratory for Materials Testing and Research,
Empa, Dübendorf, Switzerland**

**Lily. D. Poulikakos
Remy Gubler
Manfred Partl**

**Ecole Polytechnique Fédérale de Lausanne (EPFL) –
Laboratoire des voies de circulation (LAVOC)**

**Michel Pittet
Laurent Arnaud
Alejandro Junod
André-Gilles. Dumont**

**Canton Vaud
Eric Simond**

**Forschungsauftrag 1999/280 auf Antrag der
VSS Vereinigung Schweizerischer Strassenfachleute**

Datum (Dezember 2006)

.....

Eidgenössische Materialprüfungs- und Forschungsanstalt
Laboratoire fédéral d'essai des matériaux et de recherche
Laboratorio federale di prova dei materiali e di ricerca
Institut federal da controllo da material e da retschertgas
Swiss Federal Laboratories for Materials Testing and Research

EMPA
Überlandstrasse 129
CH-8600 Dübendorf
Tel. +41-1-823 55 11
Fax +41-1-821 62 44



FACULTE DE L'ENVIRONNEMENT NATUREL, ARCHITECTURAL ET CONSTRUIT
INSTITUT DES INFRASTRUCTURES, DES RESSOURCES ET DE L'ENVIRONNEMENT
LABORATOIRE DES VOIES DE CIRCULATION - LAVOC

EPFL ENAC ICARE LAVOC
Bât. GCB
Station 18
CH – 1015 LAUSANNE

Téléphone +41 21 693 23 45
Télécopie +41 21 693 63 49
<http://lavoc.epfl.ch/>



ÉCOLE POLYTECHNIQUE
FÉDÉRALE DE LAUSANNE

Mechanical Properties of Porous Asphalt, Recommendations for Standardization

Mechanische Eigenschaften von offenporigem Asphalt,
Empfehlungen für die Normierung

Propriétés mécaniques des asphalte poreux,
recommandations pour la normalisation

Research Institutions:

Swiss Federal Laboratory for Materials Testing and Resarch, Empa, Dübendorf, Switzerland
Ecole Polytechnique Fédérale de Lausanne (EPFL) - Laboratoire des voies de circulation (LA-VOC)

Authors:

Lily. D. Poulikakos, Empa
Michel Pittet, LAVOC
Laurent Arnaud, LAVOC
Alejandro Junod, LAVOC
Remy Gubler, Empa
Eric Simond, Canton Vaud
Manfred Partl , Empa
André-Gilles. Dumont, LAVOC

Forschungsauftrag 1999/280 auf Antrag der
VSS Vereinigung Schweizerischer Strassenfachleute

Dezember 2006

EXECUTIVE SUMMARY, ENGLISH

Porous Asphalt (PA) is used worldwide for its favorable splash and spray properties and its reduction of aquaplaning under rainy conditions as well as its noise reduction properties. Switzerland started using PA in 1979 with mixed results. According to a survey taken in 2004, nine of the 26 cantons use PA. In particular, canton Vaud in western Switzerland is known as one of the leaders in promoting and using PA. Currently, 1/3 of the Vaud motorways are covered with porous asphalt and the use of PA is planned to be extended to most of the motorway surfaces in the canton Vaud up to an altitude of 600m. In addition, there are several bridge trial sections with PA.

Despite its benefits, porous asphalt can suffer from problems, which can affect both its performance and its service life. The open structure exposes a large surface area to the effects of air and water, leading to rapid aging of the binder. In addition the clogging of the pores can reduce the functionality prematurely.

It is clear that porous asphalt is quite effective in providing safer conditions for drivers under rainy conditions, and in improving the environment for residents along the roads. In order to reduce the problems associated with porous asphalt and retain the benefits, in this project mechanical test procedures are compared and discussed with respect to their suitability for porous asphalt optimization and for development of improved mix designs. It is also a goal of this project to make recommendation for standardization of mechanical properties of porous asphalt.

The European Standards are in effect in Switzerland. In addition to volumetric requirements there are requirements for mechanical behavior such as water sensitivity, particle loss and horizontal and vertical permeability as well as binder drainage. The European standards are to be used in combination with a national annex. The only mechanical property specified in the current Swiss annex to this standard [SN 431-7NA] specifies an Indirect Tensile Strength Ratio (ITSR) value of ≥70 for the water sensitivity test. Additionally, in the Swiss annex, provisions are made for porous asphalt layers with max aggregate size of 8 mm which can now be used in Switzerland.

After the initial survey of the literature appropriate mechanical tests for porous asphalt were chosen (Table 8. 1). At the same time a survey of current experience with porous asphalt in Switzerland was conducted (Appendix 2). Tests were performed on laboratory prepared specimens (AG1, AG4, AG5, VD7, VD8, VD9) and cores (VD2, VD3, VD4, VD5, VS6, AG2, AG3, VD10) taken from selected pavements chosen based on the feedback from various cantons. The behavior of the selected materials was also assessed using an analytical model. Laboratory tests allowed the comparison of core performance with that of laboratory prepared specimen as well as comparison with field performance. Based on the results two mixes were optimized (VD9, AG5) and recommendations for mechanical tests appropriate for porous asphalt were made.

Experimental procedures and results

Laboratory aging of the mix

Aging of the mixture depends on both the loss of cohesion in the binder and the loss of adhesion between the binder and aggregate. Aging and subsequent testing of binder alone is not a good predictor of how a mixture will behave due to the effect of the asphalt-aggregate interaction. As a result in this investigation the mix was aged instead of aging the binder prior to mixing. The recommended short term aging procedure is the aging of the mix in a covered box for 50 minutes at compaction temperature.

Compaction

The European Standard [EN 12697-10] allows various compaction energies. 2x50 blows can provide an indication of the maximum compactability of the specimen although for some mixes this rate of compaction can cause microcracking within the specimen. It is recommended that for the purpose of mechanical tests, the specimen should be prepared with a Marshall compactor using 2x25 blows or a gyratory compactor using 40 gyrations.

Void characteristics

The European Standard [EN 12697-8] describes the procedure to calculate air void content (V_m) as well as other parameters. The air void content V_m is the volume of the air voids as percentage of total volume of that specimen.

In case of PA the amount of connected voids (capillaries) is very important as the functionality with respect to permeability is directly influenced by this property. The old Swiss standard, SN 640 433b, for PA which is followed in this project, proposed to determine the connected voids according to the French standards [NF P 98-254-2]. The test to determine the connected air void content of compacted materials makes it possible to measure the connected voids located inside the materials, at their surfaces and at the interface between them that allow the drainage of surface water. The connected voids are determined from the water mass introduced into the core sample whose side walls and the bottom part were sealed. A factor of correction depending on the maximum diameter of the solid grains allows determining the effective volume of the connected voids without taking into account the voids at the surface of the sample. Table 6. 5 and Table 6. 6 list the relevant void characteristics for the materials used in this study.

Water Permeability

Loss of permeability due to rapid clogging of the pores is one of the disadvantages of porous asphalt. In this laboratory test procedure [EN 12697-19], carried out at ambient temperatures of 15 and 25°C, a column of water was applied with a constant height of 300 mm to a cylindrical specimen. In situ water permeability was measured using the Yverdon permeameter according to the Swiss standard SN 640 430. It was apparent from the measured values that maintaining the recommended value of 15 l/min after the pavement has been put in service is unlikely. It is also important to note that although permeability values were below current recommendations in situ performance regarding aquaplaning is not reduced. It can be seen that the air void content alone does not allow to assess the permeability; the quality of the voids as well as dimensions of the capillaries, and amount of interconnected voids should be considered. Furthermore it is recommended to use 15 l/min as an initial value of permeability to be used for laboratory prepared samples and initial tests in the field and reducing required in situ permeability to 10 l/min. The experience accumulated in canton Vaud (DINF LEM Yverdon) indicates that in situ permeability is reduced to 2/3 of the initial value after two years in service.

Particle loss

One of the disadvantages of porous asphalt is the rapid loss of particles. The European test procedure for particle loss evaluation [EN 12697-17] addresses this characteristic by an attempt to reproduce the in situ deterioration in the laboratory. It was seen that using the cantabro particle loss method the cohesion of the mix could be checked with results that duplicated field experience. The results show that water conditioning and frost thaw cycles at 25°C and -10°C had a minor effect on the results of the particle loss values. In order to assure proper cohesivity of the mix cantabro loss values are recommended as stated in Table 13.2. The effect of aggregate hardness on cantabro loss was studied and it can be concluded that with respect to reduction in particle loss the effect of aggregate hardness is minor in comparison to the effect of polymer modified binder.

Indirect tensile strength

The purpose of the indirect tensile test in this investigation was to assess the resistance to thermal cracking at low temperatures. Hence, the testing temperature was chosen to simulate roads in winter. The Indirect Tensile Strength (ITS) of selected cores and laboratory produced specimen were determined in accordance to European Standards [EN 12697-23] and conducted at 5 °C it was seen that the ranking of the materials was strongly temperature dependant. The ITS results at 5°C was completely different with the rankings at 25°C obtained from the water sensitivity tests. In order to assure proper resistance to thermal cracking an ITS value at 5°C of 1.5MPa is recommended (Table 13.2).

Water sensitivity

The test method for water sensitivity [EN 12697-12] is also part of the European standards and has been evaluated as suitable for porous asphalt. The purpose of this standard test is to determine the effect of saturation and accelerated water conditioning on the Indirect Tensile Strength of cylindrical specimen. Most of the “well” performing materials tested could fulfill the recommended $ITSR=70\%$ set by the standards [SN 640 431-7NA]. Based on current results it is recommended that this value be retained. A study on the effect of the type of compaction proved that the Marshall compaction process (2x50 blows) leads to a decrease of the $ITSR$ in spite of a lower porosity compared to the Marshall compaction with 2x25 blows and the gyratory compaction with 40 gyrations, probably related to an embrittlement of material due to micro fissuring

Stiffness

In order to assess the stiffness of the materials three different test procedures were used: Coaxial shear, direct tension and two point bending test. The modulus for most materials did fall within a band. This band can be used as a guideline for acceptable modulus that would lead to acceptable field performance. Water sensitivity of the material could be clearly characterized using the Coaxial shear test (CAST).

Direct tensile test

The direct tensile test at low temperatures allows to approach the rupture phenomena at low temperature for low strain rates similar to rates that occurs in asphalt mix subjected to a temperature fall. The aim of this test is to load a bituminous mix sample by a uniaxial tension at a constant strain rate and at low temperatures in a range of -10°C to -30°C . In this study, the dimensions of the samples and strain rates were adjusted for porous asphalt. The results for three different types of PA that were tested show a significant difference in failure strain and deformability.

Modeling

Appropriate modeling techniques can provide the pavement designer with the necessary tools to predict the behavior of a potential pavement before construction leading to substantial economic benefits. In the program used for this project [NOAH] the structure is represented by several bonded elastic layers (i.e. no slippage) allowing continuity of displacement at interfaces. For comparison material properties of AG1, AG2, AG3, VD5 and VD9 were used in the model. It can be concluded from the results that the modulus of the porous asphalt does not have a strong effect on the horizontal strains at the bottom of the asphalt layer and hence does not have a strong influence on the design life of the structure. Hence it is important that the asphalt layer under the porous asphalt layer has a reasonable thickness in order to distribute the load before transmitting it to the subgrade layer.

Maintenance and Rehabilitation

Because of the lower thermal conductivity of porous asphalt in winter, this surface may be colder than dense asphalt. Therefore, on the porous asphalt surface, snow tends to settle earlier and remain longer. The winter maintenance of porous asphalt is different than dense asphalt. It is necessary to adjust the practices for winter maintenance often and to react quickly to the actual weather conditions. Specifically more salt has to be used at the first application.

A rehabilitation period of 15 years has been necessary due to the loss of functionality resulting from loss of permeability or noise reduction properties.

Conclusions

In the framework of this research program a wide range of PA mixes with heterogeneous composition and performance have been studied.

Porous asphalt is characterized by high porosity, consequently a high macro roughness, a lower thermal conductivity, a strong permeability to water, and less contact points between the stones in comparison to the traditional dense graded mixes. The choice of a binder of excellent quality, aggregates and additives adapted to the conditions of traffic and to the situation of the road is imperative in the design of high performing mixtures. The key point is to ensure cohesion and adhesion of the surface particles subjected to the mechanical loads. To this end, polymer modi-

fied binders have been shown to improve the performance of PA. Improvements in performance are however not limited to polymer modifications to the binder. The results in this research program indicate that in most cases standard EN recommended laboratory tests corroborated field performances. Specific recommendations for standardization of mechanical tests for PA have been made.

With design and maintenance adapted, current experience shows good long term behavior (mechanical, permeability, acoustical) with remarkable service life.

This research project could demonstrate that with the use of proper mechanical tests the in situ performance of PA could be to a certain extent predicted and improved.

The road administration recommends that with this type of pavement it is necessary to adapt the maintenance practices in order to retain the desired serviceability especially in winter.

EXECUTIVE SUMMARY, DEUTSCH

Offenporiger Asphalt (PA) wird weltweit zur Reduktion von Sprühfahnen und Aquaplaning bei Regen sowie zur Lärmreduktion eingesetzt. In der Schweiz begann der Einsatz 1979, die Ergebnisse waren unterschiedlich. Eine Übersicht aus dem Jahre 2004 zeigt, dass in 9 Kantonen PA eingebaut worden ist. Dabei ist der Kanton Waadt führend. 1/3 der Nationalstrassen im Kanton VD weisen Deckschichten aus PA auf. Der Kanton plant zudem, den grössten Teil des Nationalstrassennetzes unter 600 m über Meer so auszuführen. Auch wurde versuchsweise auf mehreren Brücken PA eingebaut.

Neben seinen Vorteilen weist der PA auch erhebliche Mängel auf, die seine Gebrauchstauglichkeit herabsetzen und seine Nutzungsdauer einschränken. Die offene Struktur setzt eine grosse Oberfläche der Einwirkung von Wasser und Luft aus. Das Verstopfen der Poren kann zu einem vorzeitigen Verlust des Drainagevermögens führen.

PA liefert einen Beitrag zur Verkehrssicherheit bei regnerischem Wetter und reduziert die Lärmbelastung für die Anwohner. Um Wege zu finden, die mit dem PA verbundenen Mängel unter Beibehalten seiner Vorteile reduzieren zu können, wurden mechanische Prüfungen in Hinblick auf ihre Aussagefähigkeit verglichen, wobei es gilt optimale Mischungen finden zu können und das Mix Design zu verbessern. In diesem Sinne macht der Forschungsbericht auch Vorschläge für die Normierung.

In der Schweiz werden laufend europäische Normen ins Normenwerk integriert. Damit werden neben volumetrischen Anforderungen zunehmend auch mechanische wie Wasserempfindlichkeit und Kornverlust sowie Bindemittelablauf und Wasserdurchlässigkeit in vertikaler und horizontaler Richtung in den Nationalen Anhängen zu den EN festgelegt. Gemäss aktuellem Stand wird in [SN 640 431-7NA] nur der ITSR mit 70% als Anforderung gestellt. Neu ist in der Schweiz auch der PA 8 für Deckschichten normiert.

Aufgrund einer vorgängigen Literaturrecherche wurden die in Table 8. 1 aufgeführten mechanischen Prüfungen für PA ausgewählt. Parallel dazu wurde eine Umfrage zu Erfahrungen mit PA in der Schweiz durchgeführt (Appendix 2). Diese diente auch der Auswahl der zu untersuchenden Beläge. (AG1, AG4, AG5, VD7, VD8, VD9) und (VD2, VD3, VD4, VD5, VS6, AG2, AG3, VD10). Zudem wurde für eine Reihe von Aufbauten eine numerische Modellierung des Verhaltens durchgeführt. Das erlaubt es, das Verhalten von Bohrkernen und Laborprüfkörpern untereinander und mit dem Verhalten in Situ zu vergleichen. Aufgrund der Ergebnisse wurden zwei Mischungen optimiert (VD9, AG5) und Vorschläge zur Normierung mechanischer Prüfungen gemacht.

Prinzipien der Prüfungen und Ergebnisse

Altern des Mischgutes im Labor

Das Alterungsverhalten hängt von Bindemittel und der Adhäsion zwischen den Bindemitteln und Mineralstoffen ab. Altern und anschliessendes Prüfen von Bindemittel allein genügt nicht, um vorherzusagen, wie das Mischgut sich in Praxis verhalten wird. Deshalb wurde in dieser Untersuchung das Mischgut und nicht das Bindemittel gealtert. Das empfohlene Alterungsverhalten für Mischgut besteht im Lagern in einer geschlossenen Schachtel während 50 Minuten bei der Verdichtungstemperatur.

Verdichtung

Die EN 12697-10 erlaubt verschiedenen Verdichtungsenergien. Mit 2 x 50 Schlägen im Marshallgerät wird der maximale Verdichtungsgrad erreicht. Es besteht aber das Risiko der Bildung von Mikrorissen. Es wird darum vorgeschlagen die Prüfkörper für mechanische Prüfungen mit dem Marshallverdichtungsgerät bei 2 x 25 Schlägen oder mit dem Gyrator bei 40 Umdrehungen zu verdichten.

Charakterisieren der Hohlräume

Die EN 12697-8 definiert die Berechnung des Hohlräumgehaltes (V_m) und weiterer Parametern. Der Hohlräumgehalt V_m ist der Anteil des Porenvolumens am Gesamtvolumen.

Im Falle von PA sind die verbundenen Hohlräume (Kapillaren) sehr wichtig für das Drainagevermögen, das als Wasserdurchlässigkeit gemessen wird. Nach der nicht mehr gültigen aber in dieser Forschung verwendeten SN 640 433b werden die verbundenen Hohlräume gemäss der französischen Norm [NF P 98-254-2] bestimmt. Dieser Test erlaubt es, zu messen, welcher Anteil der Hohlräume im Inneren des verdichteten Mischgutes zugänglich ist und damit einen Beitrag zur Drainage des Oberflächenwassers leisten kann. In diesem Projekt wurden die verbundenen Hohlräume als die Menge Wasser bestimmt, die ein zylindrischer Prüfkörper mit abgedichteter Mantel- und Bodenfläche aufnehmen kann. Ein vom Grösstkorn abhängiger Korrekturfaktor ergibt dann das tatsächliche Volumen der verbundenen Hohlräume, korrigiert um die Oberflächenrauigkeit. Die relevanten Charakteristiken der Hohlräume sind in Tabelle 6.6 zusammengestellt.

Wasserdurchlässigkeit

Der Verlust der Durchlässigkeit durch Verstopfen ist einer der Nachteile von PA. In der bei Umgebungstemperatur (15 bis 25 °) durchgeführten Laborprüfung [EN 12697-12] wurde mit einer Wassersäule von 300 mm über dem Prüfkörper gearbeitet. In Situ wurde die Durchlässigkeit mit dem Durchflussmessgerät Yverdon [SN 640 430] ermittelt. Die Ergebnisse zeigen klar, dass der geforderte Durchfluss von 15 l/min bei Deckschichten nach wenigen Jahren unter Verkehr nicht mehr erreicht werden kann. Dabei wurde allerdings die Gebrauchstauglichkeit der Strasse in Hinblick auf Aquaplaning trotz der nicht normgerechten Werte als ausreichend beurteilt. Die Untersuchungen zeigen auch, dass der Hohlräumgehalt allein nicht zur Beurteilung des Drainagevermögens ausreicht. Mit hinein spielen die Qualität der Hohlräume, der Porendurchmessers und der Anteil verbundener Hohlräume. Die Forschungsstellen empfehlen, den Anforderungswert von 15 l/min nur für Laborprüfungen und frisch eingebaute Decken zu verwenden, während für Decken nach Verkehrsübergabe 10 l/min genügt. Die Erfahrungen des Kantons Vaud zeigen nämlich [DINF LEM Yverdon], dass die In Situ Durchlässigkeit unter Verkehr auf etwa 2/3 absinken.

Kornverlust

Ein Nachteil des PA ist der vorzeitige Kornverlust. Die europäische Prüfung [EN 12697-17] hat zum Ziel, die Schädigung der Strassenoberfläche im Labor nachzuvollziehen. Grundsätzlich eignet sich dieser Cantabro-Test, die Kohäsion des verdichteten Mischgutes zu erfassen und die Ergebnisse korrelieren mit dem Praxisverhalten. Es zeigte sich, dass Wasserlagerung und Frost-Tau-Wechsel (25 °C / -10 °C) die Ergebnisse nur geringfügig beeinflussten. Um die Kohäsion sicherzustellen schlägt die Tabelle 13.1 Anforderungswerte vor. Die Studie zeigt einen geringfügigen Einfluss der Gesteinshärte und einen wesentlicheren Einfluss des Bindemitteltyps auf.

Indirekter Zugfestigkeit

In dieser Untersuchung wurde der indirekte Zugfestigkeit eingesetzt, um den Widerstand gegen thermische Rissbildung im Tieftemperaturbereich zu erfassen. Die Prüftemperatur als relevant für winterliche Verhältnisse gewählt. Die Prüfung wurde in Anlehnung an EN12697-23 an Laborprüfkörpern und Bohrkernen aus der Strasse bei 5 °C und mit den Ergebnissen bei 25 °C aus der Bestimmung der Wasserempfindlichkeit verglichen. Es zeigt sich, dass die Rangfolge stark von der Temperatur abhängt. Die Resultate bei 5 °C ergeben ein völlig anderes Bild als jene bei 25 °C. Um den Widerstand gegen thermische Rissbildung mit dieser Prüfung zu erfassen, schlagen die Forschungsstellen einen Grenzwert von 1.5 MPa bei 5°C vor (Tabelle 13.1).

Wasserempfindlichkeit

Die Europäische Prüfmethode [EN 12697-12] erwies sich als geeignet für die Charakterisierung von PA. Die Prüfung bestimmt den Einfluss der Wassersättigung und der beschleunigten Wasserlagerung auf die indirekte Zugfestigkeit eines zylindrischen Prüfkörpers. Die meisten der Materialien mit gutem Gebrauchsverhalten erreichten das von der Norm [SN 640 431-7NA] geforderte ITSR von 70%. Eine Studie zum Einfluss der Verdichtungsenergie ergab bei einer Verdichtung mit 2 x 50 bei der Herstellung der Prüfkörper einen verringerten ITSR-Wert, obwohl die erreichte Verdichtung besser war als bei 2 x 25 Schlägen. Als Ursache wird die Bildung von Mikrorissen durch die höhere Verdichtungsenergie angenommen.

Steifigkeit

Drei Methoden wurden zur Bestimmung der Steifigkeit benutzt: der Koaxiale Schubtest KAST, der direkte Zugversuch und die Zweipunktbiegung. Die Modulwerte liegen bei den meisten Mate-

rialien in einem engen Band. Dieses Band erlaubt es, Anforderungen an die Steifigkeit zu stellen, deren Einhalten zu guter Gebrauchstauglichkeit führt. Wenn die Wasserempfindlichkeit mittel der Modulabnahme erfasst werden soll, bietet sich der KAST als Versuch an.

Direkter Zugversuch

Der direkte Zugversuch kann zur Untersuchung des Widerstandes gegen Bildung von Kälterissen eingesetzt werden. Die Prüfkörper wurden bei Temperaturen von -10°C bis -30°C mit einer konstanten Dehnrate belastet. Für das Prüfen von PA wurden die Abmessungen der Pürfkörpern und die Dehnraten angepasst. Drei unterschiedliche PA-Mischgüter wurden geprüft und es zeigten sich signifikante Unterschiede in der Verformbarkeit und der Dehnung beim Bruch.

Modellierung

Passende Modellierungsverfahren sind ein nötiges Hilfsmittel, um die Tauglichkeit eines Belagsaufbaues vorhersagen zu können und so einen ökonomischen Nutzen zu erreichen. In dieser Forschung wurde das Programm NOAH eingesetzt um repräsentative Aufbauten mit mehreren elastische Schichten mit vollem Verbund (Kontinuität der Verschiebungen an der Schichtengrenze) durchzurechnen. Zum Vergleich wurden die Materialeigenschaften von AG1, AG2, AG3, VD5 und VD9 im Modell verwendet. Die Resultate zeigen, dass der PA nur einen unwesentlichen Einfluss auf die Dehnungen an der Unterseite des Belages hat und daher auch die angestrebte Lebensdauer des Aufbaus nicht wesentlich beeinflusst. Es ist aber wichtig, dass die Tragschichten unter dem PA eine ausreichende Schichtdicke aufweisen und die Auflast verteilt wird, bevor sie in die ungebundenen Schichten weitergeleitet wird.

Unterhalt

Da der PA Wärme schlechter als dichter Asphalt leitet, sind tiefere Oberflächentemperaturen im Winter zu erwarten. Daher bleibt der Schnee auf PA früher und länger liegen. Der Winterdienst muss deshalb diese Unterschiede berücksichtigen und schneller auf Wetterumschläge reagieren. Insbesondere muss die Menge des Salzes bei der erste Dosierung vermehrt werden.

Nach Erfahrung der PA musste nach 15 Jahre wegen schlechter Funktionalität ersetzt werden

Folgerungen

Im Rahmen dieser Forschungsprogramme wurde ein grosser Bereich von PA-Mischguten unterschiedlicher Zusammensetzung und Gebrauchstauglichkeit untersucht.

PA ist durch ein hohes Porenvolumen und damit durch eine hohe Makrorauigkeit, eine geringere thermische Leitfähigkeit und eine hohe Wasserdurchlässigkeit charakterisiert. Zugleich weist aber auch das Korngerüst weniger Kontaktstellen auf als bei dichten Belägen. Die Wahl von qualitativ hochwertigen Bindemitteln, geeigneten Mineralstoffen und Zusätzen muss der Situation von Verkehr und Strasse entsprechen, um eine gute Gebrauchstauglichkeit zu erreichen. Entscheidend sind die Kohäsion des verdichteten Belags und die Adhäsion der mechanisch belasteten Mineralkörner der Oberfläche. Diese Forschung zeigte klar, dass polymermodifizierte Bindemittel entscheidend zur Gebrauchstauglichkeit beitragen. Sie schliesst damit andere Wege nicht aus. Die Forschung wies nach, dass die durch die EN definierten Untersuchungen im Normalfall die Gebrauchstauglichkeit im Feld richtig aufzeigen. Darum wurden entsprechende Vorschläge für Anforderungen mechanischer Prüfungen wurden ausgearbeitet.

Korrektes Design und am Belagstyp angepasster Unterhalt vorausgesetzt, können nach aktuellen Erfahrungen ein befriedigendes Langzeitverhalten (mechanisch, die Entwässerung betreffend und akustisch) und eine gute Dauerhaftigkeit erreicht werden.

Das Forschungsprojekt zeigt, wie mit mechanischen Prüfungen das Gebrauchsverhalten in gewissen Grenzen vorhergesagt und dadurch verbessert werden kann.

Die Strassenämter haben festgestellt, dass der Unterhalt des Strassennetzes bei diesem Typ von Deckschichten angepasst werden muss, um die gewünschte Befahrbarkeit im Winter zu erreichen.

EXECUTIVE SUMMARY, FRANCAIS

Les asphalte poreux (PA) sont utilisés aujourd’hui dans le monde entier pour leurs qualités de drainage de l’eau de pluie, d’augmentation de l’adhérence sur chaussées humides ainsi que pour la diminution du bruit. La Suisse a commencé à les employer en 1979 avec des résultats hétérogènes. Un bilan datant de 2004 montre que 8 des 26 cantons ont des réalisations en asphalte poreux. En particulier le canton Vaud situé en Suisse occidentale est connu en tant que principal maître d’œuvre favorisant l’emploi d’asphalte poreux. Actuellement, 1/3 des autoroutes de ce canton sont recouvertes d’asphalte poreux et la volonté est de poursuivre l’application des asphalte poreux pour les autoroutes dans le canton jusqu'à une altitude de 600m. De plus, plusieurs couches de roulement de ponts sont réalisées en asphalte poreux.

Malgré des avantages environnementaux, les asphalte poreux peuvent présenter des problèmes pouvant affecter leur performance et leur durée de vie. La structure ouverte expose une superficie importante du matériau aux effets de l’air et de l’eau menant à un vieillissement rapide du liant ainsi qu’au colmatage des pores. Il est clairement établi que ce type de matériau constitue une solution très efficace pour la sécurité des conducteurs en conditions pluvieuses ainsi que contre les nuisances sonores affectant les riverains. Une étude a été menée dans le but de réduire les faiblesses de ce matériau et d’en développer les avantages. Elle porte sur divers mélanges comparés à partir de méthodes d’essais mécaniques. Une phase d’optimisation est ensuite menée. Un autre objectif de ce projet est de formuler des recommandations relatives aux propriétés mécaniques des asphalte poreux.

Les normes suisses seront progressivement remplacées par les normes européennes. En plus des vides, des exigences sont requises pour le comportement comme la sensibilité à l’eau, la perte de matériaux, la drainabilité et les perméabilités horizontale et verticale. Les normes européennes doivent être utilisées en prenant en compte les annexes nationales. La seule propriété mécanique considérée dans l’annexe suisse de cette norme [SN 431-7NA] porte sur l’essai de sensibilité à l’eau et fixe une valeur ITSR ≥ 70 . De plus, l’annexe suisse fait état de dispositions applicables à l’avenir en Suisse pour des asphalte poreux avec une dimension maximale des granulats de 8 mm.

De la recherche bibliographique, des essais mécaniques appropriés à l’étude de ces matériaux ont été choisis (Table 8. 1). De même, un inventaire des expériences avec des asphalte poreux menées en Suisse a été établi (Annexe 4). Des essais de performance ont été réalisés d’une part à partir d’échantillons préparés en laboratoire (AG1, AG4, AG5, VD7, VD8, VD9) et d’autre part sur des carottes (VD2, VD3, VD4, VD5, VS6, AG2, AG3, VD10) prélevées *in situ* en fonction de l’expérience acquise par les responsables des cantons. Le comportement de ces matériaux a été également évalué en utilisant une approche analytique. Les essais réalisés ont permis la comparaison des performances du matériau préparé au laboratoire avec celles des échantillons prélevés *in situ*. Sur la base des résultats obtenus, deux mélanges ont été optimisés (VD9, AG5) et des recommandations pour définir des essais mécaniques appropriés aux asphalte poreux ont été faites.

Procédures expérimentales et résultats

Vieillissement de l’enrobé en laboratoire

Le vieillissement de l’enrobé dépend à la fois du bitume et du granulat. Les essais sur bitume vieilli ne donnent pas une bonne prédiction du comportement de l’enrobé en raison des interactions liant/granulat. Ainsi donc la recherche a été menée en vieillissant l’enrobé. La procédure de vieillissement recommandée consiste à vieillir l’enrobé dans un récipient fermé durant 50 minutes à la température de compactage.

Compactage

Selon la norme européenne [EN 12697-10] la compactibilité peut être déterminée avec des éner-

gies de compactage variables. L'énergie de 2X50 coups Marshall donne une indication sur la compacité maximale que l'on peut atteindre néanmoins pour certaines formules une énergie plus faible est suffisante. Il est recommandé de ne pas surcompacter l'enrobé pour éviter un affaiblissement par microfissurations. Un compactage de 2x25 coups Marshall ou de 40 girations PCG est recommandé pour les PA dans le cas de la détermination des performances mécaniques.

Caractéristiques des vides

La norme européenne [EN 12697-8] décrit la procédure pour calculer la teneur en vides (V_m) ainsi que d'autres paramètres. La teneur en vides est définie comme le volume des vides d'air en pourcentage du volume total de l'échantillon.

Dans le cas des enrobés drainants la quantité des vides communicants est très importante pour la perméabilité qui est directement liée à cette propriété. L'ancienne norme suisse SN 640 433b pour les enrobés drainants, retenue dans la présente étude, propose de suivre la norme française [NF P 98-254-2] pour la détermination des vides communicants. L'essai de détermination des vides communicants des matériaux liés permet de mesurer les vides communicants situés dans la masse des matériaux communicants entre et avec la surface qui permettent le drainage de l'eau superficielle. Dans la présente recherche les vides communicants sont déterminés par la masse d'eau qui percole dans l'échantillon alors que ses parois et son fond sont rendus étanches. Un facteur de correction est appliqué en fonction de la taille maximale du grain pour obtenir le volume effectif des vides communicants donc sans tenir compte des vides à la surface de l'échantillon. Table 6.5 et Table 6.6 décrit les caractéristiques des vides retenus pour cette étude.

Perméabilité à l'eau

La chute de perméabilité due au rapide colmatage des pores est un des désavantages des enrobés drainants. En laboratoire l'essai [EN 12697-19] est réalisé à température ambiante (15 et 25°C) en appliquant une colonne d'eau de 300 mm à un échantillon cylindrique. Les mesures de perméabilité in situ ont été menées avec le perméamètre d'Yverdon conformément à la norme suisse SN 640 430. Il apparaît au travers des valeurs mesurées que la valeur recommandée par la norme EN (15 l/min) n'est pas applicable à un revêtement en service. Il est également important de relever que lorsque les valeurs de perméabilité sont au-dessous des recommandations les performances vis-à-vis de l'aquaplaning ne sont pas toujours réduites. On constate que les vides d'air ne peuvent à eux seuls évaluer la perméabilité mais qu'il faut considérer la dimension des capillaires et la quantité de vides communicants. De plus il est recommandé de retenir la limite de 15 l/min pour les essais sur les échantillons préparés en laboratoire ainsi que les essais initiaux in situ et une valeur réduite à 10 l/min pour les essais ultérieurs de perméabilité in situ. L'expérience acquise par le laboratoire des routes nationales du canton de Vaud [DINF LEM Yverdon] montre que la perméabilité résiduelle, après deux ans de service représente environ les 2/3 de la perméabilité initiale mesurée à l'état zéro.

Perte de matériaux

Un des désavantages de l'asphalte poreux réside dans la perte prématurée de matériaux. L'essai européen de perte de matériaux [EN 12697-19] aborde cette caractéristique par une tentative de reproduire en laboratoire le mécanisme de la détérioration in situ. On a vu qu'en utilisant la méthode de perte de matériaux "Cantabro" la cohésion du mélange pourrait être vérifiée avec des résultats représentatifs de l'expérience in situ. Les résultats montrent que l'immersion dans l'eau et les cycles de gel ont un effet mineur sur les résultats des valeurs de perte de matériaux à 25°C et à -10°C. Afin d'assurer une cohésion appropriée, des valeurs de perte à l'essai Cantabro sont recommandées comme indiqué dans tableaux 13.1.

L'étude de l'incidence de la dureté de granulats, dont le coefficient Los Angeles est compris entre 19 et 27, montre qu'il n'y a pas d'influence sur le résultat à la température d'essai Cantabro de 25°C. Pour l'essai réalisé à -10°C, un léger effet de la dureté du granulat est constatée. L'essai effectué avec le granulat plus dur indique une perte plus importante de l'ordre de 4 à 5% à 300 tours.

Essai de traction indirecte

Le but de l'essai de traction indirecte dans cette recherche était d'évaluer la résistance à la fissuration aux basses températures. Par conséquent la température d'essai a été diminuée pour simuler des routes en hiver. La résistance à la traction indirecte (ITS) a été déterminée à 5°C selon les normes européennes [EN 12697-23] sur des carottes sélectionnées et sur des échantillons produits en laboratoire. Il a été constaté que le classement des matériaux était fortement dépendant de la température. Les résultats à 5°C étaient complètement différents de ceux obtenus à 25°C avec des essais de sensibilité à l'eau. Afin d'assurer une résistance appropriée à la fissuration thermique une valeur de traction indirecte à 5°C de 1.5 MPa est recommandée (Table 13.2).

Sensibilité à l'eau

La méthode d'essai pour la sensibilité à l'eau, EN 12697-12 fait partie des nouvelles normes européennes et a été évaluée comme applicable aux enrobés drainants. Le but de cet essai normalisé est de déterminer l'effet accéléré de la saturation d'eau d'échantillons cylindriques sur la résistance à la traction indirecte. La plupart des bons matériaux examinés ont remplis la recommandation des normes [SN 640 431-7NA] soit $\text{ITSR}=70\%$. Sur la base des résultats actuels les auteurs recommandent que cette valeur soit maintenue.

Une étude sur l'incidence du type de compactage et de l'énergie appliquée a montré que le compactage Marshall (2x50 coups) générait une diminution du ratio ITSR malgré une teneur en vides plus faible par rapport au compactage Marshall 2x25 coups et PCG à 40 girations, probablement liée à une fragilisation du matériau par microfissuration.

Module de rigidité

Afin d'évaluer la rigidité des matériaux trois méthodes d'essai différentes ont été employées : L'essai coaxial de cisaillement, la traction directe et l'essai de flexion deux points. Le module pour la plupart des matériaux se situe dans un fuseau. Ce fuseau peut être employé comme directive pour le module des matériaux *in situ*. La sensibilité à l'eau du matériau a pu être clairement caractérisée en utilisant l'essai CAST.

Essai de traction directe

L'essai de traction directe permet d'approcher les phénomènes de rupture à basse température pour de faibles taux de déformations, semblables à ceux qui sont produits dans un béton bitumineux soumis à une chute de la température. Le but de cet essai est de solliciter un échantillon d'enrobé bitumineux par une traction uniaxiale à une vitesse de déformation constante et dans un domaine de basses températures comprises entre -10°C et -30°C. Dans cette étude, les échantillons d'essai et la vitesse de déformation ont été ajustés à des valeurs plus appropriées à l'asphalte poreux. Les résultats obtenus pour trois différents types de PA testés montrent une différence significative autant pour la contrainte de rupture que la déformabilité.

Modélisation

Des techniques de modélisation appropriées peuvent fournir au concepteur de chaussée les outils nécessaires à la prédiction du comportement d'un revêtement avant sa mise en place amenant ainsi des avantages économiques substantiels. Dans le programme utilisé pour ce projet (NOAH) la structure est représentée par plusieurs couches élastiques collées (c.-à-d. aucun glissement) maintenant la continuité des déplacements aux interfaces. Pour la comparaison les propriétés des matériaux des planches AG1, AG2, AG3, VD5 et VD9 ont été modélisées. Il est possible de conclure d'après les résultats que la valeur de module de l'asphalte poreux n'a pas un effet important sur la contrainte horizontale au fond de la couche de revêtement et par conséquent n'a pas une influence considérable sur la durée de vie de la structure. Néanmoins il est important que la couche d'asphalte sous la couche d'enrobé drainant ait une épaisseur raisonnable afin d'absorber la charge avant de la transmettre à la couche de fondation.

Maintenance et entretien

En raison de la conductivité thermique inférieure de l'enrobé drainant cette surface peut être, en hiver, sensiblement plus froide qu'un enrobé dense. Par conséquent, sur la surface poreuse la neige tend à se fixer plus tôt et à rester plus longtemps. L'entretien hivernal de l'asphalte poreux est différent de celui de l'enrobé dense. Il est nécessaire d'ajuster les pratiques de l'entretien hivernal en intervenant plus souvent et en réagissant rapidement aux conditions du moment.

Conclusions

Dans le cadre de ce programme de recherche un large éventail de mélanges de PA avec des compositions et performances hétérogènes a été étudié.

L'asphalte poreux est caractérisé par la porosité élevée, par conséquent une macrorugosité élevée, une conductivité thermique plus faible et une forte perméabilité à l'eau mais il comporte moins de points de contact entre les granulats par rapport aux mélanges denses traditionnels. Le choix d'un liant d'excellente qualité, de granulats et d'additifs adaptés aux conditions du trafic et à la situation de la route est impératif dans la conception de mélanges à haute performance. Le point clé est d'assurer la cohésion et l'adhérence à la surface des matériaux soumis aux sollicitations mécaniques. A cet effet, les liants modifiés aux polymères ont été retenus pour améliorer les performances des PA. Les améliorations de performances ne sont cependant pas limitées aux liants modifiés par des polymères. Les résultats obtenus dans ce programme de recherche indiquent que dans la plupart des cas les essais en laboratoire standards ont corroboré les performances obtenues *in situ*. Des recommandations spécifiques pour la normalisation des essais mécaniques pour les PA sont proposées.

Avec une conception et un entretien adaptés, les expériences montrent un bon comportement à long terme (mécanique, perméabilité, acoustique) avec une durée de vie remarquable.

Ce projet de recherche a démontré que l'utilisation d'essais mécaniques appropriés pouvait mener à prévoir et améliorer dans certaines limites les performances, *in situ*, des PA.

Les administrations routières ont observé qu'avec ce genre de couche de roulement il y a lieu d'adapter l'exploitation des réseaux en particulier en ce qui concerne la viabilité hivernale.

TABLE OF CONTENTS

Executive Summary, English	4
Executive Summary, Deutsch	8
Executive Summary, Francais	11
Table of Contents	15
List of Figures	18
List of Tables	20
List of Symbols and Abbreviations	21
1. Introduction	24
1.1. Summary of the advantages and disadvantages of porous asphalt	24
2. Porous Asphalt in Switzerland	27
2.1. Swiss Standards [SN 640433b]	29
2.2. European Standard [EN13108-7]	31
3. State of the Art in Research Pertaining to Porous Asphalt	31
3.1. Research in Switzerland	31
3.2. International Research	33
4. Objective and Program of Investigation	34
5. Performance Survey on Porous Asphalt in Switzerland	36
6. Material Selection	36
7. Field Evaluation of Selected Pavements	44
8. Experimental Program	45
9. Experimental Procedures	46
9.1. Laboratory Aging of Mix	46

9.2. Void Characteristics [EN 12697-8]	49
Connected Network of Voids	50
9.3. Vertical Water Permeability [EN 12697-19]	51
9.4. Horizontal Water Permeability [EN 12697-19]	53
9.5. In situ Water Permeability [SN 640 430]	54
9.6. Particle Loss using the Cantabro Test [EN 12697-17]	56
9.7. Indirect Tensile Strength [EN 12697-23]	56
9.8. Water Sensitivity [EN 12697-12]	57
9.9. Stiffness	58
Coaxial Shear Test	58
Two Point Bending Test [EN 12697-26]	59
Direct Tensile Test (DTT)	61
9.10. Binder Rheological Properties using the Dynamic Shear Rheometer, DSR	62
10. Experimental Results	64
10.1. Compaction	64
Effect of Binder Content and Gradation on Compaction	64
Void Content Distribution in Specimen Produced using a Roller Compactor	65
10.2. Total Air Voids and Interconnected Air Voids	67
10.3. Vertical Water Permeability	67
10.4. Horizontal Water Permeability, Effect of Height	69
10.5. Particle Loss using the Cantabro Test	70
Effect of Aggregate Hardness (Los Angeles) and Binder Type	70
Effect of Compaction Energy	73
10.6. Indirect Tensile Strength (5°C)	76
10.7. Water Sensitivity- Indirect Tensile Strength (25°C)	78
Effect of compaction mode	81
Effect of aging on the indirect tensile strength	81
10.8. Rheology of the Binder Using the Dynamic Shear Rheometer DSR	84
10.9. Stiffness	84
Coaxial Shear Test (CAST)	84
Two Point Bending Test	87
Direct Tension	88

11. Modeling	90
12. Maintenance and Rehabilitation	98
13. Conclusions and Recommendations	99
14. Acknowledgements	102
15. Literature	103
Appendix1: Summary of Literature Survey on Test Methods	107
Appendix 2: Summary of Results of the Survey from Various Swiss Cantons	108

LIST OF FIGURES

Note: The German and French captions are included under the English caption in the body of the report

Figure 2. 1 : Porous asphalt in Switzerland in bold red (Status 1.9.2005)	29
Figure 3. 1: Comparative noise reduction properties of the test sections in [28]. Porous asphalt twin-lay are indicated by PA4+8 and PA 8+16. With 0 reduction corresponding to 100% traffic, 3.0 dB(A) to 50% and 6.0 to 25% [24]	32
Figure 3. 2 Noise reduction of porous asphalt (Morges) in comparison to dense graded asphalt (Montreux).....	33
Figure 4. 1: Structure of the research program.....	35
Figure 6. 1: Top view of twinlay VD10, top layer (top left), bottom layer with pores (top right), bottom layer with pores filled with SAMI (bottom left), Twinlay (Bottom right)	39
Figure 9. 1 : Residual penetration of 4 binders after various aging periods.....	47
Figure 9. 2 : Retained penetration, softening point and IP of Colflex N55 binder at original state, 60 min, 120 min, 180 min, and 240 min oven aging, base and recovered bitumen.....	47
Figure 9. 3 : Mix AG4 prepared in a metal pan for aging	48
Figure 9. 4 : Voids in the mineral aggregate VMA, Void content V_m , Volume of the aggregate V_a and volume of the bitumen V_{br}	49
Figure 9. 5 : Apparatus for vertical permeability (dimensions in mm)	51
Figure 9. 6: Test set up for vertical permeability (LAVOC).....	52
Figure 9. 7 Apparatus for horizontal permeability (dimensions in mm)	53
Figure 9. 8: Test set up for horizontal Permeability (LAVOC)	54
Figure 9. 9: Detail scheme of the test device (dimensions given in mm)	55
Figure 9. 10: Scheme of the Yverdon permeameter (dimensions given in mm)	55
Figure 9. 11: Schematic representation of the indirect tensile test (left) and a specimen during a test (right) at Empa	57
Figure 9. 12: Schematic depiction of the CAST setup, left and cut view of a CAST specimen, right at Empa.....	58
Figure 9. 13 : Two point bending equipment at LAVOC.....	60
Figure 9. 14: Assembly of the sample in the conditioning chamber at LAVOC for the direct tension test	61
Figure 9. 15 : DSR (right) and schematic depiction of the DSR testing configuration (left) Empa	63
Figure 10. 1 : Mix design VD5 - Grading curve A with 4 various binder contents	64
Figure 10. 2 : Mix design VD5 - Grading curve B with 4 various binder contents	65
Figure 10. 3 Air void content distribution [vol %] in a specimen compacted using a steel roller at Empa.....	66
Figure 10. 4 : Final stage of compaction (left) and the sample (right).....	66
Figure 10. 5 : Relation of connected voids versus total voids and ratio	67
Figure 10. 6 : Results of the vertical permeability in laboratory and permeability in situ using the standard Yverdon method SN 640 430a.....	68
Figure 10. 7 : Results of vertical permeability in lab vs. permeability in situ and construction dates	69
Figure 10. 8 : VD9 PA11 Bitumen Rubber - Results of the vertical and horizontal permeability in laboratory and permeability in situ (Yverdon method) with samples of different heights (SN 640 430a).....	70
Figure 10. 9 : Particle loss (Cantabrian) at 25°C after 300 and 500 revolutions, effect of hardness of aggregate with different binders (compaction Marshall 2 x 25 blows)	71
Figure 10. 10 : Particle loss (Cantabrian) at -10°C after 300 and 500 revolutions, effect of hardness aggregate with different binders (compaction Marshall 2 x 25 blows).....	71

Figure 10. 11 : Particle loss (Cantabrian) at -10°C after 300 and 500 revolutions, effect of aggregate hardness with different binders (compaction Marshall 2 x 50 blows).....	72
Figure 10. 12 : Particle loss (Cantabrian) at -10°C after 300 and 500 revolutions, effect of hardness of aggregate with different binders (compaction 2 x 25/50 blows) and air voids.....	72
Figure 10. 13 : Particle loss (Cantabrian) at 25°C after 300 and 500 revolutions, with respect to the compaction mode.....	73
Figure 10. 14 : Particle loss (Cantabrian) at -10°C after 300 and 500 revolutions with respect to the compaction mode.....	74
Figure 10. 15 : Particle loss (Cantabrian) at 25°C after 300 revolutions – Results of standard test, after water conditioning and freeze-thaw cycles	74
Figure 10. 16: Particle loss (Cantabrian) at 25°C after 500 revolutions – Results of standard, water conditioning and freeze-thaw cycles tests.....	75
Figure 10. 17: Particle loss (Cantabrian) at -10°C after 300 revolutions – Results of standard test, after water conditioning and freeze-thaw cycles	75
Figure 10. 18: Particle loss (Cantabrian) at -10°C after 500 revolutions – Results of standard test, after water conditioning and freeze-thaw cycles	76
Figure 10. 19 : Indirect Tensile Strength (ITS) at 5°C	77
Figure 10. 20: Load displacement diagram of AG2 and AG3 showing a ductile behavior of AG3 in the displacement controlled test	78
Figure 10. 21: Peak load to failure at 25	79
Figure 10. 22 : Indirect tensile strength (ITS) at 25°C with error bars indicating maximum and minimum values.....	79
Figure 10. 23 : Indirect Tensile Strength Ratio (ITSR) at 25°C	80
Figure 10. 24 : Indirect Tensile Strength at 5°C and 25°C	80
Figure 10. 25: Indirect Tensile Strength Ratio (ITSR) at 25°C - Effect of compaction mode	81
Figure 10. 26: Effect of aging as characterized by the indirect tensile strength (ITS).....	82
Figure 10. 27: Effect of aging as characterized by the indirect tensile strength ratio (ITSR)	82
Figure 10. 28: Failure of the twinlay system at 25°C left and example of brittle fracture at 5°C right	83
Figure 10. 29 : Conditioning of the specimen in a water bath (left) and fracture surface of the twinlay after ITS test at 5°C.	83
Figure 10. 30 : Black diagrams for the recovered binders	84
Figure 10. 31: Master curves from CAST, at reference temperature of 25°C	85
Figure 10. 32: Results of CAST ; Black diagrams.....	85
Figure 10. 33: Water sensitivity of AG1 dry specimen under repeated loading left, and wet specimen under repeated loading right.....	86
Figure 10. 34: Water sensitivity of AG2 dry specimen under repeated loading left, and wet specimen under repeated loading right.....	87
Figure 10. 35: Water sensitivity of AG3 dry specimen under repeated loading left, and wet specimen under repeated loading right.....	87
Figure 10. 36 : Master curves from Two Point Bending Test, at ref. temperature of 15°C	88
Figure 10. 37 : Results of the Direct Tensile Test for AG1.....	89
Figure 10. 38: Results of the Direct Tensile Test for VD9	89
Figure 10. 39: Results of the Direct Tensile Test for VD7	90
Figure 11. 1: Design life of a pavement	91
Figure 11. 2 : Modeling of the load	91
Figure 11. 3: Geometrical scheme of the pavement indicating modeled parameters.	92
Figure 11. 4: Design life vs. modulus of the wearing course.....	96
Figure 11. 5: Design life in comparison with modulus	96
Figure 11. 6 : Strain [10^{-6}] distribution as a function of depth.....	98
Figure 12. 2 : Change of surface temperature of two sections of porous asphalt (enrobé drainant) between sections of dense graded asphalt. The position is indicated by the x-axis. [54]	99

LIST OF TABLES

Note: The German and French captions are included under the English caption in the body of the report

Table 2. 1 Inventory of porous asphalt on National Roads in Switzerland (Status 2004)	28
Table 2. 2 : Thickness requirements.....	30
Table 2. 3 Gradation requirements and binder content.....	30
Table 2. 4 : Required void content for Marshall specimen	30
Table 3. 1 : Noise reduction	33
Table 6. 1: Stage I selected sections for coring	36
Table 6. 2: Stage II selected laboratory prepared mixes.....	37
Table 6. 3: Stage III optimization of selected mixes.....	37
Table 6. 4: Optimization process of VD9 based on VD5.....	41
Table 6. 5: gradation, air void content, binder type and binder content of cores (Pmb stands for polymer modified binder)	42
Table 6. 6: Gradation, binder type and binder content of laboratory compacted mixes for stage II selected laboratory prepared mixes and stage III optimization of selected mixes	43
Table 7. 1: Summary of surface inspections	44
Table 8. 1: Test program.....	45
Table 9. 1: CAST test parameters.....	58
Table 9. 2: Two point bending parameters.....	60
Table 11. 1: Summary of modeling results.....	95
Table 11. 2: Summary of modeling results of VD5.....	97
Table 13. 1 : Summary of recommendations for mechanical tests for PA standardization.....	101
Table 13. 2 : Summary of recommendations for mechanical tests to be introduced for PA standardization.....	102

LIST OF SYMBOLS AND ABBREVIATIONS

A(E*)	Coefficient function derived from FEA by recursive iteration
AASHTO	American Association of State Highway and Transportation Officials
AB	Asphalt-Beton, Asphalt concrete
Ad	Admissible
A-Gr.	Asphalt-Granulat
A _i	Surface area
ASTRA	Bundesamt für Strassen (Swiss Roads Authority)
a _T	shift factor, determined with Arrhenius (or WLF) relationship
b	Slope of the linear regression for the fatigue law (for bituminous materials b=-0.2)
BAFU	Bundesamt für Umwelt, Federal office for the environment
CAST	Coaxial Shear Test
D	Maximum size of solid particle, amplitude of displacement
D, d	Diameter of the specimen
DRA	Drainasphalt, previous designation of porous asphalt in Swiss standards
E*	Complex modulus
Empa	Eidgenössische Materialprüfungs- und Forschungsanstalt (Swiss federal laboratory for materials testing and research)
EN	Europäische Norm, European standards
f	Frequency
F	Amplitude of sinusoidal load
F _a	Force amplitude along the steel core
f _r	Frequency of loading at the reference temperature
H	Height of the specimen
h	The conventional height of the core sample
HMF	<u>Heissmisch</u> fundationsschicht, binder course
HMT	<u>Heissmisch</u> tragschicht, wearing course
HRA	Hot roled asphalt
I	Thickness of specimen
I ₁	Global degeneration weighted index

ITS	Indirect tensile strength
ITSR	Indirect tensile strength ratio
k_r	Risk coefficient chosen according to factors of a confidence interval around thickness and around fatigue tests' results (depends on risk percentage, if 5% $k_r=0.787$)
k_s	Coefficient of reduction to take into account the effect of a lack of uniformity in the bearing capacity of a soft soil layer underneath treated layers (usually $k_s=1$)
K_v, K_h	Vertical and Horizontal permeability
LAVOC	Laboratoire des voies de circulation – EPFL
LTOA	Long term oven aging
M	Mass of introduced water
M1	Mass of dried sample
M2	Mass of the sample for which the connected voids are filled [g] Note that this definition is not the identical to the French denomination (in the standard)
MR	Rauasphalt, Roughasphalt, Macro-rugeaux
NE	Number of axle equivalents
P	Peak load
PA	Porous asphalt
Pc	Percentage of connected voids
PCG	Pine gyratory compactor
PL	Particle loss
Pmb	Polymer modified binder
Q_v, Q_h	Vertical and horizontal flow rate
r	Radius of the core sample
RM	Recycling-Mineral
RTFOT	Rolling thin film oven test
S_i	Severity of degeneration
SN	<u>Schweizer Norm</u> (Swiss Standard)
SPA	Splittasphalt, thin layer with fine aggregates, not standardized
STOA	Short term oven aging
V	The conventional volume of the core sample
v	Volume of introduced water
V_m	Air void content of the mixture
VMA	Voids in mineral aggregate

VSS	<u>Vereinigung Schweizerischer Strassenfachleute</u> (Organization of the Swiss road specialists)
V_{wasser}	Volumen of Water
W1, W2	Initial and final specimen mass

Greek Symbols

ρ_e	Density of water
ϕ	Phase shift angle between the applied max strain and the max stress
δ_a	Displacement amplitude along the steel core
α	Parameter describing the span between max and min value of E^*
β, γ	Parameters describing the shape of the sigmoidal function
Δ	Parameter describing the minimum value of E^*
Θ	Temperature
Θ_{eq}	Equivalent temperature (15°C)
ρ_b	Bulk density of the specimen, [EN12697-6]
ρ_m	Maximum density of the mixture [EN12697-5]
ε	Fatigue strain data obtained with the fatigue law
γ	Factor depending on the specimen dimensions
ω	Angular frequency
η	dynamic viscosity

1. INTRODUCTION

Porous asphalt or open graded asphalt is widely used for water drainage and noise reduction in order to improve traffic safety and comfort for both drivers and residents living in the vicinity of roads. The structure of porous asphalt differs completely from conventional dense mixes. It consists mainly of coarse aggregate with small amounts of sand and filler, thus creating an open texture and a permeable structure with high porosity. Porosity in excess of 20 % is common in this type of asphalt pavements. The character of porous asphalt is quite unique due to the high proportion of large sized aggregate and its gap gradation. Due to its rough surface texture and large amount of pores, porous asphalt improves skid resistance and provides good visibility while reducing spray and splash on wet surfaces. These improvements on traffic safety can well contribute to maintain road capacity in rainy days. Many in situ studies show traffic noise level on the roads also reduced considerably.

Despite its environmental benefits, porous asphalt can suffer from problems, which can affect both its performance and its service life. The open structure exposes a large surface area to the effects of air and water, leading to rapid aging of the binder as well as clogging of the pores.

In order to improve durability of porous asphalt and retain the benefits, in this project, test procedures are compared and discussed with respect to their suitability for porous asphalt optimization and for development of improved mix design. It is also a goal of this project to make recommendation for standardization of mechanical properties of porous asphalt. Resulting from the survey taken at the beginning of the project, porous asphalt used as a drainage course (DRAS) was not included in this project due to its limited use.

Structural Contribution

Depending on the mix design for each country, the subject of the structural contribution of porous asphalt to heavy traffic roads is debatable. An investigation by Potter and Halliday in Britain showed that 40 mm thickness of porous wearing course was found to be equivalent to a 20 mm HRA [17]. The old Swiss standard for the DRA [69] suggested that 1 cm thickness of the traditional Swiss base course mix (HMT) is equal to 12.5 cm of the DRA, and that the structural contribution of the DRA is equal to 65% strength of other surface mixes, including Gussasphalt and the SMA [69]. The Japanese experience shows in terms of layer thickness contribution for pavement structure no significant difference on the durability of asphalt pavement (crack resistance against traffic loading) with 40 mm porous asphalt, compared with conventional section with 40 mm dense graded asphalt surface, [16].

1.1. Summary of the advantages and disadvantages of porous asphalt

Advantages and disadvantages of porous asphalt have been well established in the literature; below a summary is listed:

Advantages

Reduction in splash and spray, reduced aquaplaning

Compared to dense mixes, surface water can drain through porous asphalt due to the large amount of continuous pores in the structure. The material provides good visibility under rainy conditions, thus preventing the reduction in traffic flow volumes, which normally accompany rain. In addition, the absorption of surface water is effective in reducing aquaplaning which occurs when vehicles move at high speeds on a thin water layer. It has been shown that porous asphalt contributes to the reduction of the number of accidents in rainy days [1].

Reduction in light reflection and headlight glare

Because porous asphalt acts as a drainage layer, enabling rainwater to percolate through the mix, thus light reflection and headlight glare, some of the dangerous factors for drivers especially in night time, decrease dramatically and lane markings are enhanced clearly on wet surfaces.

Noise Reduction

Road surfaces are laid with coarse macro-texture, which are in contact with the tire tread. This texture is known to contribute to the noise absorption between the surface and the tire. Many trial sections show lower noise levels on porous asphalt, which may be 6 dB (A) lower than concrete layers [2] or 2 to 6 dB(A) lower than the HRA [3]. According to the Swiss standards, under dry conditions in a 70 dB(A) area by using porous asphalt a noise reduction of 5 dB(A) can be achieved [69].

Swiss experience also indicates an advantage on the high speed traffic lanes in excess of about 80 km/h. Although the noise level of porous asphalt on the lower speed lanes is almost the same as other conventional dense mixes, porous asphalt is still effective in reducing the noise in the frequency range of 1.25 to 2 kHz at 60 km/h [6].

The experience in the Netherlands indicates that on the lower traffic speed lanes less than 70 km, the noise level of porous asphalt is even higher than dense mixes due to its rough macro-texture on the surface. To improve this aspect, 2 layer porous asphalt (Twinlay) was developed [7]. It consists of a bottom layer of the porous asphalt with a coarse single grained aggregate (11/16 mm) and a thin top layer of fine graded porous asphalt (4/8 mm). This double-layer structure can contribute to reduce the traffic noise at any vehicular speed. According to their report, additional advantages of the Twinlay are better clog resistance against dirt and better cleaning properties. Therefore, this unique structure is expected to be introduced in their urban areas on a regular basis to meet the high environmental demand.

Japanese experience reveals that porous asphalt is effective in noise reduction, but that this advantage is gradually lost over the years due to a decrease in mix porosity, especially in snowy areas where tire chains are used [8].

As an example from the USA in Oregon, two types of noise measurements were taken. The first was roadside noise and the second was interior vehicle noise. The results indicated that porous asphalt pavements reduce the noise in the higher-frequency zones. This conclusion is supported mostly from the roadside measurements and not from those taken in the interior of the vehicle, possibly since the higher frequencies are dampened by the vehicle shell. As high-frequency noises have a shorter wavelength, they are more apt to be reflected off the vehicle's thin shell [9].

Improvement in Skid Resistance, Reduction in vehicle rolling resistance

Increasing skid resistance under wet conditions is one of the main reasons for using porous asphalt. Assuming that a rougher wearing course would increase frictional properties. In Oregon friction properties of porous asphalt were compared with dense graded asphalt. The data accumulated indicated that porous asphalt mixes had slightly improved friction properties in dry conditions and a much improved friction properties during rainy conditions when free water was present on the pavement [9].

Skid resistance is a function of macro and micro textures. At high speeds, the contribution of the macro texture is more dominant. In the A38 Burton trial section, 1987, Porous asphalt showed a skid resistance at least as good as that of the HRA [10]. In Japan, it is reported that the skid resistance of porous asphalt was initially the same as conventional non-porous asphalt, but this value increased gradually during the service life, whereas the dense mixes did not show any significant change. In addition, fresh porous asphalt layers may have a reduced skid resistance due to the bitumen film on the aggregates exposed to the surface. It is noteworthy to mention that some Swiss experts recommend not using porous asphalt with aggregate size in excess of 16 mm on wearing courses. According to their experience, the use of larger top size aggregates may provide less skid resistance on wet road surfaces.

Rut-resistance

In Japan, despite its high porosity, a number of trial sections show lower permanent deformation on porous asphalt than other dense mixes. Tighter aggregate skeleton in porous asphalt may contribute to withstand the load under traffic [11].

On the 1987 Burton trial in the UK, the deformation rate of this porous asphalt section in the near side lanes was less than 2 mm/year and 0.5 mm/year on average after 8 years trafficking. This result was evaluated as an acceptable rate in Britain. Although deformation of pavement depends on several conditions, such as climate, traffic intensity and loads, porous asphalt may provide acceptable rut resistance compared to other dense mixes [10].

Disadvantages

Aging and Stripping

Although porous asphalt has many obvious advantages, there are also some disadvantages. One of the most critical factors in the performance of bituminous mixes is the tendency of the binder film on the surface of the aggregate to be continuously exposed to oxygen, sunlight, water etc. This results in binder hardening and a reduction in pavement service life [12]. When bitumen hardens, aggregates can be stripped easily from the asphalt mixes. It is well known that, due to its high porosity, porous asphalt ages much faster than conventional dense mixes. In full-scale road trials in the UK, the results conclude that the life of porous asphalt is ultimately limited by binder hardening with likely failure when its penetration drops below 15 pen [10].

Another potential disadvantage of porous asphalt is the water sensitivity of the mix. Rainwater can penetrate through the porous matrix. Sometimes the water remains in the structure keeping the asphalt in wet condition for a long time. This moisture can cause some extra damage in porous asphalt by stripping the binder film from the aggregate surfaces.

Reduction in Porosity

During service life, the pores tend to be clogged by dirt, dust or other clogging agents. On high speed lanes, tires produce a self-cleaning effect [13]. Thus clogging is more serious on low speed lanes or minor roads. With the loss of pores, the advantages of noise reduction and drainage function will gradually disappear.

This is another serious problem for road maintenance. To overcome this disadvantage many types of cleaning methods, including vacuum vehicles with hydraulic jet water, have been developed to maintain the advantage of porous asphalt long term. However, no conclusion on the optimum type of cleaning method can be recommended. Porosity loss is also caused by secondary traffic compaction, especially on heavy routes.

Shorter Service Life

Due to the above listed disadvantages, the service life of porous asphalt surfaces is shorter than that of dense mix layers. In addition, it depends on several factors such as binder content and type, aggregate gradation, traffic volume and climate. Although previous experiences show an optimistic life expectancy of around 15 years, some maintenance should be necessary within about 5 to 8 years according to the results in many countries. Such maintenance costs for porous asphalt (from cleaning the clogged pores to replacement of those layers, which lost their drainage function) are considered higher than for the conventional asphalt. However, this does not mean that cost-effectiveness of porous asphalt surface is lower than that of other surface mixes. When this issue is discussed, the significant contribution of this pervious layer for social benefits, such as traffic safety and environmental issues, can not be ignored.

Winter Maintenance

Snow and ice removal from porous surfaces requires at least twice the quantity of de-icing salt treatment compared to that of other dense mixes. However, the damage to porous asphalt due to salt is still unclear. Vehicular tire chains, spiked tires and snow ploughing sometimes cause severe damage on the open textured mixes requiring additional repair when the aggregates are stripped from the surface. Swiss standards recommend explicitly that porous asphalt not be used in areas where chains and spiked tires are used [69]. CEN suggests an abrasion test by studded tires to evaluate the chain damage [63]. Japan also applies either a similar test for porous asphalt, which was originally developed for dense mixes in snowy areas, or a decrease in the temperature down to - 20 °C in the Cantabro test [16]. It should be noted that, because of the lower thermal conductivity of the porous asphalt, in winter this surface may colder than dense asphalt [6]. Therefore, on the porous asphalt surface, snow tends to settle earlier and remain longer, also ice forms earlier when the roads are wet [5]. Winter maintenance is discussed further in section 12.

2. POROUS ASPHALT IN SWITZERLAND

Porous asphalt (PA) in Europe has typically air void contents in the order of 20% as opposed to the North American open graded friction courses (OGFC) which typically have a lower air void content of 14%. One square meter of porous asphalt with a thickness of 4cm has a void volume of ca. 9 liters of which 7 liters are communicating voids capable of draining 7 liters of water [18]. Switzerland started using PA in 1979 with mixed results. Based on the survey taken in 2004, nine of the 26 Cantons use PA. Table 2.1 and Appendix 2 show a summary of this survey. The mixed results with PA in Switzerland is on the one hand due to the variety of climate and design practices and on the other hand due to the lack of proper maintenance practices. Canton Vaud in western Switzerland is known as one of the leaders with respect to their promoting and using porous asphalt. As a result of their positive experience, currently, 1/3 of the Vaud motorways are covered with porous asphalt and the use of PA will be extended to most of the motorway surfaces in that Canton up to an altitude of 600m. In addition, there are several bridge trial sections with PA.

According to the responses accumulated through a recent survey and attached in Appendix 2, as of January of 2004, 131 km of Swiss motorways are paved with porous asphalt. Table 2.1 shows the summary of this survey. Figure 2.1 shows the location of PA sections in Switzerland as of 2005.

In 1987, the Institute for Transport Planning and Systems (IVT) of the Swiss Federal Institute of Technology (ETH) received a contract from the Swiss Federal Roads Office (FEDRO, ASTRA), to investigate the long-term behavior of PA in comparison with other pavement types including concrete [6]. This project focused on the acoustic characteristics of porous asphalt as well as durability and maintenance. The survey was executed on different test sections in Canton Zurich for 10 years starting in 1982. The results conclude that the drainage function is gradually decreased during its life, and would be significantly reduced within approximately 5 to 6 years on cantonal roads and within 8 to 10 years on motorways.

A recent study comparing Swiss porous asphalt from Canton Aargau and Japanese standard porous asphalt mix showed that the binder type plays an important role in the performance of porous asphalt [19, 20].

Table 2. 1 Inventory of porous asphalt on National Roads in Switzerland (Status 2004)*D: Inventar des offenporigen Asphalts in der Schweiz (Stand: 2004)**F: Inventaire et situation des asphalte poreux du réseau des routes nationales (état 2004)*

Canton	Road	Location	Length [km]	Designation
Aargau	N1 (M)	Oftringen-Gränichen-Safenwil	13.83	AG1, AG2, AG3
Freiburg	N1 (M)	Séreaz-Payerne	2.5	
Zürich	N1 (M)	Wülflingen, Winterthur	2.0	
Geneva	N1 (M)	Descente lac	1.7	
	N1 (M)	Airport zone -Palexpo	0.6	
Jura	H18 (C)	Soyhières	0.365	
Neuchâtel	N5 (M)	Vaumarcus-Bevaix	3.0	
Uri	N2 (M)	Gotthard Tunnel	9.9	
Valais	N9 (M), A21 (C)	Various locations	26.75	VS6
Vaud	N1 (M), N5 (M), N9 (M)	Various locations	70.4	VD2, VD3, VD4, VD5, VD9, VD10
		Total	131.045	

M=Motorway, C=Cantonal Road (status 2004)

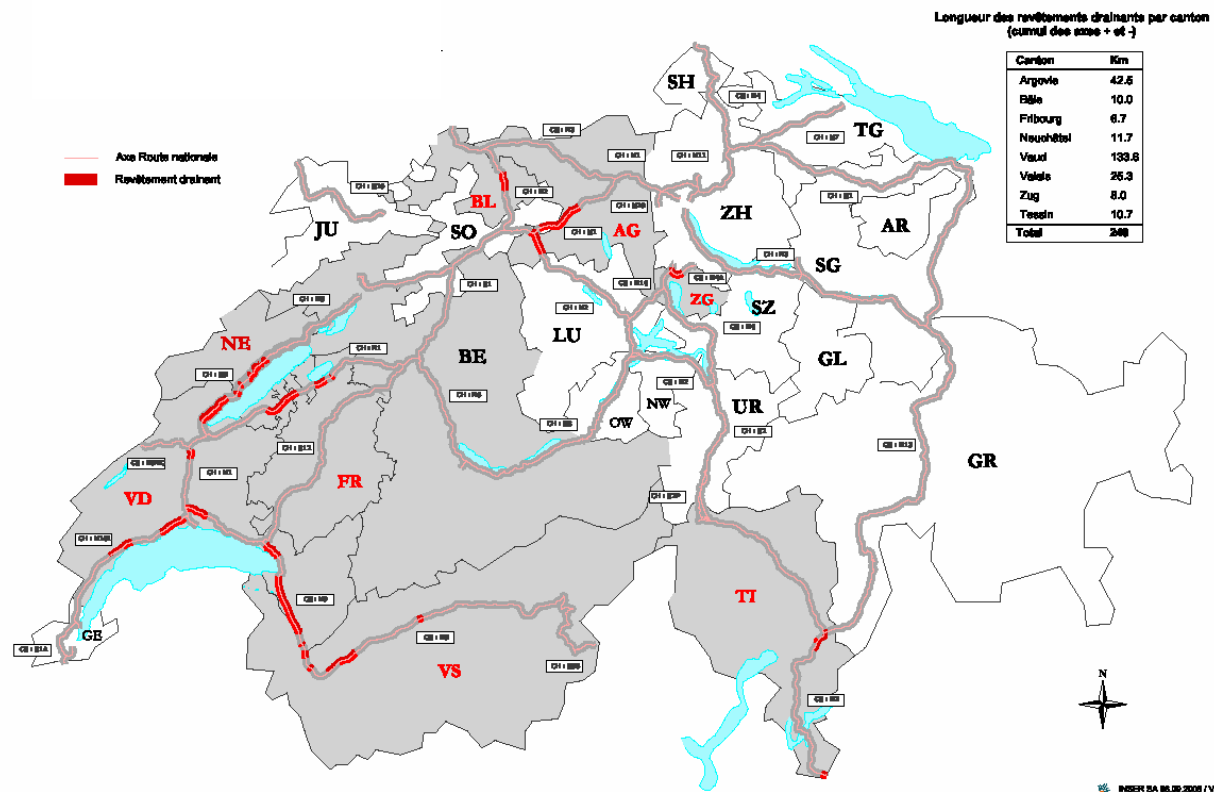


Figure 2. 1 : Porous asphalt in Switzerland in bold red (Status 1.9.2005)

D: Offenporiger Asphalt in der Schweiz in fett rot (Stand 1.9.2005)

F: Revêtements drainants en Suisse en gros rouge (état au 1.9.2005)

2.1. Swiss Standards [SN 640433b]

This research project is based on the Swiss standards [69] valid from 2001 to 2005 and contains requirements for surface course, base course and drainage course and lists volumetric requirements such as mineral gradation and void content on Marshall specimens as well as permeability requirements in accordance to the Yverdon [73] method. However in contrast to the standards for dense courses no requirements on mechanical behavior such as water sensitivity or on acoustic absorption factors are listed. As porous asphalt is used increasingly more often in Switzerland such requirements are deemed necessary for the construction of durable and safe porous pavements. As the pavements discussed in this report were constructed in compliance with the current Swiss standards a short summary of the important requirements are listed below.

The thickness of the PA layers and max aggregate size should be in accordance to Table 2. 2 and the gradation and binder content requirements are listed in Table 2. 3.

Table 2. 2 : Thickness requirements.*D: Anforderungen an die Schichtdicke**F: Epaisseur nominale fonction des types de PA*

	Mix type	Layer thickness [mm]
Surface course	DRA6 for sport arenas	20...30
	DRA11	30...50
Base course (T)	DRAT	40...80
	DRAT	60...150
	DRAT	80...200

DRA6 indicates max aggregate size is 6mm. T- base course, S-drainage course

Table 2. 3 Gradation requirements and binder content.*D: Anforderungen an Korngrösseverteilung und Bindemittelgehalt**F: Fuseau des valeurs nominales de la granularité et teneur en liant*

Sieve Size	Mix type				
	Surface course % Passing		Base course % Passing		
	DRA6	DRA11	DRAT16	DRAT22	DRAT32
45.0					...100
31.5				...100	90...100
22.4			...100	90...100	30...65
16.0		...100	90...100	25...60	20...35
11.2	...100	90...100	20...50	15...30	15...28
5.6	90...100	15...40	10...25	10...20	8...18
2.8	15...40	8...20	7...17	6...15	5...14
0.5	4...10	4...10	4...10	4...10	4...10
0.09	3...5	3...5	3...5	3...5	3...5
Binder content	5.0...6.0	4.5...5.5	(3.5) 4.0...5.0	(3.0) 3.5...4.5	(2.5) 3.0...4.0

Note: DRA6 indicates max aggregate size is 6mm. T- base course

The minerals used in PA should fulfill requirements of SN 670 130 [74], with a PSV of at least 50. Only polymer modified binder should be used. On surfaces that do not experience traffic such as drainage surfaces or sport arenas, un modified binder may be used. The required void content of specimen compacted using the Marshall hammer is listed in Table 2. 4.

Table 2. 4 : Required void content for Marshall specimen*D: Anforderungen an die Verdichtung der Marshall Prüfkörper**F: Teneur en vides Marshall requise*

	Void content [%]	Communicating voids [%]
Surface course	≥22	≥15
Base course	≥22	≥15
Drainage course	≥17	≥11

2.2. European Standard [EN13108-7]

Currently the European Standards are in effect for Switzerland [63]. In addition to volumetric requirements there are requirements for mechanical behavior such as water sensitivity and particle loss and horizontal and vertical permeability and binder drainage. The European standards are to be used in combination with a national annex. The only mechanical property specified in the current Swiss annex to this standard, SN 640 431-7NA [71], specifies an Indirect Tensile Strength Ratio (ITSR) value of ≥ 70 for the water sensitivity test.

In the Swiss annex, provisions are made for porous asphalt layers with max aggregate size of 8mm which could be used in Switzerland in the future.

3. STATE OF THE ART IN RESEARCH PERTAINING TO POROUS ASPHALT

The porous nature of PA can be restrictive in the use of many conventional test methods. Some test equipments lend themselves to be more appropriate for this material.

3.1. Research in Switzerland

An ongoing project in Switzerland by Angst et al [24] is investigating the use of quiet pavements for urban areas. To this end, in summer 2004, 10 pavement types were built in various urban locations in Switzerland. Pavement tests as well as acoustic measurements were made on all test sections at regular intervals. Following the current practice to reduce noise, pavements with fine aggregates as well as PA were used including a twin-lay PA. In addition, in one test section porous minerals were used to determine this effect on noise reduction. The highest reduction in acoustic emission, up to 7 dB(A) was measured on the twin-lay PA. An initial reduction of 5.5 and 7 dB(A) was obtained as a result of a combination of fine aggregates, concave surface absorbing the noise and the dual layer. In terms of noise impact this corresponds to a reduction of traffic to 25% which is of great benefit to the community.

Figure 3. 1 shows comparative noise reduction properties of the test sections in [24]. The effect on the population can be represented as a reduction in traffic which is shown on the right; with 0 reduction corresponding to 100% traffic, 3.0 dB(A) to 50% and 6.0 dB(A) to 25%. In general the best results were achieved using a double layer porous asphalt, twin-lay (PA4+8 and PA 8+16) followed by the thin layer with fine aggregates (SPA4 and MR4) with a noise reduction of 4 to 5dB(A).

A cooperative research program by Empa and Japan Highway public corporation [19, 20] demonstrated the effect of an improved gradation for porous asphalt known as the "Packed Theory" originally developed in the UK [26]. Different tests concerning both durability and functional properties of porous asphalt were carried out. The packed theory demonstrated better resistance against over-compaction than specimen produced using empirical methods. Although the different mixes could be distinguished before aging, after aging the mixes could not be distinguished.

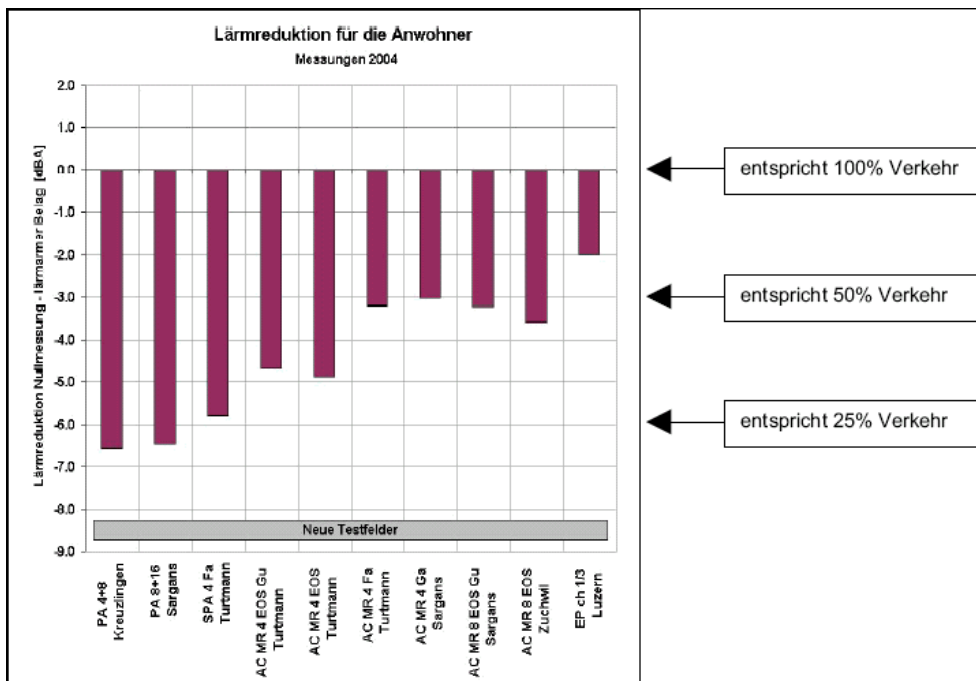


Figure 3. 1: Comparative noise reduction properties of the test sections in [28]. Porous asphalt twin-lay are indicated by PA4+8 and PA 8+16. With 0 reduction corresponding to 100% traffic, 3.0 dB(A) to 50% and 6.0 to 25% [24]

D: Vergleichende Lärmminderung der Teststrecken in [28]. Zweischichtiger PA ist mit PA4+8 und PA 8+16 andeutet. Die Reduktion 0 entspricht 100%, 3.0 dB(A) 50% und 6.0 dB(A) noch 25% des Verkehrs [28]

F: Comparaison des réductions du niveau de bruit de différentes sections tests [28]. L'asphalte poreux bicouches est indiqué par PA4+8 et PA 8+16. La valeur de référence de 0 dB(A) correspond à 100% de trafic, une diminution de 3 dB(A) à 50% et de 6 dB(A) à 25% [28]

The results of tests conducted at Empa and other research institutions [19, 20] indicate that the LCPC French wheel tracking machine as used for conventional mixes is not suited for porous asphalt. Furthermore, reports from various cantons indicate that rutting is not a primary problem for porous asphalt [Appendix 2].

The experience at Empa [20] shows that the Co-axial Shear Test (CAST) developed at Empa is an important and diverse tool for the experimental determination of the Modulus. Experiments have been carried out on dry, wet and freeze-thawed sample [28].

The environmental protection law in Switzerland requires improvement in noise properties on the roads [33]. In this cooperative project funded by the Swiss roads authority, ASTRA and Swiss office for the environment BAFU various types of bituminous pavement materials were evaluated and recommendations were made as to their suitability for noise emission reduction. For the reduction on noise a porous asphalt pavement is recommended outside the cities, under 600m elevation and under 80km/h speed.

Numerous studies have shown that porous asphalt has significant influence on the reflexive properties of noise. From a physical point of view, it is now well known that acoustical waves are scattered on the porous surface and resulting waves propagate inside the open porous network and are attenuated due to the viscous behavior of air. Damping leads to noise reduction the level of which depends mainly on the frequency spectrum of the emitted noise, the direction of propagation and the characteristics of the porous network (pore size, air permeability and tortuosity). The main point is related to the size and the continuity of the pore network.

LAVOC has performed in situ noise measurements for different kinds of vehicles and conditions of driving on recently built highways with porous wearing courses (Ashish Bhaskar et al)

In situ performance of various test sections in Switzerland is discussed in detail in [18] and [25]. Reduction in noise through the use of porous asphalt vs. dense graded asphalt at various locations with an average reduction of 6 dB(A) is reported in Table 3.1. Long-term development of noise reduction was recorded for two sites as shown in Figure 3. 2 , indicating that at these sites the noise reduction capability of porous asphalt was maintained even after 9 years.

Table 3. 1 : Noise reduction

D:Lärmminderung

F: Réduction de bruit

Installation date	Location	Reduction in noise after the installation of porous asphalt [dB(A)]
1991	Pertit	4.1 ... 6.2
1993	Morges	5.4 ... 8.6
1999	Lonay	6.2 ... 8.4
1999	Bex	4.5 ... 6.0

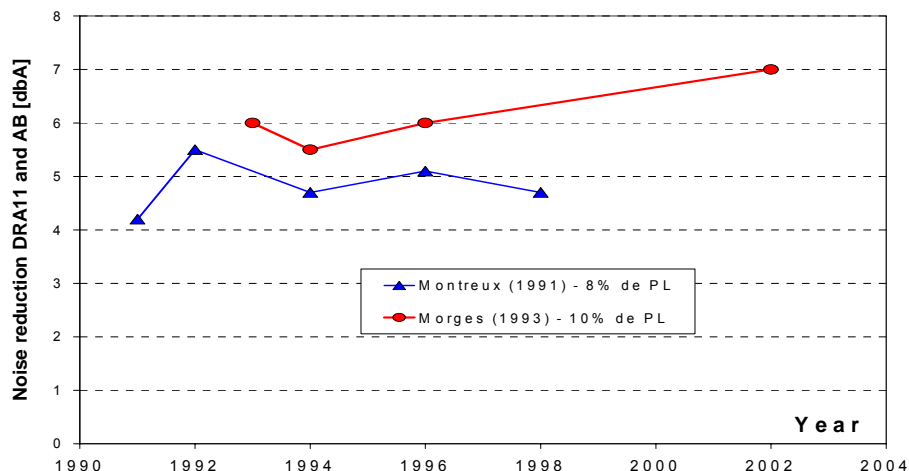


Figure 3. 2 Noise reduction of porous asphalt (Morges) in comparison to dense graded asphalt (Montreux)

D: Lärmminderung für offenporigen Asphalt (Morges) in Vergleich zu dichtem Asphalt (Montreux)
F: Diminution du niveau de bruit d'un asphalte poreux (Morges) par comparaison avec un enrobé dense (Montreux)

3.2. International Research

The evolution of physical parameters after exposure to traffic was studied by Losa et al [21]. The parameters considered included: percentage of communicating air voids and air flow resistance, which is the reciprocal of permeability. Spain has been using porous asphalt since 1980 with good results. The procedure used in Spain is based on the optimization of two fundamental properties: Particle loss using the Cantabro test and permeability using the in situ Laboratorio de Caminos de Santander (LCS) permeameter [14]. It is recommended that cohesion and bonding characteristics of the mix be closely scrutinized as inadequate cohesion and bonding is the ultimate cause of raveling of the pavement. Marshall Stability is assessed as not being appropriate for open graded mixes. Furthermore, high dispersion rate and insufficient sensitivity to mix components were noted in the wheel tracking and indirect tensile tests. As a result, the Cantabrian

test for abrasion loss was developed which reproduces the in situ mechanism of deterioration in the laboratory.

The prediction of material behavior through the stiffness modulus has become an integral part in international research, such as the AASHTO Mechanistic Empirical Design Guide 2002 [23].

Noise reduction using porous asphalt is reported to be about 3.0 dB(A) at highway speeds which is a 50% reduction in noise pressure. Unfortunately the clogging of pores leads to degradation of this very important property over time. A recent study in Italy attempts to describe this degradation with traffic of both physical parameters and acoustical properties [21]. The acoustical performance of the pavement was evaluated using the acoustical absorption factor. Standard procedures exist for both in situ [64] and laboratory [65] measurements. It was shown that in situ and laboratory results were in agreement, with the double layer material showing better results after a certain number of vehicle passes. In addition the evolution of physical parameters after exposure to traffic was studied. The parameters considered included: percentage of communicating air voids and air flow resistance, which is the reciprocal of permeability and their influence on acoustical properties.

Fiber stabilizers are used to prevent drain down during construction. Drain down or separation of binder from the coarse aggregates can occur during the storage and transportation process of the mix. Without a fiber stabilizer, mixtures can be produced that are binder rich with no air voids in some parts and with little binder and high air voids in other parts which are susceptible to raveling.

Polymer modified binders improve the drain down susceptibility of porous asphalt. It is reported that mixtures containing modified and non-modified binders densify at the same rate.

4. OBJECTIVE AND PROGRAM OF INVESTIGATION

Figure 4.1 gives an overview of the various activities in this project. After the initial survey of the literature, appropriate mechanical tests for porous asphalt were chosen. At the same time a survey of current experience with porous asphalt in Switzerland was conducted. Tests were performed on specimen produced from laboratory prepared mixes and bore cores taken from selected pavements, chosen based on the feedback from various cantons. The behavior of these selected materials was determined using a numerical model. Laboratory tests allowed the comparison of bore core performance with laboratory prepared specimens and comparison with field performance. Based on the results, two mixes were optimized and recommendations for mechanical tests appropriate for PA were made.

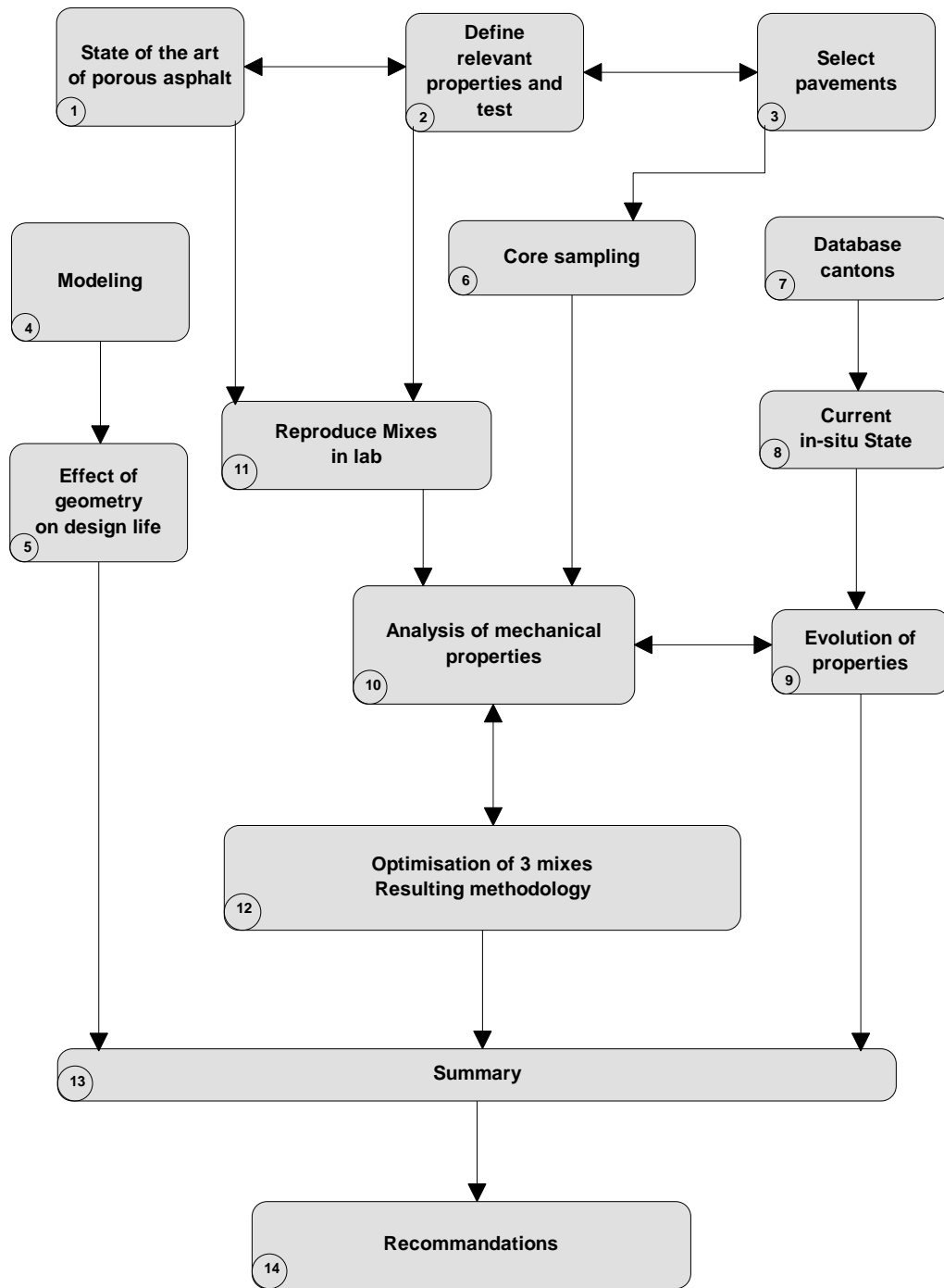


Figure 4. 1: Structure of the research program

D. Ablauf des Forschungprogramms

F. Structure du programme de recherche

5. PERFORMANCE SURVEY ON POROUS ASPHALT IN SWITZERLAND

A questionnaire was sent to all 26 cantons regarding their use and experience with PA. Table 2.1 shows a summary with location and length of the porous asphalt pavements in Switzerland as reported by the cantons. A more detailed table is included in Appendix 2. As of 2004 only 9 cantons had experience with PA. The inventory shows a total of 131km of road paved with PA with 97km (69%) in the two cantons of Valais and Vaud. Depending on the individual cantons there is considerable variety in the Swiss motorways paved with PA in terms of structure, loading conditions, application and mix design (e.g. binder type). Table 6.5 and Table 6.6 show typical results for different PA pavement sections. The performance survey indicated also that the in situ experience varied. For example in canton Vaud, the road section labeled VD5 was high performing whereas in canton Aargau, the section labeled AG2 was low performing and already rehabilitated. Chapter 7 presents some results of the in situ inspection of selected sections.

6. MATERIAL SELECTION

Based on performance feedback from the cantons listed in Chapter 7 and Appendix 2, pavements from motorways have been selected for further study in three stages. This further study included in situ inspection as well as laboratory tests on cores and particular laboratory produced specimen and field tests. In stage I, a number of existing pavements from Swiss motorways were chosen for further investigation. The criteria for choosing these pavements were age, performance and binder type. In stage II some of the mixes in stage I were reproduced in the laboratory. In stage III, based on results of experiments with materials from stages I and II, mixes were optimized. Table 6.1, Table 6.2 and Table 6.3 summarize the materials in Stages I, II and III. Table 6.1, Table 6.2 and Table 6.3 list the material parameters in detail.

Table 6. 1: Stage I selected sections for coring

D : Etappe I- Wahl der Strecken für Bohrkernentnahmen

F : Etape I - Carottes des planches sélectionnées

Criteria	Source	Material Designation	Comments
Distress	Aargau	AG2	Original aged
		AG3	Replaced, new Contains calcium hydroxide
	Valais	VS6	
Binder	Vaud, N9	VD4	Styrelf 13/80
	Vaud, 1999, N9	VD5	Bitumen+Rubber
	Vaud, 1993, N1GL	VD3	Practiplast
Age	Vaud, 1991, N9	VD2	Colflex N
Twin layer	Vaud	VD10	Styrelf 13/80

Table 6. 2: Stage II selected laboratory prepared mixes*D: Etappe II- Auswahl von im Labor herzustellendem Mischgut**F: Etape II - Reconstitution en laboratoire des mélanges sélectionnés*

Criteria	Source	Material Designation	Comments
Distress	Aargau	AG1	Original mix (AG2 aged)
		AG4	Replaced new mix Contains calcium Hydroxide (AG3)
Binder	Vaud, N9	VD7	Choex+13/80 Styrelf (VD4)
	Vaud, 1999, N9	VD8	Choex + CTS special bitumen + Rubber (VD5)

Table 6. 3: Stage III optimization of selected mixes*D: Etappe III- Optimierung ausgewählten Mischgutes**F: Etape III - Optimisation des mélanges sélectionnés*

Optimization Criteria	Source	Material Designation	Comments
Distress Polymer modified binder to improve mech prop. cohesivity	Aargau	AG5	AG1 minerals+Styrelf
Water sensitivity	Aargau	AG4	Lab prepared AG3 Contains calcium Hydroxide
Binder+ Gradation Cantabro, in situ performance	Vaud	VD9	VD5 gradation changed with more filler and sand Choex + Bitumen + Rubber

Brief description of cores obtained from the pavements in service (AG2, AG3, VD2, VD3, VD4, VD5, VS6, VD9 VD10)

AG2

These are the original cores located in Offtringen in Canton Aargau before the pavement was rehabilitated in 2004. The cores were taken under fine weather with temperature of ca 20°C at the 74.638 km of the fast lane.

AG3

These are the cores of the pavement located in Offtringen in Canton Aargau that replaced AG2 in 2004 due to excessive raveling of that pavement.

VD2

As shown in Table 6. 1 and Appendix 2, this pavement located in canton Vaud is one of the oldest sections in Switzerland and therefore chosen for this investigation.

VD3

These cores are from the pavement section at km 61.35 to 54.95 of the A9 motorway located in canton Vaud. They were chosen due to their binder type that is polymer modified.

VD4

These cores are from the pavement section at km 0.5 to 8.2 of the A9 motorway located in canton Vaud. They were chosen due to their binder type that is polymer modified.

VD5

VD5 cores are from Canton Vaud Motorway A9 Lot 52/807 section Aigle/Bex south. This mix was field optimized using traditional polymer modified binders. As a rubber additive is used for this mix, one percent more binder was added.

VS6

This pavement section located in canton Valais had shown premature loss of permeability and therefore chosen for this project.

VD10

VD10 denotes the twinlay PA cores from Canton Vaud. The use of twinlays is still at an experimental stage in Switzerland. However the canton has been satisfied with the performance of this section which had to be replaced for other purposes not related to its performance. The top layer consists of 8mm max aggregate size, 24.1% total air voids, 17% communicating air voids and 4.77 vol % binder content. Whereas the lower layer has a 22mm max aggregate size, 14.8% total air voids, 12% communicating air voids and 4.8 vol % binder content. The two layers considered together have total geometric voids of 17.6% and communicating voids of 12%. The Styrelf 13/80 polymer modified binder was used in both cases. It was observed that the bottom layer has in many cases a SAMI layer that has filled the voids in the lower layer so that in some cases the void rich layer is only 20mm deep. As the top layer is only ca 22mm and the second layer ca 55mm (average of three cores), it was decided to test the two layers as a system. All specimens consist of a dual layer porous asphalt. Figure 6. 1 shows various observations made on these cores. Evaluation of the results of the tests presented in Chapter 9 should bear in mind the larger in homogeneity of these cores and therefore more scatter is expected. It should be noted that the cross sections in Figure 6. 1 are cut at ca 60mm from the top so the observed filled voids are located about the middle toward the bottom of the lower layer and not at the border of the 2nd and 3rd layers.

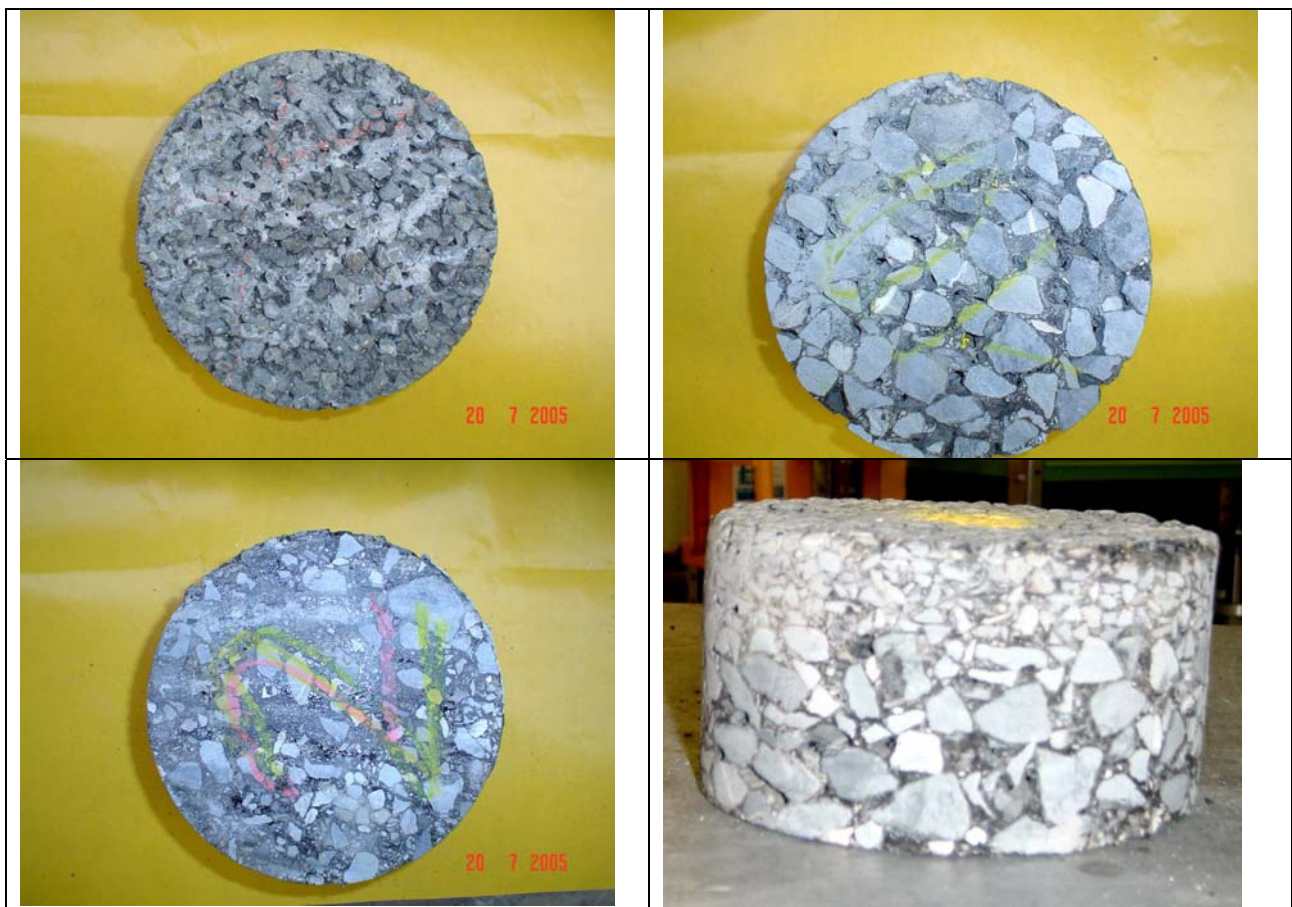


Figure 6. 1: Top view of twinlayer VD10, top layer (top left), bottom layer with pores (top right), bottom layer with pores filled with SAMI (bottom left), Twinlayer (Bottom right)

D: Obere Seite des oberen Schicht des zweischichtigen Aufbaus VD10 (oben links), untere Seite der unteren Schicht (oben, rechts), untere Schicht, Poren mit SAMI gefüllt (unten links), ganzer Bohrkern (unten rechts)

F : Vue de dessus du bicouches VD10, couche supérieure (haut, gauche); couche inférieure (haut, droite); couche inférieure avec pores colmatés par le SAMI (bas, gauche); bicouches (bas, droite)

Brief description of the laboratory produced mixes and mixes from the job site (AG1, AG4, VD7, VD8)

AG1

This is the mix corresponding to AG2 which was received from the job site at canton Aargau and stored in a cool location at Empa. It is assumed that no aging had taken place prior to the fabrication of the specimen.

AG4

This is the laboratory produced mix of AG3. The mix gradation was based on the average of values reported by the company Consultest on the mix at the km 74.600 location and the design values received from Canton Aargau. This mix has a 2% calcium hydroxide additive based on the mass of the minerals. That is the filler was reduced by 2% calcium hydroxide. AG3 gradation, which is based on the cores, varied slightly with the Consultest results so it was not used to produce this mix.

AG4 was in addition considered as one of the optimized mixes as it contains calcium hydroxide. On the job site in Canton Aargau the lanes in direction Bern-Zürich contain calcium hydroxide whereas the lanes Zürich-Bern do not. This way the advantages of using calcium hydroxide over the years can be studied. Calcium hydroxide is added to the mix to improve the bond between the binder and aggregates. It is easy to add to the asphalt mixture as it can be added like a filler and it is economical.

VD7

VD7 is the laboratory prepared mix of VD4 that consists of maximum 11mm Famsa-Choex minerals and 4.8% Styreelf 13/80 polymer modified binder. Two mixes were prepared at LAVOC and Empa. The laboratory produced mix at Empa reproduces the design gradation as close as possible whereas the laboratory produced mix at LAVOC reproduces the average gradation obtained from in situ analysis after construction and before traffic and the lab results.

The design void content is assumed to be 23 vol % which is what is obtained by Marshall compaction (2X25 blows). The void content of VD4 cores are on the average 22.8%. This current void content is influenced by the fact that the cores are already exposed to traffic and post compaction as well as aging and stripping of the binder have taken place. The Empa produced mixes were not aged whereas the LAVOC produced mixes were aged.

VD8

VD8 is the laboratory prepared mix of VD5 that consists of maximum 11mm Famsa-Choex minerals and 6% CTS binder with rubber additive. Two mixes were prepared at LAVOC and Empa. The laboratory produced mix at Empa reproduces the design gradation as close as possible whereas the laboratory produced mix at LAVOC reproduces the average gradation obtained from in situ analysis after construction and before traffic and the lab results. The extracted binder content in this case of 5.35% is lower than the design values (ca 6%) because rubber being insoluble will not show up in the extraction process. The design information indicates that the mix was field optimized for a traditional polymer modified binder that led to 4.9% binder content. The binder content was increased by ca 1% to account for the rubber therefore reducing the resulting void content. It was attempted to reproduce a void content of 17.2% which is what is obtained by the Marshall compactor (2X25 blows). The void content of the corresponding cores (VD5) are on the average 15.3%. This current void content is influenced on the one hand by the fact that the cores are already exposed to traffic and post compaction on the other hand aging and stripping of the binder. The Empa produced mixes were not aged whereas the LAVOC produced mixes were aged.

Brief description of the optimized laboratory produced mixes (AG3, AG4, AG5, VD9)

Four mixes were chosen for the purpose of optimization at stage III. For a detailed description of AG4 see above.

AG5

This is one of the optimized mixes produced in the laboratory. The premature deterioration of AG1 (AG2 cores) was attributed to the lack of polymer modified binder. To study this point closely it was decided to extract the binder from AG1 and replace it with the polymer modified binder Styreelf resulting in AG5.

VD9

VD9 is the optimized version of VD5 with less filler and sand using Choex with polymer modified bitumen and rubber additive. Satisfactory field performance led to the choice of VD5 for optimization. Keeping the gradation based on VD5 as shown in Table 6. 4, the binder content was varied to produce variations A1, A2, A3 and A4. As seen, in order to achieve target porosity of ca 22% and communicating voids to >15% based on SN640 433b, the binder content had to be lowered in variations A3 and A4. As a result, in a second step the gradation was changed to B, with B2

resulting in the desired void content of 22.1 V%, communicating voids of 16.5 V % and binder content of 6.2 vol % as shown in Table 6. 4.

Table 6. 4: Optimization process of VD9 based on VD5

D: Optimierungs-Prozess für VD9 basierend auf VD5

F: Procédé d'optimisation de VD9 sur la base de VD5

	DRA11 - Aggregates FAMSA/Choëx + rubber binder CTS								
	Sieve curve design A Mix design VD5					Sieve curve design B Modified mix design VD5			
	VD5 Mix design	A2	A1	A3	A4	B2 Selected mix	B1	B3	B4
Sieves [mm]	Passing [%]								
16	100	100	100	100	100	100	100	100	100
11.2	97	97	97	97	97	97	97	97	97
8	52	52	52	52	52	52	52	52	52
5.6	20	20	20	20	20	17	17	17	17
4	15	15	15	15	15	13	13	13	13
2.8	13	13	13	13	13	10	10	10	10
2	11	11	11	11	11	8.5	8.5	8.5	8.5
1	8	8	8	8	8	7	7	7	7
0.5	7	7	7	7	7	6	6	6	6
0.09	4.8	4.8	4.8	4.8	4.8	3.5	3.5	3.5	3.5
Binder content theoretical	6	6.2	5.9	5.6	5.3	6.2	5.9	5.6	5.3
B/A theoretical	6.38	6.61	6.27	5.93	5.60	6.61	6.27	5.93	5.60
Rubber content [% binder]	15.0								
Real density aggregates [g/cm ³]	2.71	2.71	2.71	2.71	2.71	2.71	2.71	2.71	2.71
Binder deal density [g/cm ³]	1.04	1.04	1.04	1.04	1.04	1.04	1.04	1.04	1.04
Mix deal density [g/cm ³]	2.472	2.465	2.475	2.486	2.497	2.465	2.475	2.486	2.497
Marshall voids 2 x 50 blows	22	19.2	19.9	21.9	22.2	22.1	22	23.5	23.3
Connected voids 2 x 50 blows	>15	12.9	14.8	16	17	16.5	17	18.4	18.1
Marshall voids 2 x 25 blows	-	-	-	-	-	-	-	-	-
PCG voids 40 gyrations	-	23.3	23.5	23.9	24.7	25.4	25.7	27.4	27.3

Table 6.5 and Table 6.6 show gradation, air void content, binder type, binder content (B/A), type of additive and adhesive agent as well as years in service and selection criteria. The selected sections represent a wide variety of PA in Switzerland. As seen in this Table, binder content varies from 4.5 % to 6.2 % and air void content from 14.8% to 26.1 %. Trinidad natural asphalt (used in AG1 and AG2) is no longer used in Switzerland for PA. Note that AG1 is the mix from the AG2 job site and VD9 is the laboratory produced and optimized mix of VD5. The optimized VD9 was also installed in 2004.

Table 6. 5: gradation, air void content, binder type and binder content of cores (Pmb stands for polymer modified binder)

D: Korgrößenverteilung, Hohlräumgehalt, Bindemitteltyp und -gehalt für Bohrkerne (PmB bezeichnet polymermodifiziertes Bindemittel)

F: Caractéristiques des carottes prélevées, granularité, teneur en vides, teneur en liant et type de liant (PmB = liant modifié aux polymères)

Designation	VD 2	VD 3	VD 4	VD 5	VS 6	AG2	AG3	VD10 Twin layer	VD 9
Type SN 640433b	DRA11	DRA11	DRA11	DRA11	DRA11	DRA11	DRA11	DRA8 / DRA22	DRA11
Binder Type	PmB Colflex N	PmB Prac-tiplast M40	PmB Styrelf 13/80	PmB CTS+ Rubber additive	PmB Styrelf 13/80	B 55/70S + Trinidad NAF 501	PmB E 70/100 + calcium hydrox-ide	PmB Styrelf 13/80	PmB CTS+ Rubber additive
Sieve Size [mm]									
% Passing (by Mass)									
31.5	-	-	-	-	-	-	-	100	-
22.4	-	-	-	-	-	-	-	95	-
16	100	100	100	100	100	100	100	60	100
11.2	98	95	95	97	98	98	90	100	26
8	65	65	49	52	67	60	61	95	21
5.6	25	25	20	20	28	16	30	35	16
4	17	17	15	15	17	13	19	22	14
2.8	13	13	13	13	11	12	15	15	12
2	10	10	11	11	9	11	13	13	10
1	7	7	7	8	7	8	9	10	7
0.5	6	6	6	7	5.5	7	7	8	6
0.09	5	4	4.8	4.8	3.5	4.8	4	4.5	4
Binder [% by wght. of total mix]	4.8	4.8	4.8	6.0	4.5	4.8 + 1.8 additive	5.95	5.0	4.3
Voids cores [% by vol.]	23.3	23.4	22.8	16	20.3	26.1	18.6	24.1	14.8
Years in Service (constr date)	13 (1991)	12 (1992)	7 (1997)	6 (1998)	5 (1999)	5 (1999)	0 (2004)	4 (2000)	0 (2004)
Selection Criteria	Age	Binder type	Binder type	Binder type+ Additive	Dis-tress	Distress	Distress	Twinlay	Binder type+ Additive

Table 6. 6: Gradation, binder type and binder content of laboratory compacted mixes for stage II selected laboratory prepared mixes and stage III optimization of selected mixes

D: Korngrößenverteilung, Hohlraumgehalt, Bindemitteltyp und -gehalt für laborhergestellte (Phase II) und optimierte Prüfkörper (Phase III)

F: Caractéristiques des mélanges reconstitués en laboratoire (phase II) et des mélanges optimisés (phase III), granularité, teneur en vides, teneur en liant et type de liant.

Stage	II selected laboratory prepared mixes					III optimization of selected mixes		
	AG1	AG 4	VD 7	VD 8	AG 5	AG 4	VD 9	
Design- nation	AG1	AG 4	VD 7	VD 8	AG 5	AG 4	VD 9	
Type SN 640433b	DRA11	DRA11	DRA11	DRA11	DRA11	DRA11	DRA11	
Binder Type	B 55/70S + Trinidad NAF 501	PmB E 70/100 + calcium hydroxide	PmB Styrelf 13/80	PmB CTS+ Rubber additive	PmB Styrelf 13/80	PmB E 70/100 + calcium hydroxide	PmB CTS+ Rubber additive	
Sieve Size [mm]	% Passing (by Mass)							
Lab.	LAVOC Empa	LAVOC Empa	L	E	L	E	LAVOC Empa	LAVOC Empa
31.5								
22.4	-	-	-	-	-	-	-	-
16	100	100	100	100	100	100	100	100
11.2	98	92	95.6	92	97	94	93.3	92.1
8	60	58	56.5	58	62.8	65	58.3	58.0
5.6	16	30	28.4	25	36.4	31	24.1	30.2
4	13	16	18.5	15	24	19	15.9	15.9
2.8	12	13	15.5	12	19.7	13	14	12.8
2	11	11	13.1	10	16.6	12	11.9	11.2
1	8	9	9.8	9	12.7	9	9.2	8.8
0.5	7	7	8.1	8	9.9	8	7.7	7.4
0.09	4.8	5	5.6	7	6	6	5.4	3.5
Binder [% by wght. of total mix]	4.8 + 1.8 additive	4.51	4.63	4.8	6	5.33	4.88	4.51
Voids content [% by vol.]	21	24.8	22.2	21.8	15	19.5	21	24.1
Comments	Original mix (AG2 aged)	Replaced new mix Contains calcium Hydroxide (AG3)	Choëx minerals VD4	Choëx minerals VD5	AG1 minerals	Lab pre- pared AG3 Contains calcium Hy- droxide	Lab mix optimized VD5	

(PmB stands for polymer modified binder), E= Empa, L=LAVOC,

7. FIELD EVALUATION OF SELECTED PAVEMENTS

Before coring the selected sections listed in Table 7. 1, a visual inspection according to the Swiss standard SN 640 925b [74] was carried out. To this end, the surface degradation characteristic I_1 was assessed by inspection. The index I_1 combines degradation in terms of surface distress (polishing, bleeding), pavement degradations (wear, loss of aggregate, cracks of joints, cracking) and pavement strain (rutting). The overall state is determined as a function of the surface area A_i and severity of degeneration S_i leading to the total value $M_i = A_i \cdot S_i$. From M_i and a weighing factor G_i , a global weighted index I_1 is deduced with a rating scale which is divided in intervals of good (0 and 1), medium (1 to 2), sufficient (2 to 3), critical (3 to 4) and bad (4 to 5). Table 7. 1 summarizes the results indicating that the state of the inspected sections varied between good and sufficient Figure 7. 1 and Figure 7. 2 show the significant deterioration of AG2 and the recently paved AG3.

Table 7. 1: Summary of surface inspections

D: Zusammenfassung der Zustandserhebung

F: Inventaire des tronçons d'asphalte poreux recensés et sélectionnés

Material Designation	Overall rating Index I_1	State	Remarks
VD2	3	Sufficient to critical	significant polished aggregates and loss-no structural degradation
VD3	1.4	Medium	significant aggregate loss, minor rutting
VD4	2	Medium to sufficient	medium aggregate loss
VD5	2.6	Sufficient	significant polished aggregates and loss
VS6	1.6	Medium	
AG2	2.7	Sufficient	significant aggregate loss
AG3	-	-	new pavement- not investigated
VD10	1.4	Medium	minor aggregate loss minor rutting



Figure 7. 1: Cross section of the new porous asphalt core from canton Aargau AG3

D: Schnitt durch Bohrkern aus neuem PA, Aargau, AG3

F: Coupe de carotte du nouveau PA, Aarau, AG3



Figure 7. 2: Cross section of the old porous asphalt core from canton Aargau AG2

D: Schnitt durch Bohrkern aus altem PA, Aargau, AG2

F: Coupe de carotte de l'ancien PA, Aarau, AG2

8. EXPERIMENTAL PROGRAM

Table 8. 1 lists the tests that were chosen based on the literature review in Chapter 3 in order to determine the fundamental properties of PA. A summary of the literature review and reasons for choosing the following experimental procedures are further listed in Appendix 1. Detail experimental procedures are in chapters 9.

Table 8. 1: Test program

D: Prüfprogramm

F: Programme d'essais

Property	Test	Comment	Specimen Type	Lab
Stiffness	2-point bending§	good repeatability	Trapezoidal Lab/core	L
	CAST (Dry)	Specimen production Simulates road well -10 to 20	150 Ømm Lab/core	E
Water sensitivity	Cantabro (wet) §	Not in EN anymore Cond. 70h @ 40°C	100 Ømm 2x25	L
	CAST (wet/Dry)	Specimen production Fatigue cycles Simulates road well 25 to 30	150 Ømm Lab/core	E
	Indirect tension	25°C	150 Ømm	E
Particle Loss Cohesion, Bonding	Cantabro (Dry) §	Sensitive to variations of components in the mix like binder. Good repeatability.	100 Ømm 2x25	L
Low Temp Behavior	CAST (Freeze-thaw cycles)	G* after ea. Cycle -10 to 5	150 Ømm Lab/core	E
	Cantabro§	Freeze/Thaw cycles	100 Ømm 2x25	L
	Direct Tension	Low Temp crack formation	100x60x30	L
	Indirect tension	Consider diff. temp; 5°C	150 Ømm	E
Permeability (Lab)	Permeability prEN 12697-19			L
Permeability (In situ)	Per SN 640 430a			Canton VD, AG
Permanent Def.	Compatibility § Gyratory	Shows resistance to compaction When reaching interlock.	Gyratory	E
Compaction	Gyratory	Reproducible but does not represent compaction on the road	Gyratory	E+L
	Wheeltracking	Best represent compaction on the road, initial trials only	Wheel Tracking	E+L
Void content	geometric	Good repeatability		E+L
Aging	STOA	LAVOC Method		E+L

§=Test performed on specimen produced from lab prepared mix only, Lab= Lab prepared spec., Core= Field cored spec. L=LAVOC, E=Empa, STOA= short term oven aging

9. EXPERIMENTAL PROCEDURES

9.1. *Laboratory Aging of Mix*

It was shown by Kliewer et al [29] and data from other SHRP contractors that aging of the mixture depends on both the asphalt and the aggregate. It was also shown that aging and subsequent testing of asphalt alone is not a good predictor of how a mixture will behave due to the effect of the asphalt-aggregate interaction. As a result, in a previous study at Empa [7] and in this investigation the mix was aged as opposed to the binder.

It was shown also that aging of the mix had a different effect on mechanical properties of different mixes as seen in the results obtained from CAST [20].

As of 2005, no European standard aging procedure existed. However two aging processes are defined by AASHTO: Short term oven aging (STOA) intended to simulate the pre-compaction phase of the construction phase, and long term oven aging (LTOA) intended to simulate aging that occurs over the service life of the pavement [13]. The AASHTO procedure for STOA states that laboratory prepared loose mix asphalt should be placed in a pan at a thickness of 40mm, and conditioned in a forced draft oven for $4h \pm 5$ minutes at the mixture compaction temperature.

In this study, for selected tests, the mixture was short term oven aged. Long term oven aging was not carried out since this type of aging is done on the specimens where binder drain down can be a problem for PA.

The AASHTO short term oven aging procedure discussed above was deemed too severe for Swiss construction practices. Under standard construction conditions the mix would be laid down within an hour from leaving the mixing plant. However, in certain cases, such as binders that are very sensitive to aging, prolonged storage in hopper or working sites very far away from the place of production, the AASHTO - STOA procedure generates a severe aging rate.

The thermal history of asphalt binder has a direct influence on the mechanical performances of mixes. For reproducibility, tests have to be performed in different laboratories on samples with similar or identical thermal history. The thermal conditioning applied to the samples is described in the ongoing research project [43]. The aim of the current project is mainly to define rules of heat treatment of the bituminous mix manufactured in laboratories and cold-coated materials taken in situ and heated in the laboratory. The rate of selected aging allows to reproduce the thermal history of the material in the lab and to determine the material characteristics in the lab that correspond roughly to that obtained after the RTFOT which is similar to the aging obtained after production in the mixing plant. This process enables to manage well the conditions of heat treatment of the samples, which makes it possible to obtain test results with good repeatability and reproducibility.

The STOA procedure used in this study, explained in detail below, is based on the above ongoing research conducted in Switzerland [43] and referred to as the LAVOC aging procedure hereafter. The results presented in Figure 6.1 and Figure 6.2 [43] show a good correspondence between the penetration of the binder aged according to the RTFOT procedure and the penetration of the binder recovered from samples aged for 50 min (40 to 60 min) at the temperature of compaction.

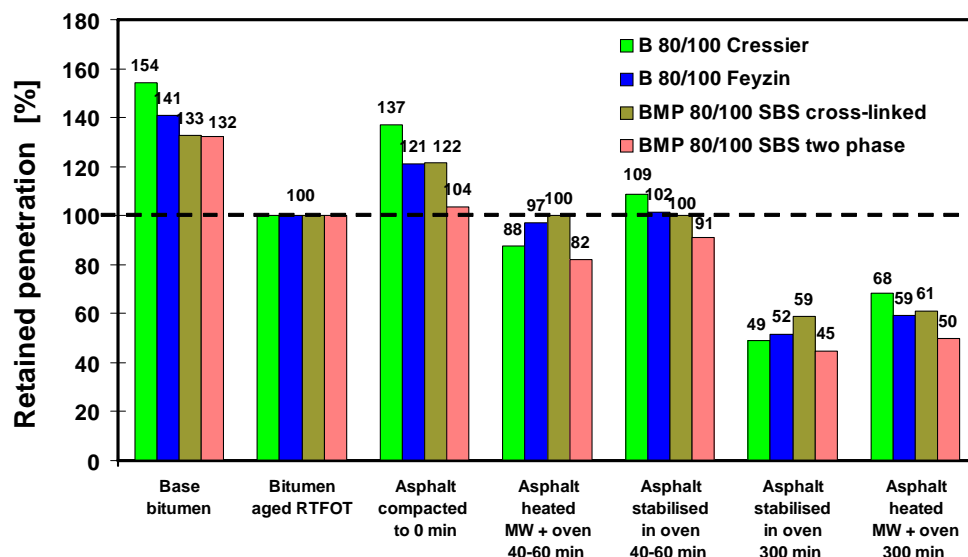


Figure 9. 1 : Residual penetration of 4 binders after various aging periods

D: Verbleibende Penetration von vier Bindemitteln nach verschiedenen Alterungsmethoden
F: Pénétration résiduelle de quatre liants types après différentes méthodes de vieillissement

The study carried out on the binder Colflex N55 (VD2) (Figure 9. 1 and Figure 9. 2) validates the LAVOC procedure using 50 min as the aging period and shows the excessive rate of aging generated by the AASHTO-STOA procedure on this binder with a residual penetration of 41% compared to the recommended minimal value of 60%. A particularly high index of penetrability is noticed after an aging of 180 min as well as 240 min, which reveals a high rate of oxidation. The adopted aging procedure duplicates the aging of the binder represented by RTFOT.

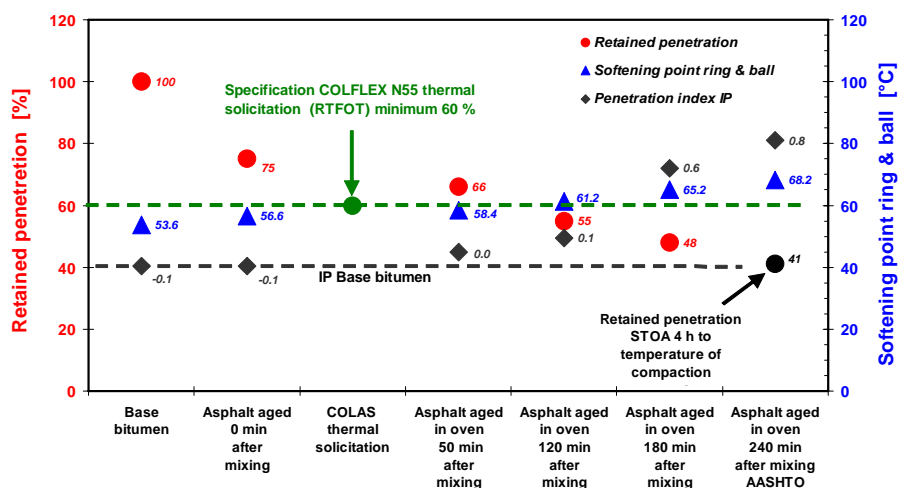


Figure 9. 2 : Retained penetration, softening point and IP of Colflex N55 binder at original state, 60 min, 120 min, 180 min, and 240 min oven aging, base and recovered bitumen

D: Verbleibende Penetration, Erweichungspunkt und PI für Colflex N55 Bindemittel im Anlieferungszustand und rückgewonnenes Bindemittel nach Alterung von 60 min, 120 min, 180 min, und 240 min

F: Pénétration résiduelle, point de ramollissement et IP de liants Colflex N55 de base et récupéré de l'enrobé vieilli. Etat 0, après vieillissement de 60 min, 120 min, 180 min et 240 min

LAVOC oven aging procedure

20-30 kg of mix is placed in a covered box (Figure 9. 3), paperboard or metal (to reduce effects of a forced draft oven) in a forced draft oven for 50 min at compaction temperature. In case of a cold mix, the mix should be pre-heated to compaction temperature (preferably in a microwave oven that minimizes the rate of aging).

Two procedures were applied:

1. Aging of laboratory prepared mixes

- Mix at fabrication temperature
- Aging of the mix in a covered box for 50 minutes at compaction temperature.
- Compaction of the specimen

2. Aging of the cold mix (from lab or work site)

- Reheat the mix to bring the temperature up to the compaction temperature (example: AG4 required 3 h in the oven, whereas, a bituminous mix sample of approximately 20 kg required between 10 min and 15 min using a microwave oven (3000 W))
- Aging of the mix in a covered box for 50 min at compaction temperature
- Compaction of the specimen

A third procedure can be applied for the bituminous mix taken and/or delivered tepid to the laboratory:

3. Aging of the tepid mix from the job site

- Reheat mix to compaction temperature if necessary (preferably with microwave oven)
- Aging of the mix in a covered box for 50 min at the compaction temperature
- Compaction of the specimen



Figure 9. 3 : Mix AG4 prepared in a metal pan for aging

D: Mischgut AG4 in Metallschale vor der Alterung

F: Récipient métallique avec enrobé AG4 préparé pour vieillissement

9.2. Void Characteristics [EN 12697-8]

The European standard [57] describes the procedure to calculate the air void content (V_m) as well as other parameters. The air void content V_m is the volume of the air voids as percentage of total volume of that specimen. VMA is the volume of inter-granular void space between the aggregate particles. It includes the air voids and the volume of the bituminous binder, expressed in percentage of total volume of specimen. These quantities are shown in Figure 9. 4. The air void content is calculated per equation 9.1.

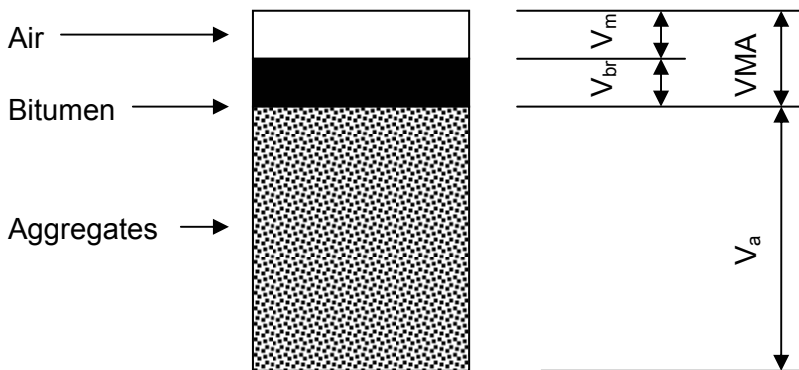


Figure 9. 4 : Voids in the mineral aggregate VMA, Void content V_m , Volume of the aggregate V_a and volume of the bitumen V_{br}

D: Hohlraumgehalt des Mineralstoffgerüsts, VMA, Hohlraumgehalt des Probekörpers V_m , Volumen der Mineralstoffe V_a , Volumen des Bindemittels V_{br}

F: Vides du squelette granulaire, VMA, vides de l'éprouvette, V_m , volume du squelette granulaire V_a , volume du liant V_{br}

$$V_m = \frac{\rho_m - \rho_b}{\rho_m} \times 100\% \quad [9.1]$$

where,

- V_m is the air void content of the mixture
- ρ_m is the maximum density of the mixture, [kg/m^3] [EN12697-5]
- ρ_b is the bulk density of the specimen, [kg/m^3] [EN12697-6]

The European standards [56] identify four methods for the calculation of bulk density. For specimen with open or course surfaces the sealed specimen and for geometric shapes including cylinders bulk density by dimension is specified. In this study, procedure D: Bulk density by dimensions is utilized.

The bulk density of a cylindrical specimen is calculated using equation 6.4:

$$\rho_{b,\text{dim}} = \frac{m_1}{\frac{\pi}{4} \times h \times d^2} \times 10^6 \quad [9.2]$$

where,

- $\rho_{b,\text{dim}}$ is the bulk density of the specimen, by dimensions, [kg/m^3]
- m_1 is the mass of dry specimen, [g]

- h is the height of the specimen, [mm]
d is the diameter of specimen, [mm]

Connected Network of Voids

The Swiss standard SN 640 433b [69] for PA proposed to determine the connected voids according to the French standards NF P 98-254-2. The test to determine the connected air void content of bounded materials makes it possible to measure the connected voids located inside the materials, at their surfaces and at the interface between them that allow the drainage of surface water. In this research project, the connected voids are determined from the weight of water introduced into the core sample whose side walls and the bottom part were sealed. A factor of correction depending on the maximum diameter of the solid grains allows to determine the effective volume of the connected voids without taking into account the voids at the surface of the sample.

the percentage of the volume of connected voids is calculated using the following equation:

$$P_c = \frac{V}{V} \times 100$$

[9.3]

Where the following quantities have to be defined

- The conventional height: $h = H - \frac{D}{20}$
- The introduced mass of water: $M = M_2 - M_1$
- The conventional volume of the core sample: $V = \pi r^2 h$
- The volume of introduced water: $v = \frac{M}{\rho_e}$ in between 15 °C and 25 °C, $\rho_e = 1 \text{ g/cm}^3$

And:

- Pc Percentage of connected voids
- V the conventional volume of the core sample (cm^3)
- D Maximum size of solid particle (mm)
- H Measured height of the core sample (cm)
- v Volume of introduced water (cm^3)
- r Radius of the core sample (cm)
- h the conventional height of the core sample (cm)
- M1 Mass of dried sample (g)
- M2 Mass of the sample for which the connected voids are filled (g) Note that this definition is not identical to the French denomination (in the standard)

M Mass of introduced water (g)

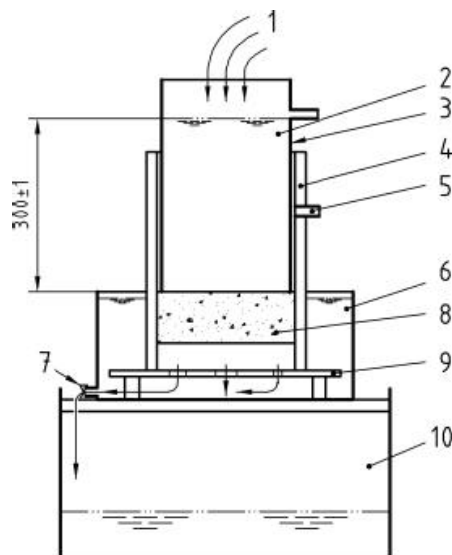
ρ_e Density of water (g/cm³)

9.3. Vertical Water Permeability [EN 12697-19]

Loss of permeability due to clogging of the pores is one of the disadvantages of porous asphalt. In this laboratory test procedure [61] carried out at ambient temperature (15 and 25°C), a column of water was applied with a constant height of 300 mm to a cylindrical specimen. Permeability K_v is evaluated from the measured flow rate of the water Q_v as follows:

$$K_v = \frac{4 Q_v I}{h \pi D^2} \quad [9.4]$$

Where, K_v is the vertical permeability (m/s); Q_v is the vertical flow rate (m³/s); I is the thickness of the specimen (m); h is the height of the water column (m) and D is the diameter of the specimen (m). Note that the requirements for dimensions of core sample are: thickness at least a quarter of the diameter (\varnothing 150 mm, $h \geq 37.5$ mm) and/or at least 2 times the maximum aggregate size (\varnothing 11 mm $h = \geq 22$ mm). No correction related to hydraulic conductivity as a function of water temperature is applied. The test set up is shown in Figure 9. 6.



Key

1 Water supply	6 Container
2 Water column	7 Outlet valve
3 Plastic tube	8 Specimen
4 Rubber cuff	9 Perforated plate
5 Overflow valve	10 Second collection tan

Figure 9. 5 : Apparatus for vertical permeability (dimensions in mm)

D: Gerät zur Bestimmung der vertikalen Durchlässigkeit

F: Appareillage pour perméabilité verticale



Permeameter (set up for vertical measurement)



Permeameter; top view



Detail of the test-tube with sleeve

Figure 9. 6: Test set up for vertical permeability (LAVOC)

D: Prüfaufbau für vertikale Durchlässigkeit (LAVOC)

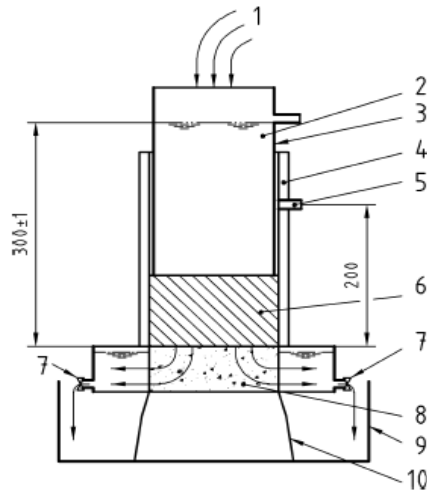
F: Essai de perméabilité verticale (LAVOC)

9.4. Horizontal Water Permeability [EN 12697-19]

As for the vertical permeability, in this laboratory test procedure [61] carried out at ambient temperature (15 and 25°C), a column of water was applied with a constant height (300 mm) to a cylindrical specimen. Permeability K_h is evaluated from the measured flow rate of the water Q_h as shown below:

$$K_h = \frac{Q_h}{(H+P+0.5l)} \frac{l}{(\pi D l)} \quad [9.5]$$

Where, K_h is the horizontal permeability (m/s); Q_h is the horizontal flow rate (m^3/s); l is the thickness of the specimen (m); h is the height of the water column (m), D is the diameter of the specimen (m), H is the distance of the lower and upper tubes (m) and P is the height of the lower tube (m). The requirements for dimensions of core samples are similar to the vertical permeability case: thickness at least a quarter of the diameter ($\varnothing 150 \text{ mm } h = \geq 37.5 \text{ mm}$) and/or at least 2 times the maximum aggregate size ($\varnothing 11 \text{ mm } h = \geq 22 \text{ mm}$). No correction related to hydraulic conductivity as a function of water temperature is applied. The test set up is shown in Figure 9. 6, Figure 9. 8



Key

1 Water supply	6 Plastic tube
2 Water column	7 Outlet valve
3 Upper tube	8 Specimen
4 Rubber cuff	9 Second collecting reservoir
5 Overflow valve	10 Support

Figure 9. 7 Apparatus for horizontal permeability (dimensions in mm)

D: Gerät für die Bestimmung der horizontalen Durchlässigkeit

F: Appareilage pour perméabilité horizontale



Figure 9. 8: Test set up for horizontal Permeability (LAVOC)

D: Prüfaufbau für horizontale Permeabilität (LAVOC)

F: Essai de perméabilité horizontale (LAVOC)

9.5. *In situ Water Permeability [SN 640 430]*

In situ water permeability was measured using the Yverdon permeameter according to the Swiss standard SN 640 430 [73]. The indirect measurement of the flow passing through the sample is determined from the water circulation with constant flow, under the base of the apparatus (fixed circular section). The interface between device and wearing course is sealed by a core joint made of synthetic mastic. The device is held down by a weight of ca. 70 to 80 kg (i.e. 1 operator). In the first step of the test the water pressure is varied in order to eliminate the air bubbles in the base. In a second step the water height of 170 mm is stabilized within 10 s. The water flow is measured using a graduated container. The test is repeated twice and the reported value in l/min is the arithmetic mean of the two values. Figure 9. 9 shows the overall view of the permeameter with Figure 9. 10 providing the detail [73].

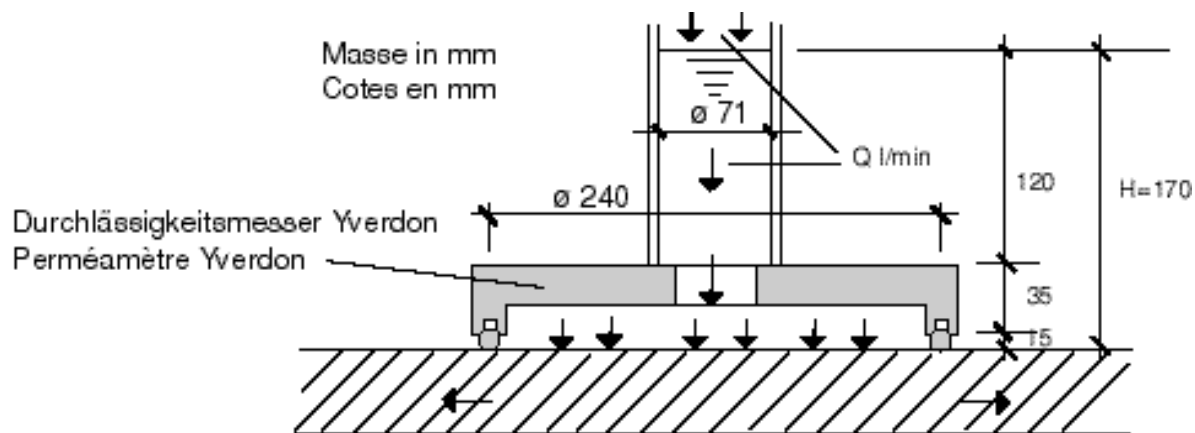


Figure 9. 9: Detail scheme of the test device (dimensions given in mm)

D: Detailliertes Schema der Prüfgerätes (Dimensionen in mm)

F: Représentation schématique du dispositif d'essai (dimensions en mm)

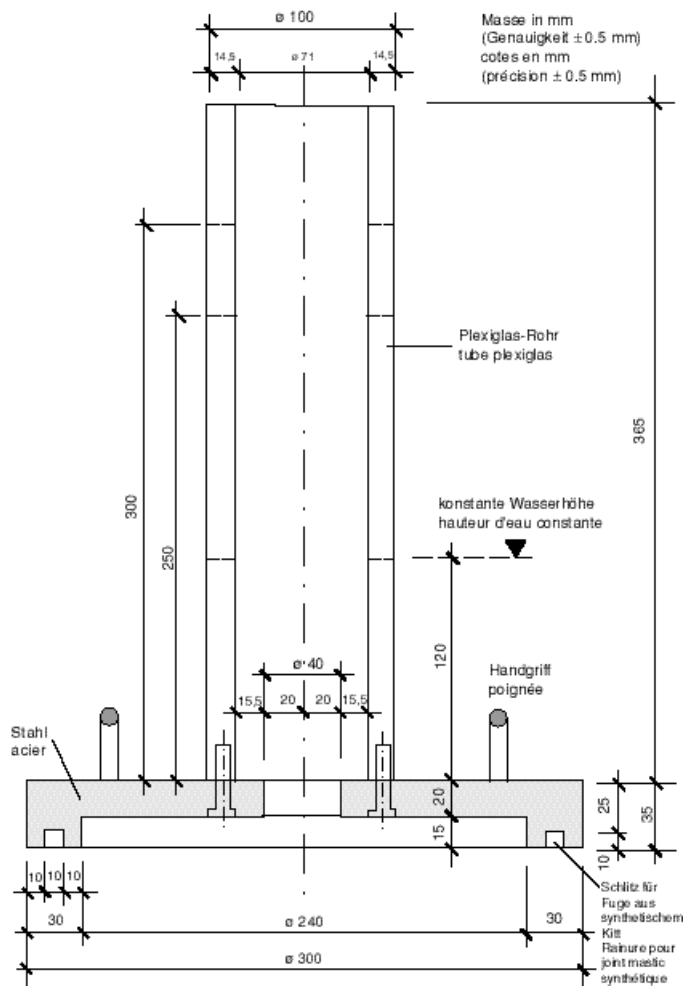


Figure 9. 10: Scheme of the Yverdon permeameter (dimensions given in mm)

D: Schema des Yverdon Permeameter (Dimensionen in mm)

F: Représentation schématique du perméamètre d'Yverdon (dimensions en mm)

9.6. Particle Loss using the Cantabro Test [EN 12697-17]

One of the disadvantages of porous asphalt is the loss of particles. The European test procedure for particle loss evaluation [60] addresses this characteristic by an attempt to reproduce the in situ mechanism of deterioration in the laboratory.

Five laboratory produced specimens were conditioned in an air chamber at 25°C for at least 4h or at -10°C for at least 6h (usually 12h). Each specimen was initially weighed (W_1) and placed separately into a Los Angeles drum. Thereafter, each specimen was weighed again after 300 and 500 revolutions of the drum (W_2) in order to determine the weight loss during testing. This weight loss is an indication of the cohesive properties of the mix. The test results are expressed as a percentage of weight loss in relation to the initial weight:

$$PL = \frac{W_1 - W_2}{W_1} \times 100 \quad [9.7]$$

Where, PL is the particle loss in percent; W_1 is the initial specimen mass [g] and W_2 is the final specimen mass [g].

9.7. Indirect Tensile Strength [EN 12697-23]

The purpose of the indirect tensile test in this investigation was to assess the behavior of the materials at low temperatures. Hence the testing temperature was decreased to simulate roads in winter. The indirect tensile test was conducted at 5 °C.

In accordance to the European standard for indirect tensile strength [62], cylindrical specimens of 150mm diameter were cut to the height of maximum 75mm if they were larger and conditioned in a temperature-controlled chamber for 4h at 5°C. Thereafter, the specimens were placed in the compression testing machine between the loading strips, and loaded diametrically along the direction of the cylinder axis with a constant speed of displacement of 50.8 mm/min until failure. Three specimens per mix type were conditioned. Thereafter, all specimens were tested immediately until fracture at peak load P. From P the indirect tensile strength for a specimen, ITS, was determined as shown below.

$$ITS = \frac{2P}{\pi DH} \quad [9.8]$$

Where,

ITS is the indirect tensile strength in GPa or MPa

P is the peak load in kN,

D is the diameter of the specimen in mm,

H is the height of the specimen in mm.

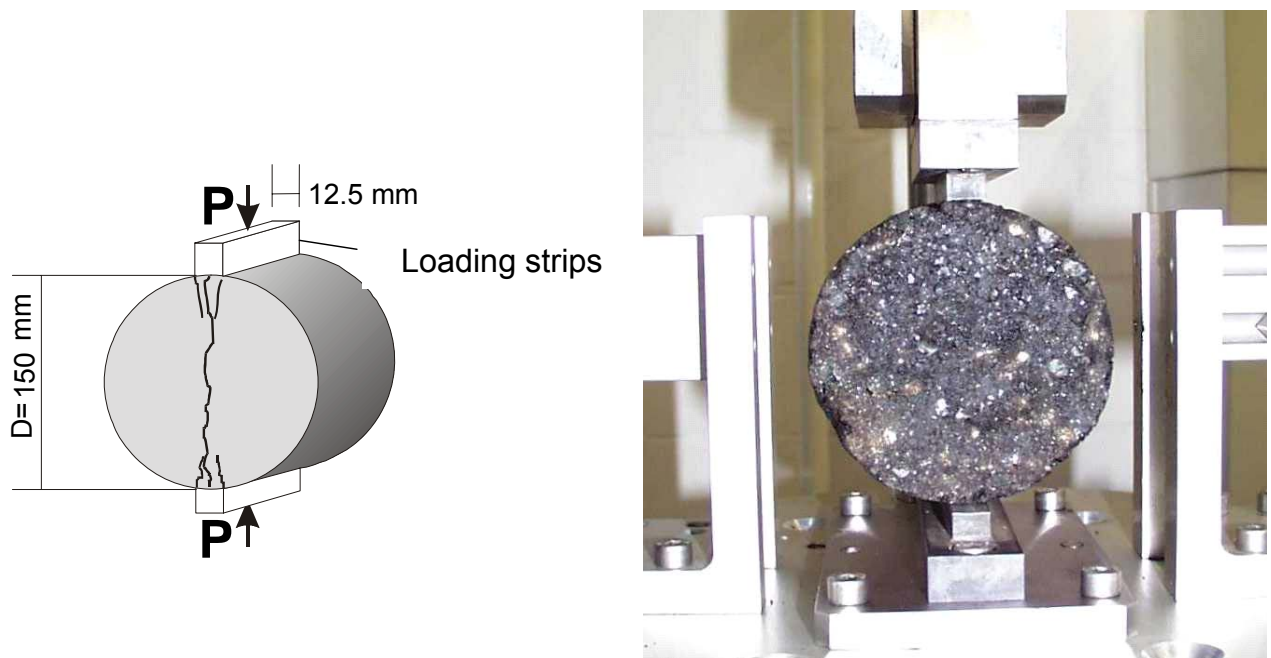


Figure 9. 11: Schematic representation of the indirect tensile test (left) and a specimen during a test (right) at Empa

D: Schema des indirekten Zugfestigkeits (links) und Prüfkörper während der Prüfung an der Empa (rechts)

F: Représentation schématique de l'essai de traction indirecte effectué à l'Empa (gauche) et test d'une éprouvette (droite)

9.8. Water Sensitivity [EN 12697-12]

The test method for water sensitivity, [20] is part of the new European standards and has been evaluated as suitable for porous asphalt. The purpose of this standard test is to determine the effect of saturation and accelerated water conditioning on the Indirect Tensile Strength of cylindrical specimens. The practical experience with this test method is not complete especially its relevance to the long term effects of water on porous asphalt pavements. In addition to this standard test particle loss and CAST on wet samples was used to assess the water sensitivity of the materials used in this project.

The standard test was modified as stated below. Six cylindrical specimens of 150mm in diameter were used. The specimens were divided into a dry and a wet group. The dry group was stored at room temperature (20 ± 5) °C while the wet group was vacuum saturated at an absolute pressure of 300mbar for 5 min then stored for 24h at 60°C. The specimens were thereafter further conditioned for 24h at the test temperature of 25°C.

In accordance to the European standard for indirect tensile strength, the test was carried out on specimens not later than one minute after they had been taken out of the water or chamber, [62]. The indirect tensile strength ratio ITS_R, is calculated by:

$$\text{ITS}_R = 100 \times \frac{\text{ITS}_w}{\text{ITS}_d} \quad [9.8]$$

Where,

ITS_R= Indirect Tensile Strength Ratio, in percent

ITS_w= Average Indirect Tensile Strength of three specimen of the wet group, kPa

ITS_d= Average Indirect Tensile Strength of three specimen of the dry group, kPa

9.9. Stiffness

In order to determine the stiffness of the specimen the coaxial shear test (CAST) the two point bending tests as well as direct tension test were carried out.

Coaxial Shear Test

The Co Axial Shear Test (CAST) is a dynamic, axial loading system to determine the complex modulus (E^*) of an asphalt pavement (Figure 9. 12). The test was first developed at Empa in 1987 [4] and further developed by Younger et al [27], Gubler et al [31] and Sokolov et al [32]. Tests are performed in a conventional, temperature controlled, servo-hydraulic tension-compression machine. The shear load is applied perpendicular to the specimen's circular surface with lateral confinement provided by a metal ring surrounding the specimen. This format allows loading along the same axis as that of traffic while the lateral confinement simulates a semi-infinite in situ situation. The Coaxial Shear Test (CAST) equipment was also used to determine the evolution of the mechanical properties under combined water action and temperature cycles. The test method produces mechanical damage due to repeated loading, temperature cycles and water immersion as described in [28]. In this case four temperature cycles from 25°C to 30°C and 30°C to 25°C each for 18000s were used.

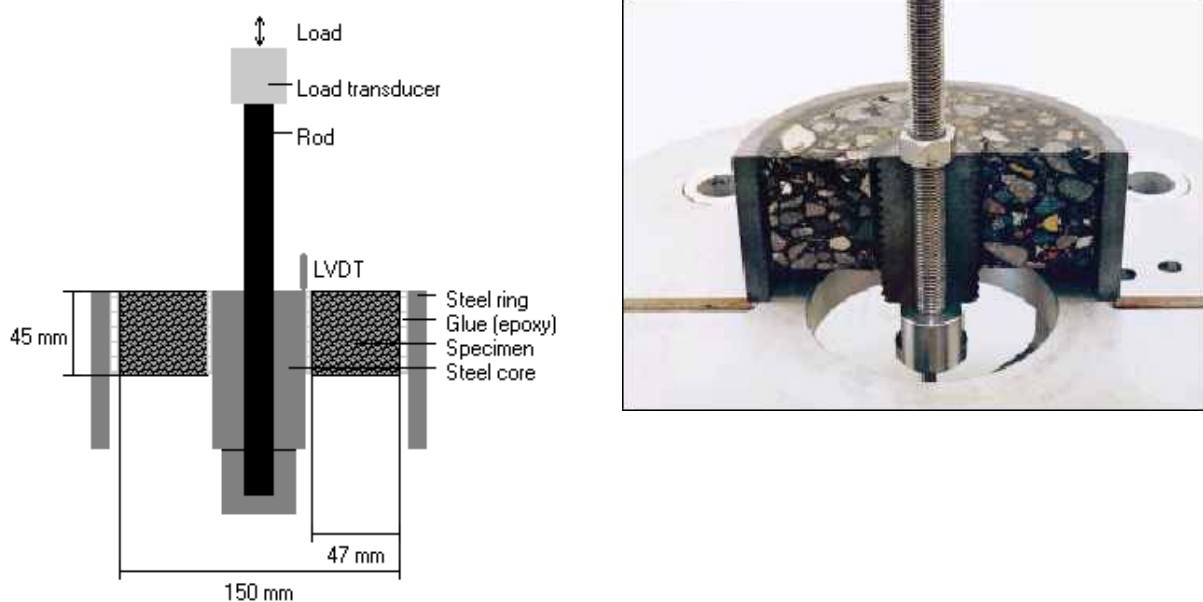


Figure 9. 12: Schematic depiction of the CAST setup, left and cut view of a CAST specimen, right at Empa

D: Schema des Prüfaufbaus KAST (links) und Schnittbild eines Prüfkörper (rechts, Empa)

F: Description schématique de l'essai CAST de l'Empa (gauche) et vue de la coupe d'une éprouvette (droite)

Table 9. 1: CAST test parameters

D: KAST Prüfparameter

F: CAST paramètres d'essai

Temp [°C]	-10, -5, 0, 5, 10, 15, 20
Frequency [Hz]	0.25, 0.5, 1, 2, 4, 8, 16
No. of modulus determinations measurements per loading condition	6
Modulus of glue [MPa]	2000

Test parameters are listed in Table 9. 1. The tests were conducted under load control and the modulus of the test specimens were calculated by the program using the following formula:

The evaluation of the results is based on a finite element analysis resulting in tables connecting the modulus E^* with deformation. The formulas used to back calculate the modulus E^* from deformation are shown below.

$$E^* = \frac{F_a}{\delta_a} \quad A(E^*) \quad [9.9]$$

Where:

E^* =Complex modulus

F_a =Force amplitude along the steel core

δ_a =Displacement amplitude along the steel core

$A(E^*)$ =Coefficient function derived from FEA by recursive iteration

Assuming linear viscoelastic behavior, the method of time temperature superposition was used to construct master curves at the reference temperature of 25°C based on the sigmoidal function as shown below [37]:

$$\log E^* = \delta + \frac{\alpha}{1 + e^{\beta(\log f_r - \log a_T)}} \quad [9.10]$$

Where,

E^* = Dynamic complex modulus

δ = Parameter describing the minimum value of G^*

f_r = Frequency of loading at the reference temperature

α = Parameter describing the span between max and min value of G^*

β, γ = Parameters describing the shape of the sigmoidal function

a_T = shift factor, determined with WLF relationship

Two Point Bending Test [EN 12697-26]

The two points bending test (2PB-TR) is carried out on trapezoidal samples. The samples are loaded in the upper part with sinusoidal cyclic deflection strain in the linear domain (ϵ is limited to 50×10^{-6} to avoid any damage). Stress and strain amplitudes are measured simultaneously. An example of the test set up is shown in Figure 9. 13. The complex modulus E^* is calculated as the ratio between stress and strain at a given moment:

$$E^* = (\sigma_0/\epsilon_0) (\cos\varphi + i \sin\varphi) \quad [9.11]$$

The modulus ($|E^*|$) is a complex number which corresponds to the modulus ratio (σ_0/ϵ_0) and the phase angle (φ). The phase angle in turn represents the difference of phase between stress and strain levels. It is possible to express this complex number as follows:

$$E^* = E_1 + i E_2 = |E^*| e^{i\phi} \quad [9.12]$$

with :

The real part $E_1 = \gamma(F/D \cos\phi)$

The imaginary part $E_2 = \gamma(F/D \sin\phi)$

F is amplitude of sinusoidal load (N)

D is amplitude of displacement (mm)

γ is Factor depending on the specimen dimensions



Figure 9. 13 : Two point bending equipment at LAVOC

D: Prüfeinrichtung für Zweipunktbiegung am LAVOC

F: Essai de flexion 2 points, appareillage du LAVOC

Table 9. 2: Two point bending parameters

D : Parameter für das Prüfverfahren Zweipunktbiegung

F: Paramètres d'essai de flexion 2 points

Dimension of samples	
Height [mm]	250
Thickness [mm]	25
Large base [mm]	70
Small base [mm]	25
Test parameters	
Temp [°C]	-10, -5, 5, 10, 15, 20, 25, 30
Frequency [Hz]	1, 3, 10, 25, 40

Direct Tensile Test (DTT)

The objective of this test is to evaluate the phenomena of adhesiveness and cohesively of various binders used in the porous asphalt mixes by a direct tensile test at low temperatures [39]. The ideal case planned at the start of the project was to combine the test results of TSRST (Thermal Stress Restrained Specimens Test) [40] with a direct tensile test at low temperatures. However, the TSRST test at LAVOC is not currently operational [41, 42]. It has been shown that the rate of strain does not play a significant role; therefore it seems possible to carry out a test at higher strain rates than in [41] which is of about $200 \cdot 10^{-6}$ m/m·h as a result a rate of $2000 \cdot 10^{-6}$ m/m·h was proposed.

The procedure initially was to define the thermal dilation coefficients of porous asphalt so as the theoretical temperature TSRST has been calculated by means of the modeling proposed in [42]. To this end, 3 samples were tested with temperature steps of 5°C around the theoretical value TSRST, followed by three others with temperature steps of 2.5°C , around the real temperature corresponding to the fracture stress.

The direct tensile test (Figure 9. 14) allows to approach the rupture phenomena at low temperature for low strain rates similar to rates that occurs in asphalt mix subjected to a temperature fall. The aim of this test is to load a bituminous mix sample by a uniaxial traction at a constant strain rate and at low temperatures in a range of -10°C to -30°C . These tests are carried out normally on samples of $30 \times 30 \times 100\text{mm}$. In the case of porous asphalt, the cross section is increased to $60 \times 30 \times 100\text{mm}$.



Figure 9. 14: Assembly of the sample in the conditioning chamber at LAVOC for the direct tension test

D: Prüfeinrichtung in Klimakammer des direkten Zugversuchs, LAVOC

F: Essai de traction directe Lavoc, montage d'une éprouvette dans l'enceinte thermique

9.10. Binder Rheological Properties using the Dynamic Shear Rheometer, DSR

Traditionally, empirical binder properties such as penetration softening point and Fraass breaking point have been used to provide an indication of the mechanical properties of binders. Modern road designs often require the use of polymer modified binders. These modifications significantly alter the rheological properties of the binder and traditional empirical methods can no longer adequately be used to characterize the properties of the binder. As a result of the SHRP program in the U.S. (1988-1993) a performance based binder specification and associated test based on rheological principles was developed. The dynamic shear rheometer (DSR) was the main test instrument that was developed as a result.

During the DSR test, sinusoidal, oscillatory stresses and strains are applied to a thin disc of bitumen, which is sandwiched between the two parallel plates (spindles) of the DSR. The tests are performed using a range of temperatures and load frequencies. In addition, testing is usually performed using small strains (testing within the linear viscoelastic region) to enable the rheological data to be transported between different frequencies and temperatures using the time-temperature principle of superposition [53].

The properties that are obtained from the DSR are the complex shear modulus G^* and the phase angle δ . G^* is defined as the ratio of the maximum shear stress to maximum strain and characterizes the resistance to deformation under shear loading. The complex shear modulus consists of an elastic part or storage modulus (G') and the viscous component or loss modulus G'' . The phase angle φ is the time lag between the applied stress and shear strain response during a test.

The following relationships hold:

$ G^* $	=Peak stress/Peak strain [Pa]
φ	= phase shift angle between the applied max strain and the max stress [°]
G'	= shear storage modulus = $ G^* \cos \varphi$
G''	= shear loss modulus = $ G^* \sin \varphi$
$\tan \varphi$	= G''/ G'
ω	= angular frequency [rad/sec]
$ \eta $	= dynamic viscosity = $ G^* /\omega$ [Pas]

Accurate temperature control is important in the measurement of rheological parameters in the DSR. Temperature gradients in the sample can lead to a reduction in the precision and accuracy of the measured data. Figure 9. 15 shows the DSR and the testing configuration. In this study an 8mm diameter spindle and a 2 mm testing gap were used which were defined as appropriate for temperatures less than 40°C. The test temperatures were 10 to 40 °C.

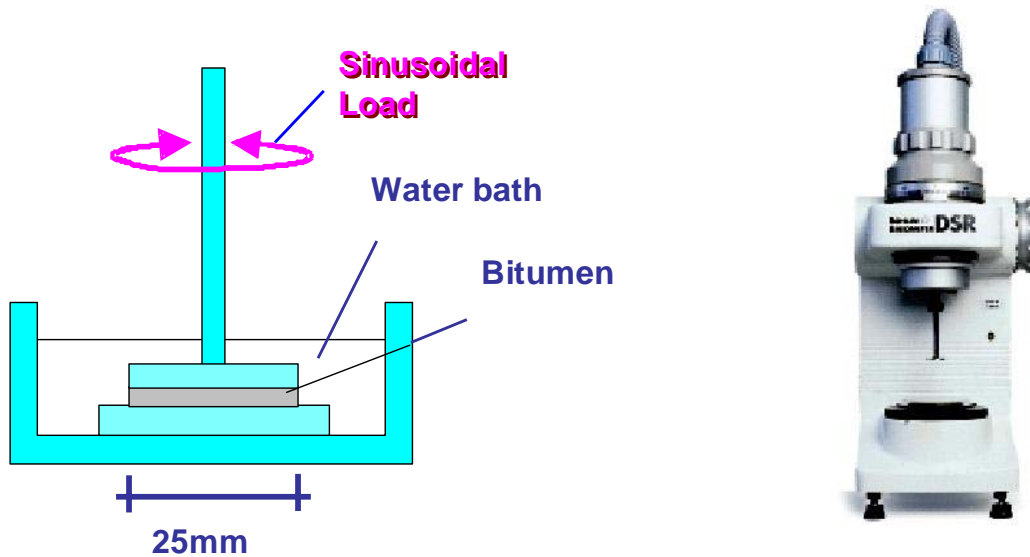


Figure 9. 15 : DSR (right) and schematic depiction of the DSR testing configuration (left)
Empa

D: DSR (rechts) und Schema der DSR-Prüfung (links) Empa

F: DSR (droite) et description schématique de l'essai DSR gauche) Empa

10. EXPERIMENTAL RESULTS

10.1. Compaction

Effect of Binder Content and Gradation on Compaction

The effect of the binder content variations and the compaction energy variations were evaluated during the optimization study of mix VD9 by means of the Marshall test. On the basis of the initial mix VD5, two grading curves and 4 binder contents were tested with the same initial state: void content obtained after 2X50 Marshall blows.

The results obtained on 100 mm diameter cylindrical samples compacted by Marshall compaction and Gyratory (PCG) compaction (after 40 gyrations) are plotted in Figure 10. 1 and Figure 10. 2. The gyratory compacted specimens are shown on the figures as those corresponding to 2x25 blows. With the grading curve A, it was not possible to obtain the minimal porosity of 22% with high binder content (6.2%). With the grading curve B (less filler and sand) it was possible to obtain the required air void content even with high binder content. One notes that compaction level achieved with PCG after 40 gyrations for this mix, corresponds to a theoretical energy for Marshall compaction of 2x25 blows. A similar trend in compaction was seen for all the mixes examined in this project. This can be attributed to the fact that after a certain level of compaction, in this case about 2X25 blows, the material runs the risk of breaking the aggregates in the process of further compaction, leading to a lower void content than intended. Figure 10.12 and Figure 10.13 illustrate how the void content is affected by the compaction energy and how the void content achieved by 2X25 blows correspond to 40 gyrations.

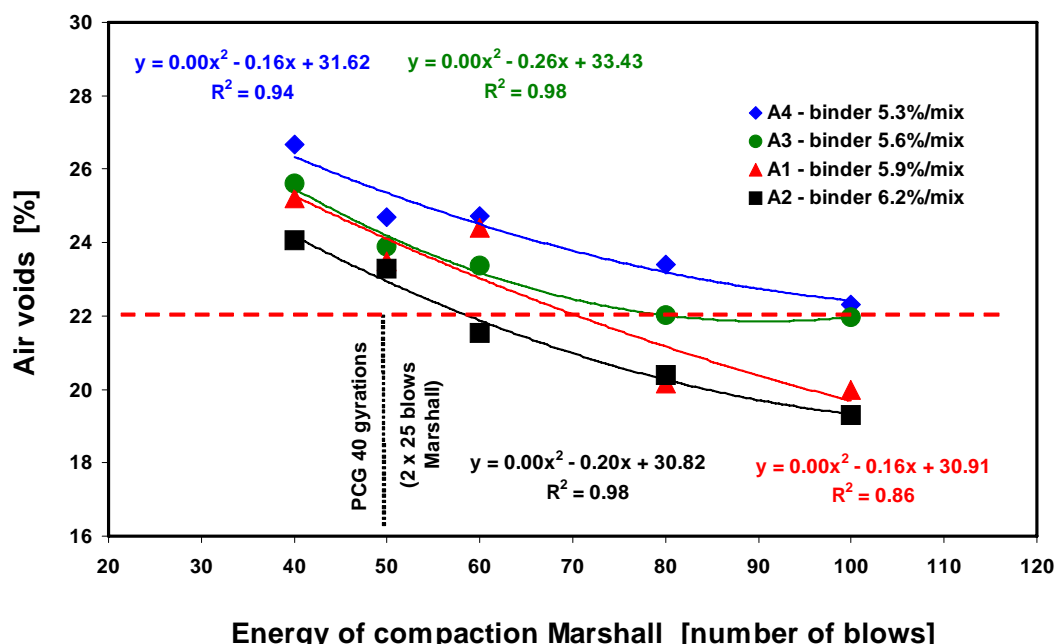


Figure 10. 1 : Mix design VD5 - Grading curve A with 4 various binder contents

D : Optimierung des Rezepts VD5- Korngrossenverteilung A mit vier Bindemittelgehalten
F : Formulation de la recette VD5 - Courbe granulométrique A avec 4 teneurs en liant

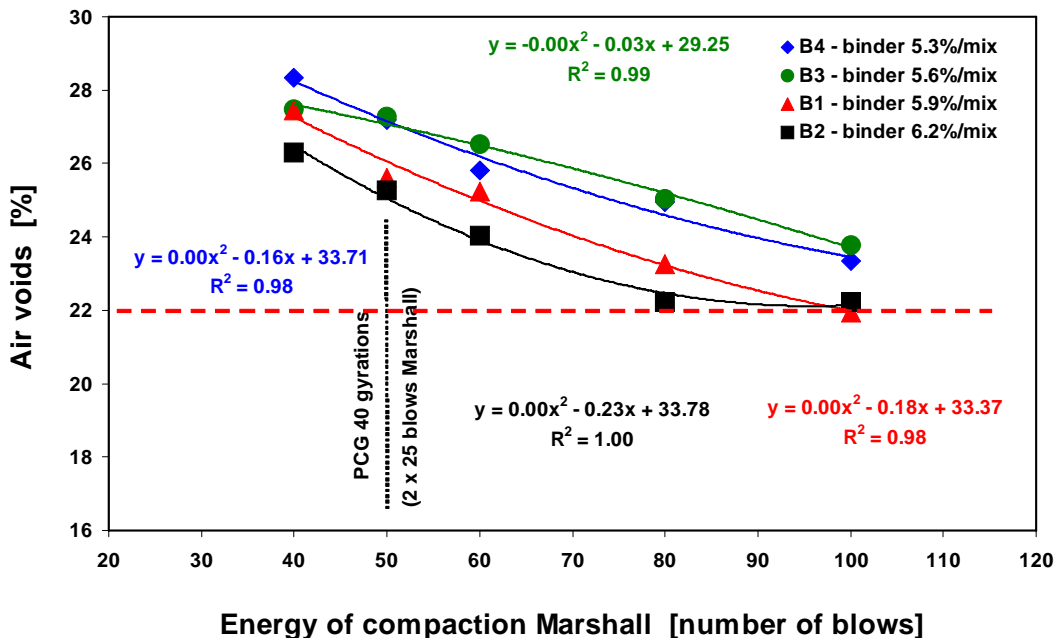


Figure 10.2 : Mix design VD5 - Grading curve B with 4 various binder contents

D: Optimierung des Rezepts VD5- Korngrossenverteilung B mit vier Bindemittelgehalten
F : Formulation de la recette VD5 - Courbe granulométrique B avec 4 teneurs en liant

Void Content Distribution in Specimen Produced using a Roller Compactor

In order to simulate field compaction, the use of the roller compactor from LCPC using the steel roller was further investigated.

To determine the void content distribution (V_m) in a wheel tracking specimen using the geometric method the material from Aargau, AG1, was extensively tested using two approaches for the roller compactor.

For the first method, used at Empa, the mix was compacted with a steel roller that fits around a pneumatic tire with 4.5 bar pressure in a steel mould (100 x 180 x 500 mm). Initially 27 passes at the center of the specimen were applied while the bottom plate was continually pushed up. At the final stage, 23 additional passes were applied.

As shown in Figure 10.3, the void content in the middle of the compacted slab (at center height) is close to the desired 22%. However, there is variability in the vertical and horizontal direction. As seen in the figure, the top and bottom portions of the slab are not adequately compacted. It is recommended that for test purposes the middle section be used.

Material: PA mix from the job site from Aargau (AG1)

Density: $\rho_m = 2.49 \text{ g/cm}^3$

Design void content: 22%

Bulk density: $\rho_b = M/V$

Where M is the mass of the specimen (g) and V is the volume (cm^3).

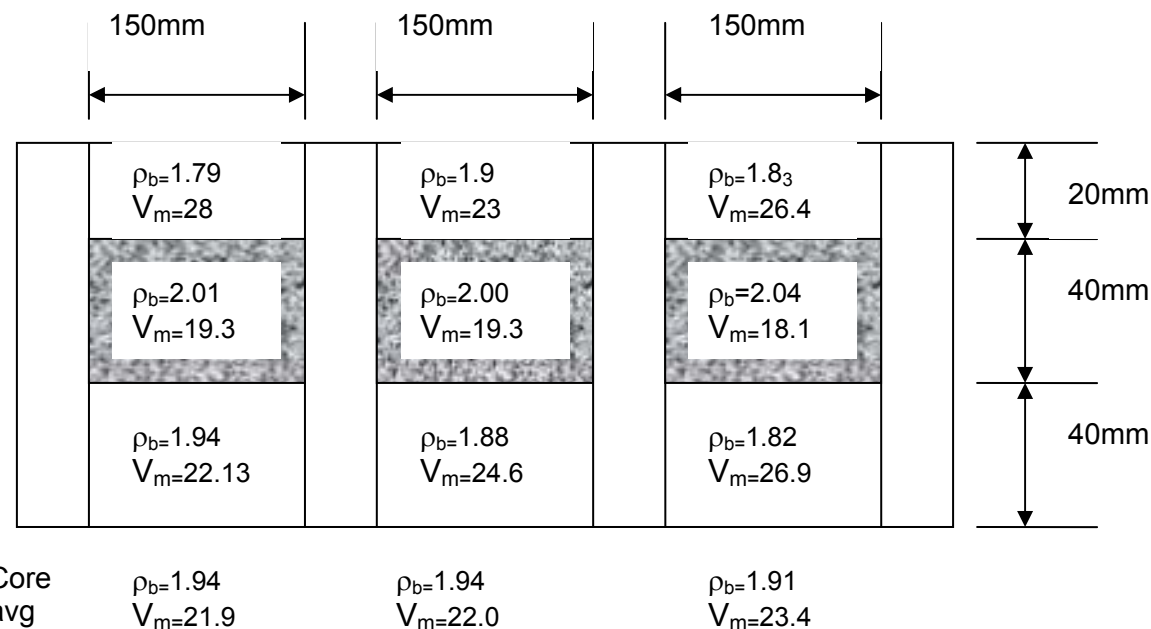


Figure 10. 3 Air void content distribution [vol %] in a specimen compacted using a steel roller at Empa

D: Verteilung des Hohlräumgehalts [vol %] in Prüfkörper, verdichtet mit einer Stahlrolle, Empa
F: Distribution des vides [vol %] de l'éprouvette, Empa

At LAVOC a similar procedure was followed. However, the specimen was initially compacted with the pneumatic tire and at the end of the compaction process a steel roller that fits around one tire was used (Figure 10. 4).



Figure 10. 4 : Final stage of compaction (left) and the sample (right)

D :End stadium der Verdichtung (links), und der Prüfkörpers (rechts)
F : Phase finale du compactage (à gauche) et état final de la plaque (à droite)

Similar results to those by Empa were obtained in this case. The middle section void content is close to the desired 22%; however, there is variability in the vertical and horizontal direction. As seen in the figure, the top and bottom portions of the slab are not adequately compacted. As a result of the compaction experience at Empa and LAVOC stated above, it is recommended that for test purposes specimen obtained from the middle section closer to the top be used if compaction with a steel roller is applied. Considering the in-homogeneity of the samples obtained by this

method and the fact that a large portion of the material would have to be discarded, it was decided to forego this method and to use the gyratory compaction as a standard compaction method. Marshall hammer compaction has also been used where indicated.

10.2. Total Air Voids and Interconnected Air Voids

In order to maintain the permeability and noise abatement properties of PA a high ratio of interconnected voids to total air voids is desirable. The average ratio between interconnected air voids over geometrical voids of the materials tested in this project was 0.71. The lowest ratio recorded was 0.44 for the VD5 mix and the highest one for VD10-22 core equals 0.83.

As seen in Figure 10. 5, AG2 had a high ratio of interconnected voids to total voids. However this is due to excessive binder loss and deterioration of the material. VD5 on the other hand had a low ratio but did perform well in situ.

In order to reach a recommendation for standardization eliminating the two outliers of AG2 and VD5 and calculating the average ratio of connected voids to total voids gives a value of 0.73. Field performance of these sections according to chapter 5 and 7 and Appendix 2 were satisfactory. This value can be recommended for standardization.

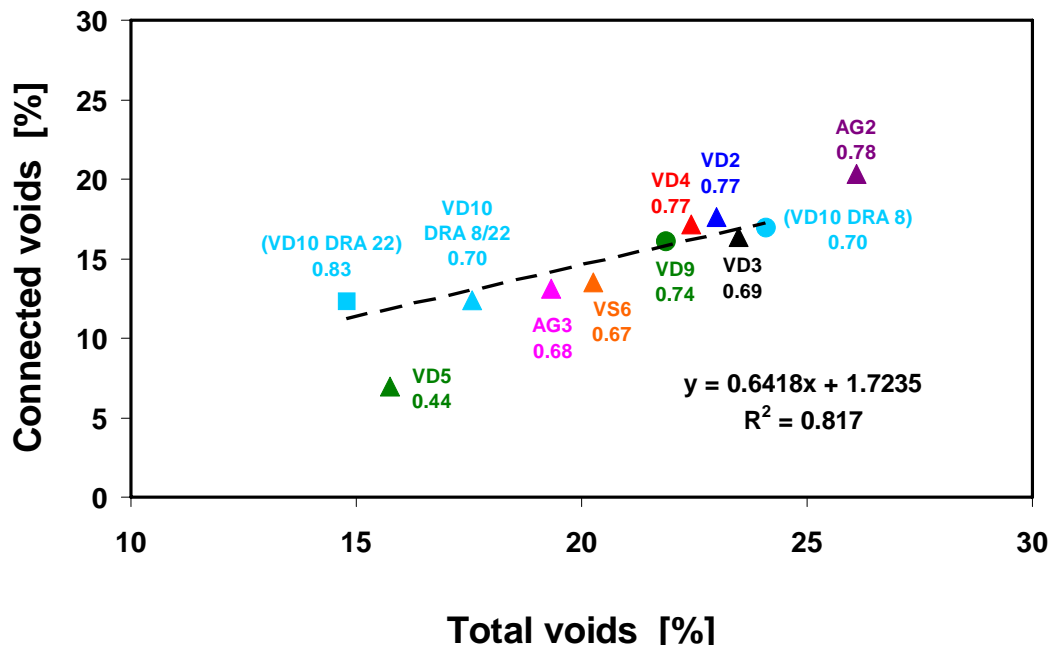


Figure 10. 5 : Relation of connected voids versus total voids and ratio

D: Zusammenhang zwischen verbundenen Hohlräumen und gesamtem Hohlraumgehalt
F : Relation entre les vides communicants et les vides totaux, ratio

10.3. Vertical Water Permeability

Figure 10. 6 shows the vertical water permeability measured in laboratory and in situ permeability as measured by the Yverdon method [73] plotted against air void content of all the cores tested. The taken samples were sawn to 10 mm of the PA/support interface so as not to take into account the filled part due to the sealing membrane (SAMI). In situ permeability of 15l/min is recommended by the standard as indicated [73]. The twinlay (VD10) was tested as a system and in addition each layer was tested separately. The 22mm layer shows good permeability as opposed to the 8mm layer; also the system consisting of both layers performs well.

The laboratory prepared samples of VD9 (VD5 optimized) show high permeability contrary to those of the VD5 cores with minimal vertical permeability in laboratory, indicating clogging of the pores. This characteristic is confirmed by in situ measurements. It is apparent from the measured values that maintaining the recommended value after the pavement has been put in service is unlikely. It is also important to note that although permeability values are below current recommendations in situ performance regarding aquaplaning is not reduced. It can be seen that the air void content alone does not allow to assess the permeability, the quality of the voids as well as dimensions of the capillaries, and amount of interconnected voids should be considered. Furthermore it is recommended to use 15 l/min as an initial value of permeability to be used for laboratory prepared samples and initial tests in the field and reducing required in situ permeability to 10l/min after 2 years in service. The experience accumulated in canton Vaud (DINF LEM Yverdon) indicates that in situ permeability is reduced to 2/3 of the initial value after two years in service.

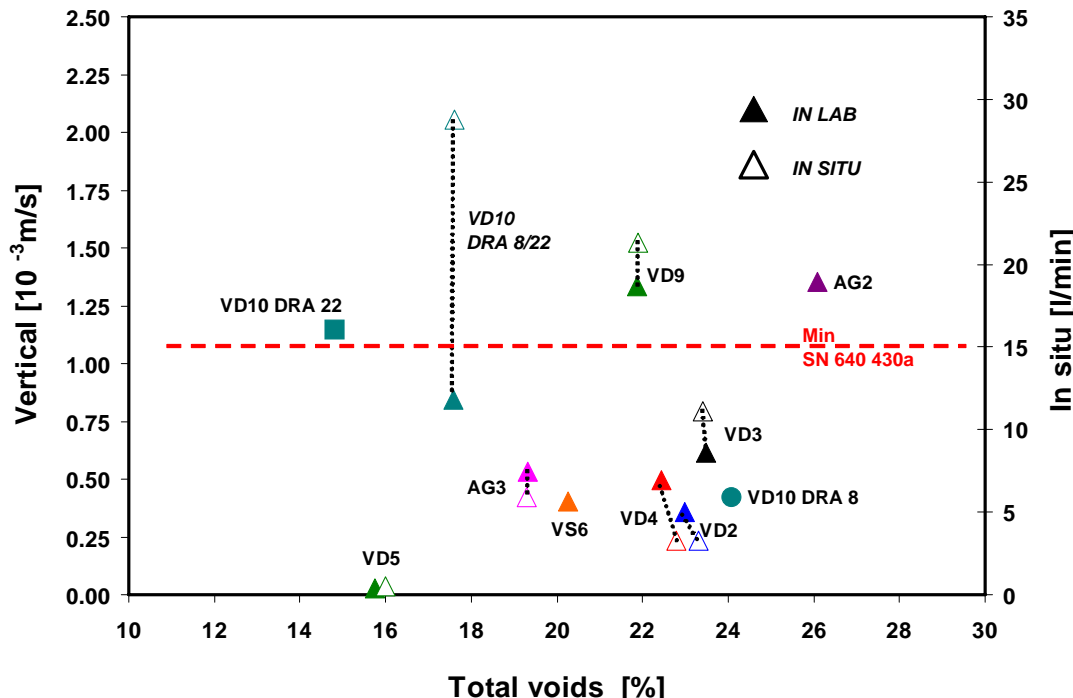


Figure 10.6 : Results of the vertical permeability in laboratory and permeability in situ using the standard Yverdon method SN 640 430a

D: Ergebnisse der vertikale Permeabilität im Labor und der Permeabilität in situ mittels gemäss SN 640-430a (Yverdon-Methode)

F : Résultats d'essai de perméabilité verticale mesurée en laboratoire et de perméabilité mesurée in situ au perméamètre d'Yverdon selon SN 640 430a

For 5 mixes VD2, VD3, VD4, VD10 and AG3 with different characteristics (Figure 10.7), a linear variation is observed between the permeability measured in situ with the Yverdon permeameter and the vertical permeability measured in laboratory on core samples. This law does not apply for two cases: mix VD5 which is very clogged characterized by a very low permeability close to 0 and the mix VD9 (optimized VD5) for which the material was not yet trafficked. In this case, we can assess that the microstructure of the layer has not been modified under vehicle loads as observed usually.

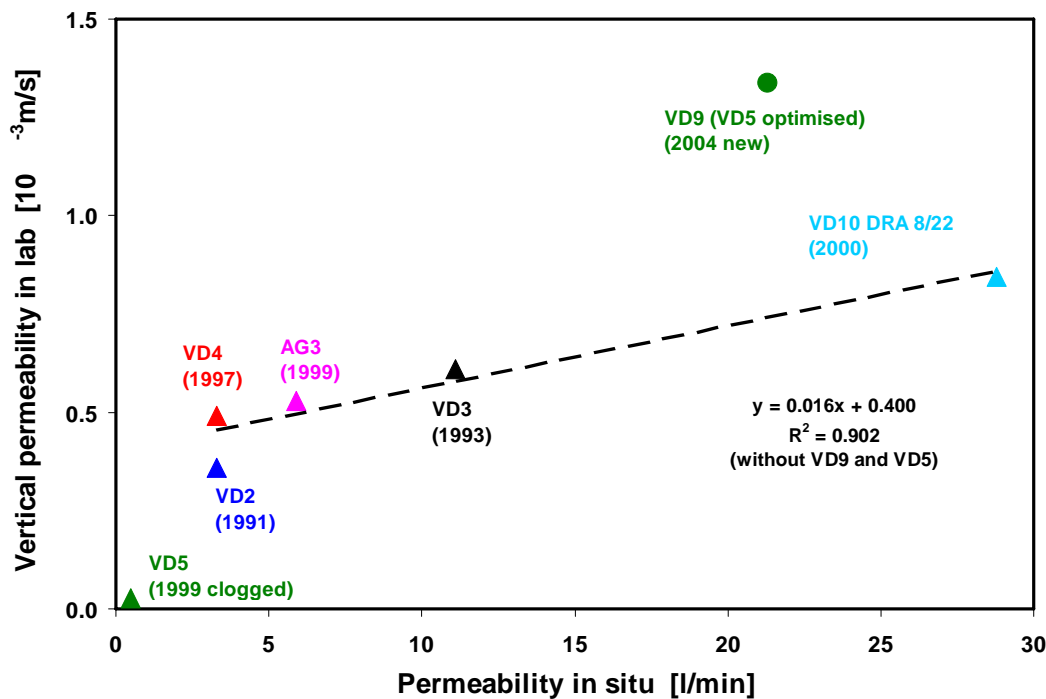


Figure 10. 7 : Results of vertical permeability in lab vs. permeability in situ and construction dates

D : Ergebnisse der vertikalen Permeabilität im Labor und in situ mit Prüfdaten

F : Résultats de perméabilité verticale fonction de la perméabilité in situ selon les dates de construction

10.4. Horizontal Water Permeability, Effect of Height

A complementary test was carried out on samples of mix VD9 compacted with the PCG and compare to those from field cores. The compacted samples have a height of approximately 75 mm. The test was also carried out on samples from PCG sawn in the middle (height 36 mm), to evaluate the influence of height. The horizontal permeability test was not carried out on in situ samples (test field A5 batch 5130 Yverdon-Concise) because the lateral surface was filled with the bituminous mastic during the coring process. A laboratory test would require a new coring at low temperature with lower diameter (100 mm) and an adaptation of the system of measurement or alternatively a coring in situ with 200 mm and a new coring with 150 mm diameter at low temperature at the laboratory.

Measurements of vertical and horizontal permeability are carried out on water saturated specimen; the results from the methods are then comparable. The measured flows depend on the sample size, for a constant diameter (150 mm), one notes a reduction in the flows related to increased thickness (effect of pressure loss).

Figure 10. 8 shows the results that were obtained on PCG samples with various heights for the 2 methods of laboratory measurement (vertical and horizontal permeability). These values are compared with the results obtained on core sample from the road with various heights and in situ results with the Yverdon permeameter. One notes a good similarity in the vertical and horizontal methods, between the flows measured in situ and the flows measured in laboratory for samples with similar heights.

It is important to keep in mind that the in situ flow measurements with the Yverdon permeameter cannot be directly compared with laboratory measurements because the in situ device senses vertical and horizontal permeability at the same time, in partially saturated conditions meaning that the volume of wet material cannot be precisely defined. It has to be mentioned that no cor-

rection is applied to take into account temperature dependence of hydraulic conductivity. Water viscosities as a function of temperatures leads to varying results concerning differences in pressure losses and then in flows. Resistance to the flow decreases with the increase in the temperature and vice versa. In laboratory, the water temperature is about 14–15°C. It is recommended that the in situ measurements be carried out at a similar temperature range (it can be 10 to 20°C).

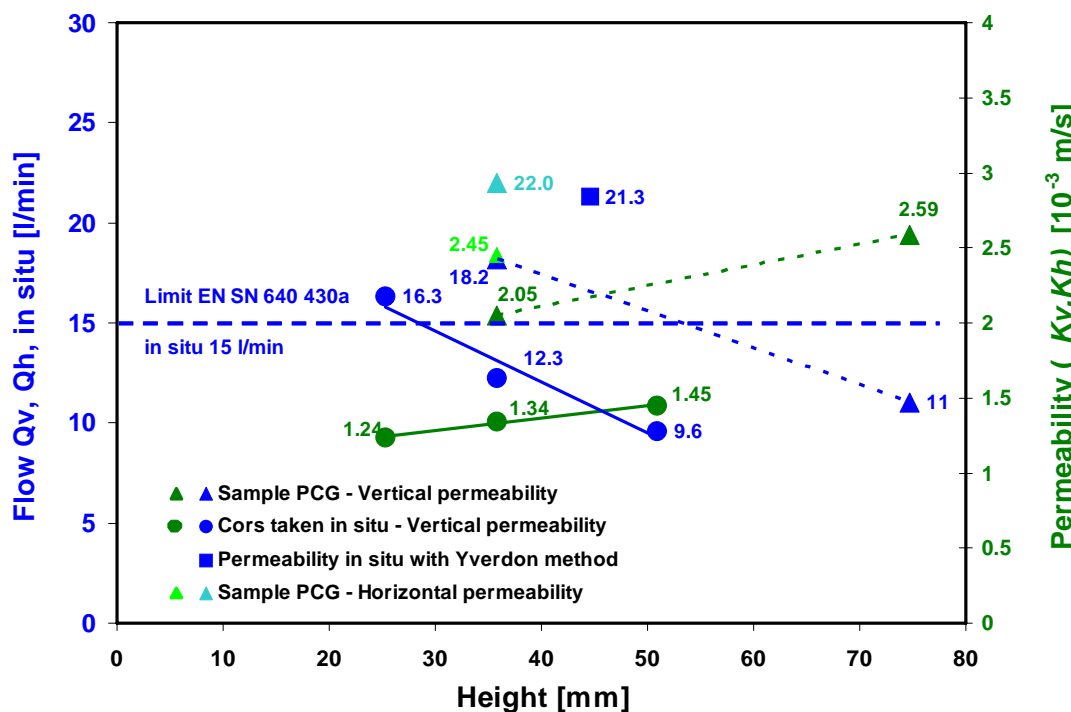


Figure 10.8 : VD9 PA11 Bitumen Rubber - Results of the vertical and horizontal permeability in laboratory and permeability in situ (Yverdon method) with samples of different heights (SN 640 430a)

D: VD9 PA11 Bitumen mit Gummi - Ergebnisse der vertikalen und horizontalen Permeabilität im Labor und in situ (Yverdon-Methode) mit Prüfkörpern unterschiedlicher Höhen (SN 640 430a)
F: VD9-PA11 bitume-caoutchouc – Résultats de perméabilités verticales et horizontales en laboratoire et in situ (méthode d'Yverdon) avec échantillons de différentes hauteurs (SN 640 430a)

10.5. Particle Loss using the Cantabro Test

Effect of Aggregate Hardness (Los Angeles) and Binder Type

In order to evaluate the effect of aggregate hardness on the cantabro test for particle loss, two types of aggregates were utilized. The first is the FAMSA Choëx with a Los Angeles coefficient according to EN of 19 (17 in SN), the other from the Bourgeoisie de Sion with a Los Angeles coefficient in accordance to EN of 27 (25 in SN). Two types of binders were utilized one polymer modified (Styrelf 13/80) and the other straight run bitumen (B 50/70). The parameters temperature, energy of compaction/porosity and a number of revolutions were evaluated. Figure 10. 9 shows the results obtained at 25°C and compaction energy of 2x25 blows. The results at 300 and 500 revolutions are consistent indicating that at 25°C the particle loss is lower for the harder aggregate (FAMSA-Choëx) in comparison to the semi hard aggregate (Bourgeoisie de Sion). The particle loss is also lower for the polymer modified binder. A reduction in particle loss due to hardness of aggregates of 3% at 300 revolutions and 6% at 500 revolutions can be seen. At -10°C the material is more brittle and a slight increase in particle loss is observed (Figure 10. 10, Figure 10. 12). This increase in particle loss for the harder aggregate is also seen when the compaction energy is increased to 2x50 blows (Figure 10. 11). However, a reduction in particle loss is observed across the board with the use of polymer modified binder.

It can be concluded that with respect to reduction in particle loss the effect of aggregate hardness is minor in comparison to the effect of polymer modified binder.

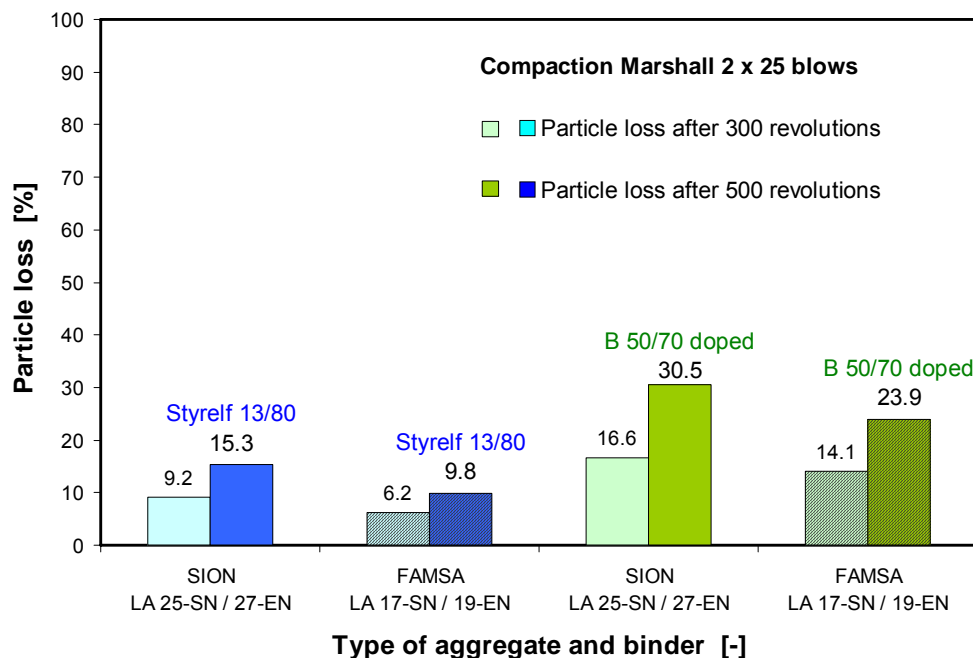


Figure 10. 9 : Particle loss (Cantabrian) at 25°C after 300 and 500 revolutions, effect of hardness of aggregate with different binders (compaction Marshall 2 x 25 blows)

D: Partikelverlust (Cantabro) bei 25°C nach 300 und 500 Umdrehungen, Effekte der Härte der Zuschlagstoffe und der Art des Bindemittels (Marshall Verdichtung mit 2X25 Schläge)

F: Perte de matériaux (Cantabro) à 25°C après 300 et 500 tours, effet de la dureté des granulats avec différents liants (compactage Marshall 2 x 25 coups)

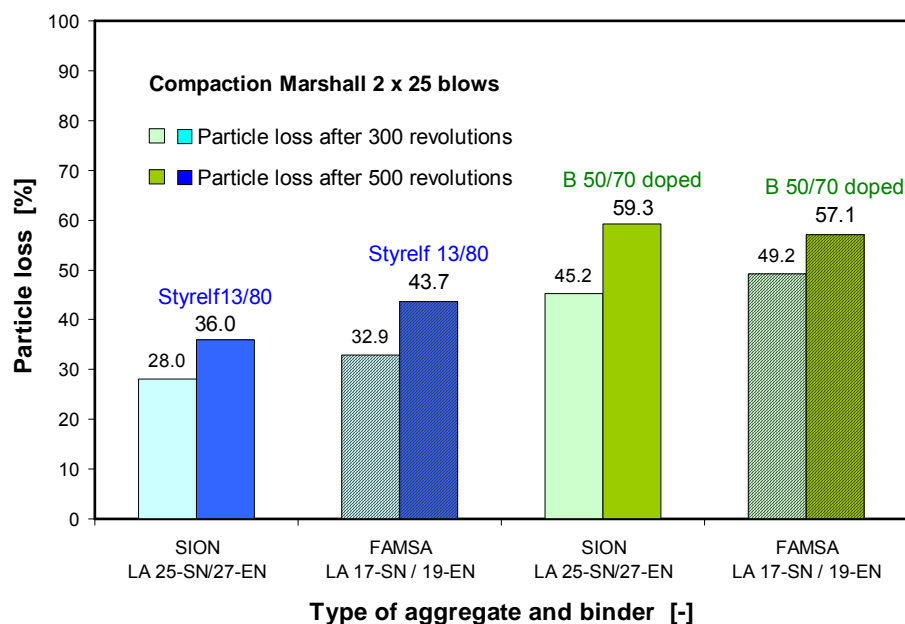


Figure 10. 10 : Particle loss (Cantabrian) at -10°C after 300 and 500 revolutions, effect of hardness aggregate with different binders (compaction Marshall 2 x 25 blows)

D: Partikelverlust (Cantabro) bei -10°C nach 300 und 500 Umdrehungen, Effekte der Härte der Zuschlagstoffe und der Art des Bindemittels (Marshall Verdichtung mit 2X25 Schläge)

F : Perte de matériaux (Cantabro) à -10°C après 300 et 500 tours, effet de la dureté des granulats avec différents liants (compactage Marshall 2 x 25 coups)

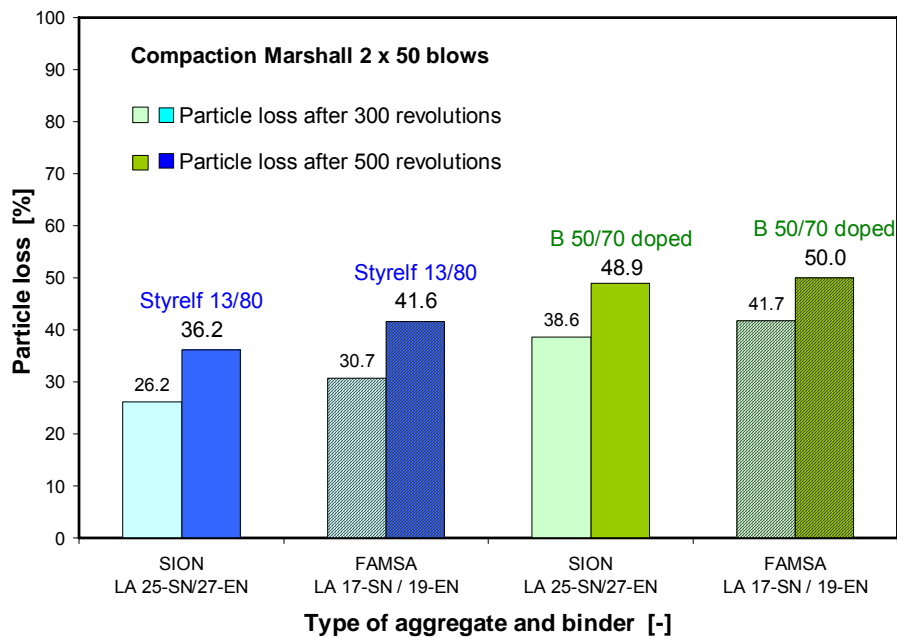


Figure 10. 11 : Particle loss (Cantabrian) at -10°C after 300 and 500 revolutions, effect of aggregate hardness with different binders (compaction Marshall 2 x 50 blows)

D: Partikelverlust (Cantabro) bei -10°C nach 300 und 500 Umdrehungen, Effekte der Härte der Zuschlagstoffe und der Art des Bindemittels (Marshall Verdichtung mit 2X25 Schläge)

F: Perte de matériaux (Cantabro) à -10°C après 300 et 500 tours, effet de la dureté des granulats avec différents liants (compactage Marshall 2 x 50 coups)

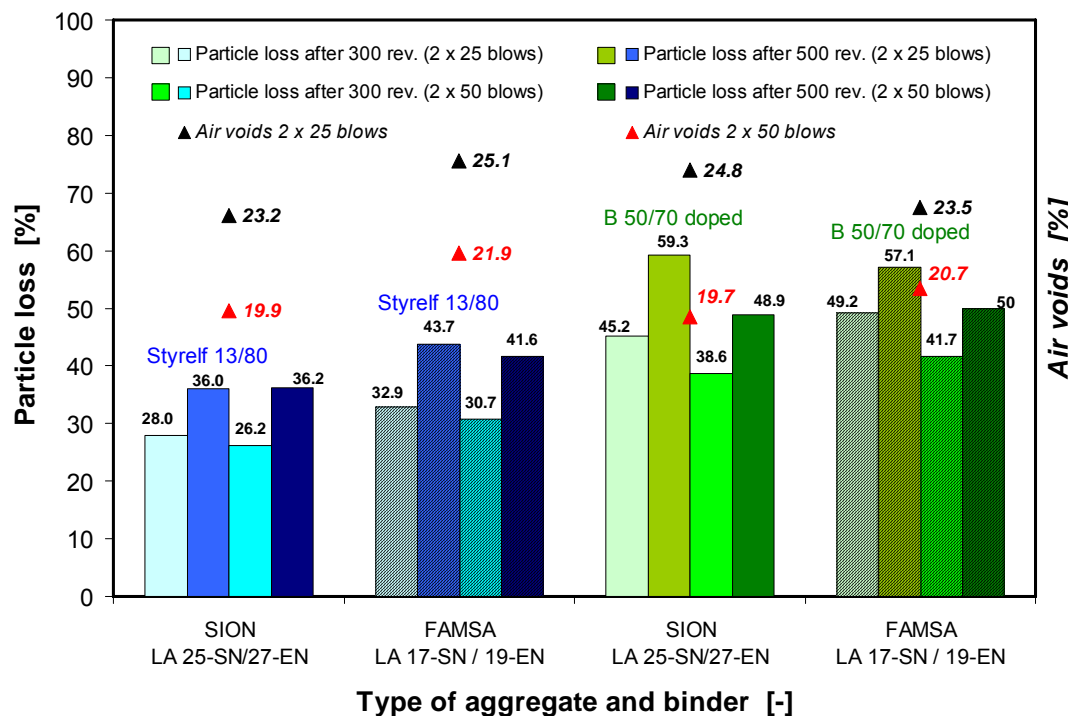


Figure 10. 12 : Particle loss (Cantabrian) at -10°C after 300 and 500 revolutions, effect of hardness of aggregate with different binders (compaction 2 x 25/50 blows) and air voids

D: Partikelverlust (Cantabro) bei -10°C nach 300 und 500 Umdrehungen, Effekte der Härte der Zuschlagstoffe und der Art des Bindemittels (Marshall Verdichtung mit 2X25 Schläge) und Hohlräumgehalt

F: Perte de matériaux (Cantabro) à -10°C après 300 et 500 tours, effet de la dureté des granulats avec différents liants (compactage Marshall 2 x 25/50 coups) et teneur en vides

Effect of Compaction Energy

Cantabrian tests on laboratory produced specimens on the high and low performing mixes, VD9 and AG1 were conducted at two different temperatures 25° and -10°C investigating also the influence of compaction using a Marshall hammer (with 2x50 and 2x25 blows respectively) and gyratory compaction with 40 gyrations.

Figure 10. 13 and Figure 10. 14 show the particle loss in percent, PL, on these two types of mixes VD9 and AG1 respectively. According to laboratory experiments at 25°C and -10°C, AG1 is more susceptible to raveling than VD9 which corroborates field performances of VD5 and AG2. However, VD9 becomes more susceptible to raveling at lower temperatures (Figure 10. 14). Note the clear dependency of particle loss on the air void content regardless of the method of compaction. At 25°C, the cohesive characteristic of the mix plays a significant role in particle loss, whereas at -10°C, the effects of binder, aggregate properties, and compaction level are combined.

In addition the effect of water conditioning and frost thaw cycles at 25°C and -10°C on the results of the Cantabro test was examined. The results for AG1, AG4, VD7, VD8 and VD9 for 300 revolutions and 500 revolutions are shown in Figure 10. 15, Figure 10. 16, Figure 10. 17 and Figure 10. 18. Again in agreement with the field experience (see section 9), in comparison with other mixes, AG1 has consistently a very high particle loss at 300 and 500 revolutions at 25°C and at -10°C. All other mixes are within acceptable limits with VD8 having the lowest particle loss. Generally particle loss of the mixes did not show a strong dependence on water conditioning or frost thaw with AG5 and AG1 being slightly more sensitive in this regard. Based on the obtained results and field performance it is recommended to use a PL=20% after 300 revolutions and a PL=30% after 500 revolutions as a limit to assure good cohesion of the mix. As seen in the figures temperature has a significant effect on the results of the Cantabro test. Therefore, in regions where consistently temperatures of around -10°C is expected PL=50% and PL=60% is recommended for 300 and 500 revolutions respectively.

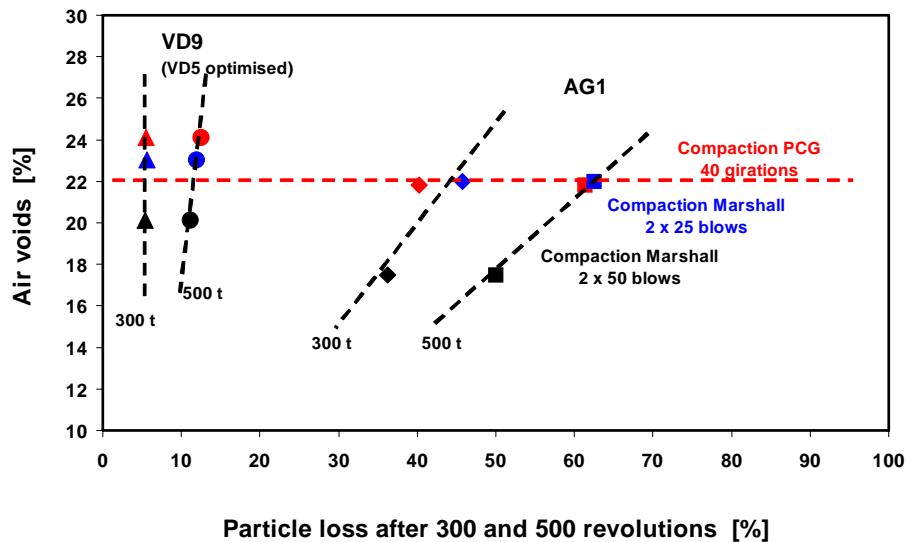


Figure 10. 13 : Particle loss (Cantabrian) at 25°C after 300 and 500 revolutions, with respect to the compaction mode

D: Partikelverlust (Cantabro) bei 25°C nach 300 und 500 Umdrehungen, Effekt der Verdichtungsmethode

F : Perte de matériaux (Cantabro) à 25°C après 300 et 500 tours fonction du mode de compactage

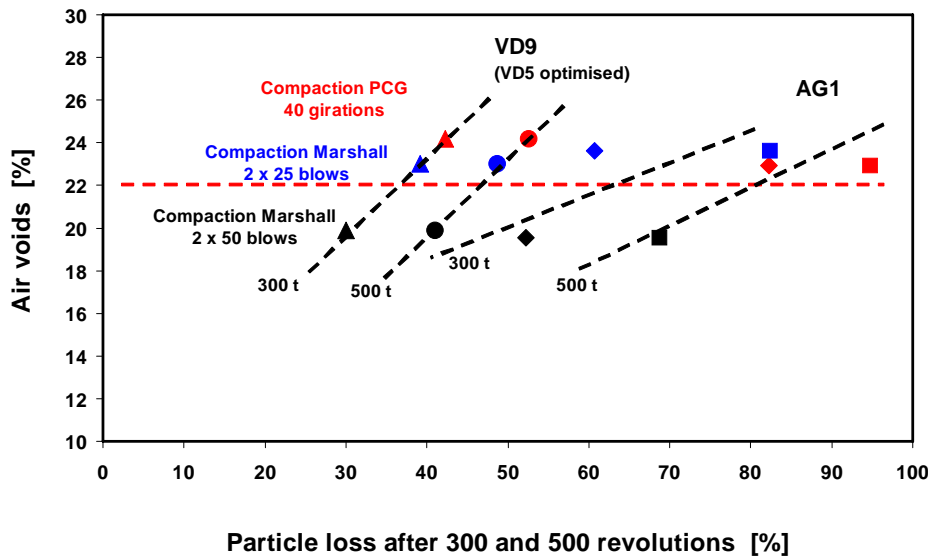


Figure 10.14 : Particle loss (Cantabrian) at -10°C after 300 and 500 revolutions with respect to the compaction mode

D: Partikelverlust (Cantabro) bei -10°C nach 300 und 500 Umdrehungen, Effekt der Verdichtungsmethode

F: Perte de matériaux (Cantabro) à -10°C après 300 et 500 tours fonction du mode de compactage

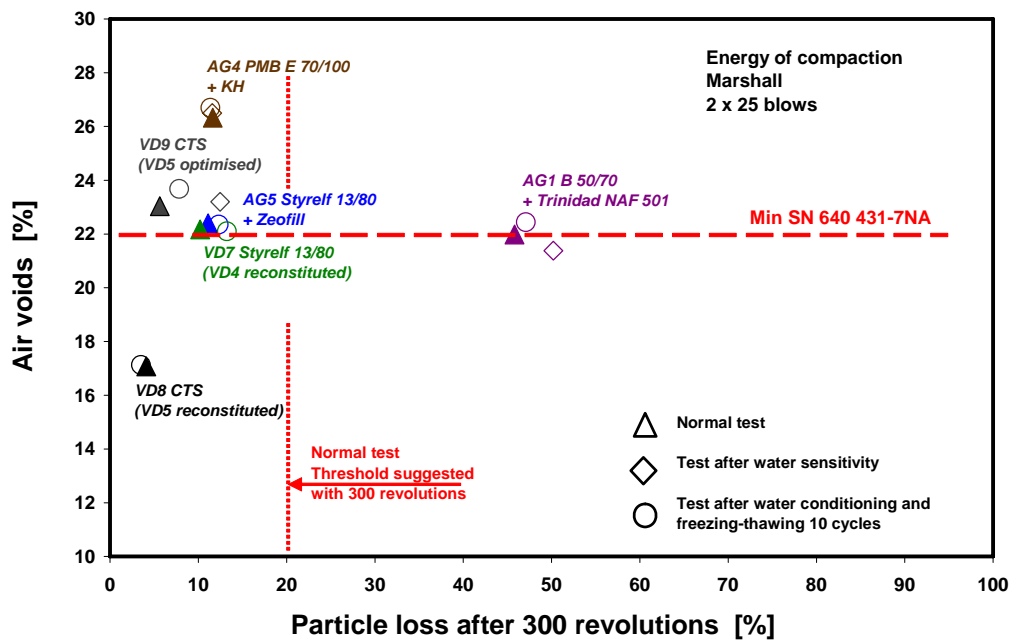


Figure 10.15 : Particle loss (Cantabrian) at 25°C after 300 revolutions – Results of standard test, after water conditioning and freeze-thaw cycles

D: Partikelverlust (Cantabro) bei 25°C nach 300 Umdrehungen, - Ergebnisse vor und nach Wasserr Lagerung und nach Frost-Tau Zyklen

F: Perte de matériaux (Cantabro) à 25°C après 300 tours - Résultats des essais selon : procédure normale, après essai de sensibilité à l'eau et après cycles de gel-dégel

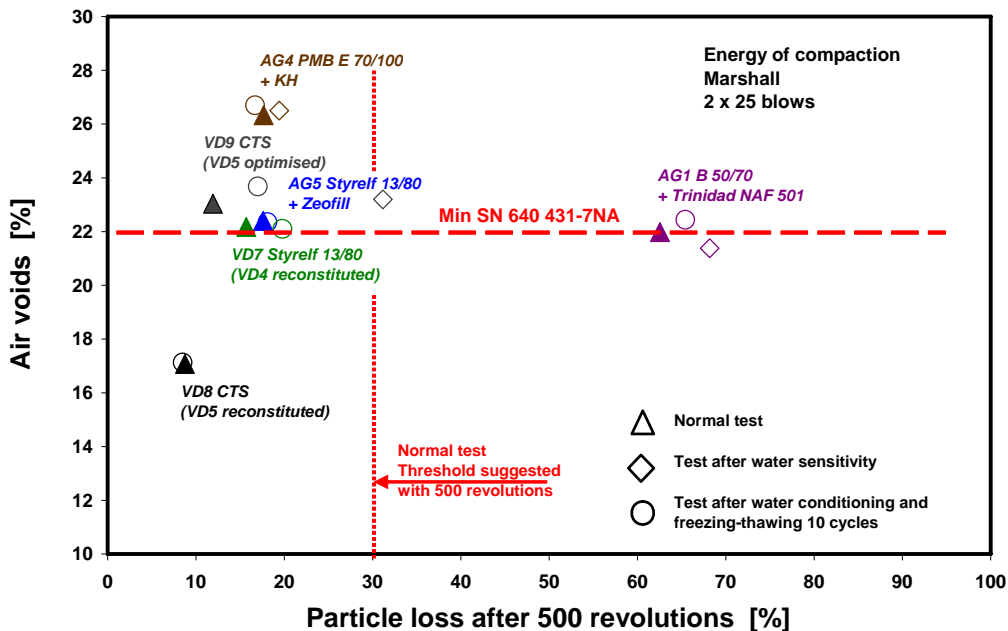


Figure 10. 16: Particle loss (Cantabrian) at 25°C after 500 revolutions – Results of standard, water conditioning and freeze-thaw cycles tests

D: Partikelverlust (Cantabro) bei 25°C nach 500 Umdrehungen, - Ergebnisse vor und nach Wasserrägerung und nach Frost-Tau Zyklen

F: Perte de matériaux (Cantabro) à 25°C après 500 tours - Résultats des essais selon : procédure normale, après essai de sensibilité à l'eau et après cycles de gel-dégel

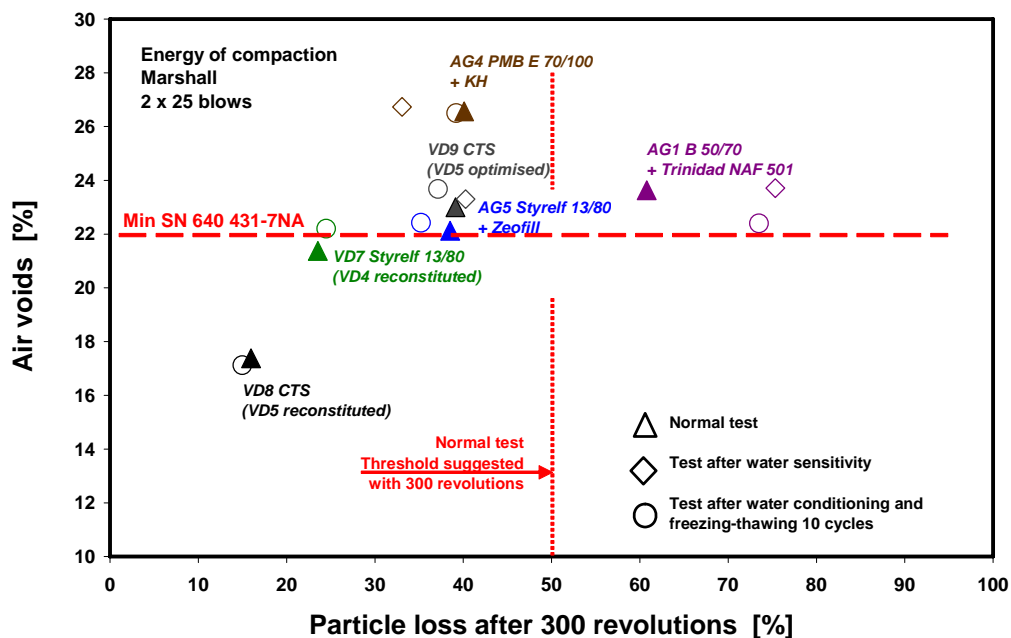


Figure 10. 17: Particle loss (Cantabrian) at -10°C after 300 revolutions – Results of standard test, after water conditioning and freeze-thaw cycles

D: Partikelverlust (Cantabro) bei -10°C nach 300 Umdrehungen, - Ergebnisse vor und nach Wasserrägerung und nach Frost-Tau Zyklen

F: Perte de matériaux (Cantabro) à -10°C après 300 tours - Résultats des essais selon : procédure normale, après essai de sensibilité à l'eau et après cycles de gel-dégel

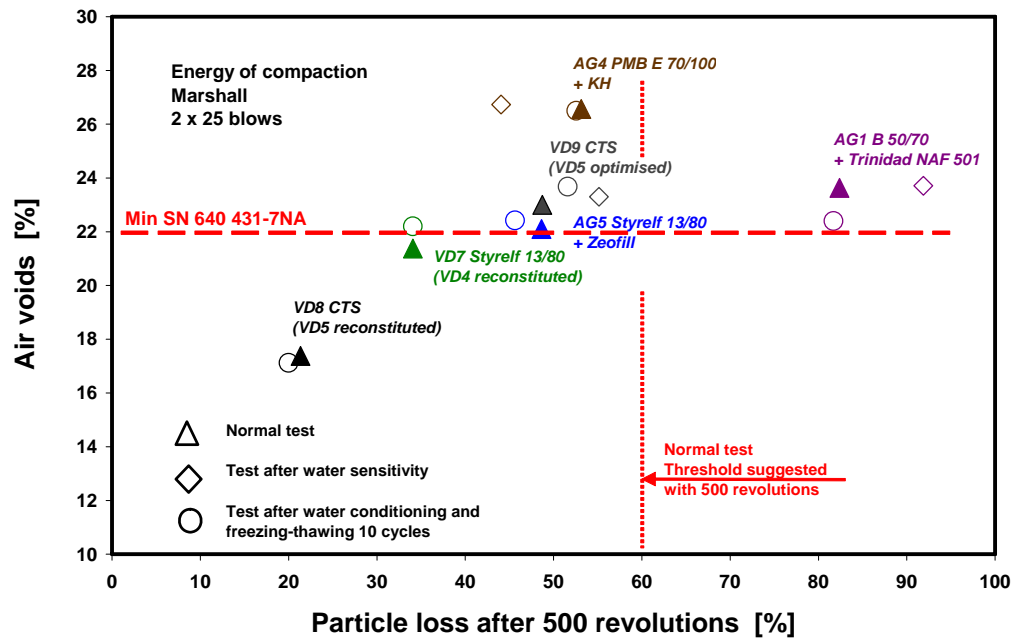


Figure 10.18: Particle loss (Cantabrian) at -10°C after 500 revolutions – Results of standard test, after water conditioning and freeze-thaw cycles

D: Partikelverlust (Cantabro) bei -10°C nach 500 Umdrehungen, - Ergebnisse vor und nach Wasserr Lagerung und nach Frost-Tau Zyklen

F: Perte de matériaux (Cantabro) à -10°C après 500 tours - Résultats des essais selon : procédure normale, après essai de sensibilité à l'eau et après cycles de gel-dégel

10.6. Indirect Tensile Strength (5°C)

The Indirect Tensile Strength of selected cores and laboratory produced specimen were determined in accordance with the pertinent European Standard [22] and as specified in detail in section 9.7. Figure 10.19 shows the indirect tensile strength of 150 mm diameter specimen tested at Empa. The measured specimen dimensions are in the range 150mm to 154mm and the height of the specimen range from 33mm to 75mm. After conditioned in an air chamber at 5°C, three specimens per material type were tested immediately with the load at a controlled speed until fracture occurred in the specimen at peak load P. From P the indirect tensile strength for a specimen ITS was determined as explained in section 9.7. As shown in the figure VD5 and VD6 were ranked the best at 5 °C.

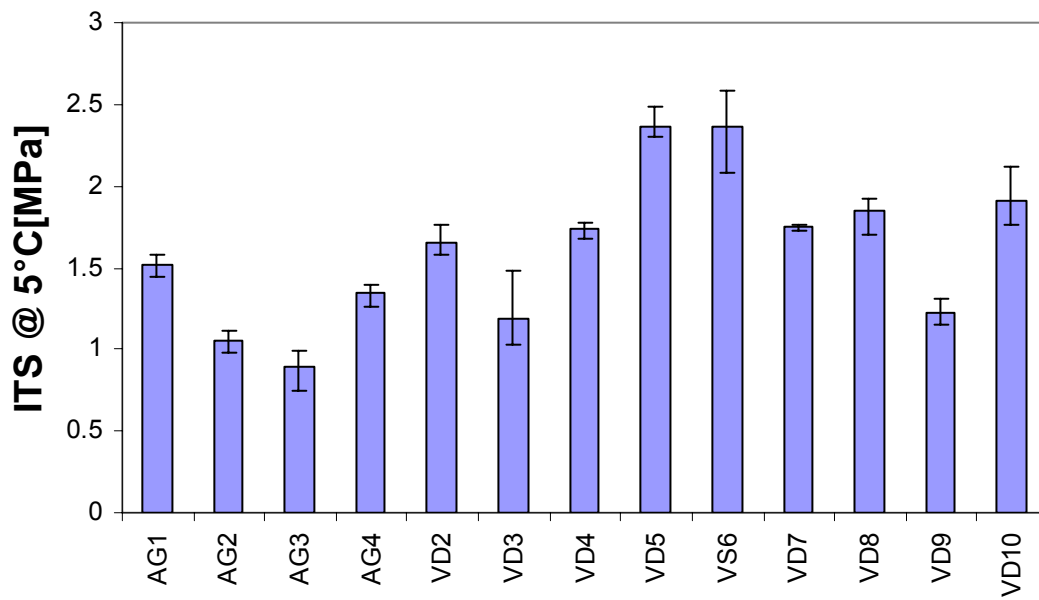


Figure 10. 19 : Indirect Tensile Strength (ITS) at 5°C

D: Indirekter Zugfestigkeit (ITS) bei 5°C

F : Résistance à la traction indirecte (ITS) à 5°

Figure 10. 22 and Figure 10. 24 are for conditioning at 5°C and at 25°C. These figures however do not draw a complete picture about the behavior of the selected materials. A closer look at the load-displacement diagram in Figure 10. 20 which compares AG2 (old Aargau core) and AG3 (new Aargau core) shows that even though both materials reached the same maximum tensile strength; AG3 shows a more ductile behavior under increased displacement leading to a better structural response under load. At cold temperatures VD5 and VS6 ranked the best whereas at 25°C VD2 ranked the best followed by AG1. This can be an indication of the behavior of the binders at various temperatures. Comparison of laboratory prepared mixes that were aimed to duplicate cores, shows good agreement for tests at 25°C and mixed results at 5°C. For example at 5°C there is good agreement between VD4 and VD7 and not a good agreement in the case of ITS between AG3 and AG4 or VD5 and VD9. It can be concluded that the ITS value obtained under warm conditions from laboratory samples correspond better to the values from field samples. However the laboratory values can be used as a valuable ranking tool.

Based on field performance combined with the laboratory test results an ITS= 1.5 MPa is recommended for tests carried out at 5°C and an ITS of 0.5MPa for specimens conditioned to 25°C.

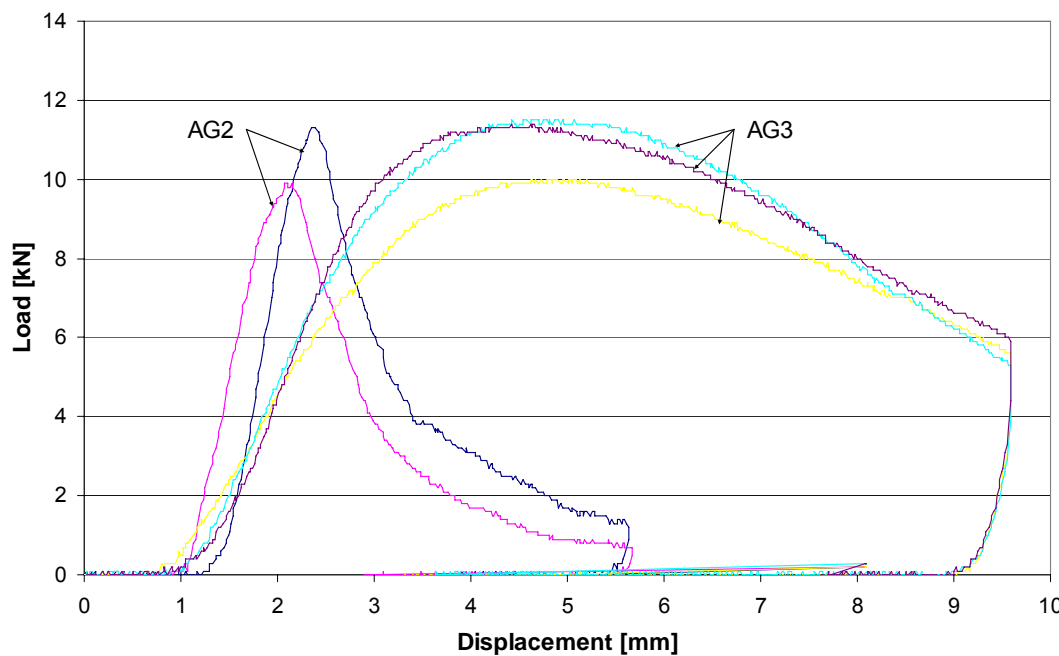


Figure 10. 20: Load displacement diagram of AG2 and AG3 showing a ductile behavior of AG3 in the displacement controlled test

D: Kraft-Weg Diagramm für AG2 und AG3 der weggeregelten Prüfung. Man beachte das duktile Verhalten von AG 3.

F : Représentation de la charge en fonction du déplacement pour les PA AG2 et AG3 montrant un comportement ductile pour AG3 dans le cas de l'essai à déplacement imposé

10.7. Water Sensitivity- Indirect Tensile Strength (25°C)

The experimental set up for water conditioning as well as the resulting fractured specimen is shown in Figure 10. 28 and Figure 10. 29. Figure 10. 23 shows the Indirect Tensile Strength Ratio (ITSR) at 25°C for selected cores and laboratory produced specimen. Figure 10. 21 and Figure 10. 22 show the peak loads to failure and the ITS at 25°C respectively. Tests were performed on the cores which means these cores with the exception of AG3 were all in an aged state. The water sensitivity criteria in the standards (SN 640 431-7NA) however is for an un-aged specimen. Still after having aged for various amounts of years all cores with the exception of AG2 and VD5 meet the criteria of $\text{ITSR} \geq 70\%$. This test did not rank VD5 as the least water sensitive. However field performance indicates that the high ITS value at 5°C (Figure 10. 19) compensates for the higher water sensitivity of this mix (Figure 10. 23). It can be deduced that the high ITS results in fewer cracks and less stripping of the binder from the aggregates.

Even though the peak load experienced by VD10 was the highest it should be noted that the specimens were deeper with a larger surface area which leads to similar values of strength when the effect of surface area is also taken into account.

To determine if the laboratory prepared specimen did predict the behavior of field cores AG3, VD4 and VD5 should be compared with the corresponding lab samples of AG4, VD7 and VD8. Even though in absolute terms the agreement is not very close (Figure 10. 22) in relative terms and as a tool for ranking of the materials there is very good agreement between the core ITS values and laboratory produced specimen (Figure 10. 25). VD2 with the Colflex binder shows the best resistance to water in absolute terms followed by AG1

However in relative terms from the indirect tensile strength ratio (Figure 10. 23) the Argau materials with the exception of AG2 are ranked best. The poor field performance of AG2 shows that even though AG1 had good laboratory performance, the lack of polymer modifiers led to premature aging and inadequate field performance. VD2 is followed closely by VS6 and VD5 for all

three cases ITS at 5°C, at 25°C and ITSR at 25°C. This high laboratory performance corroborates field experience leading the authors to recommend an ITSR=70% for standardization.

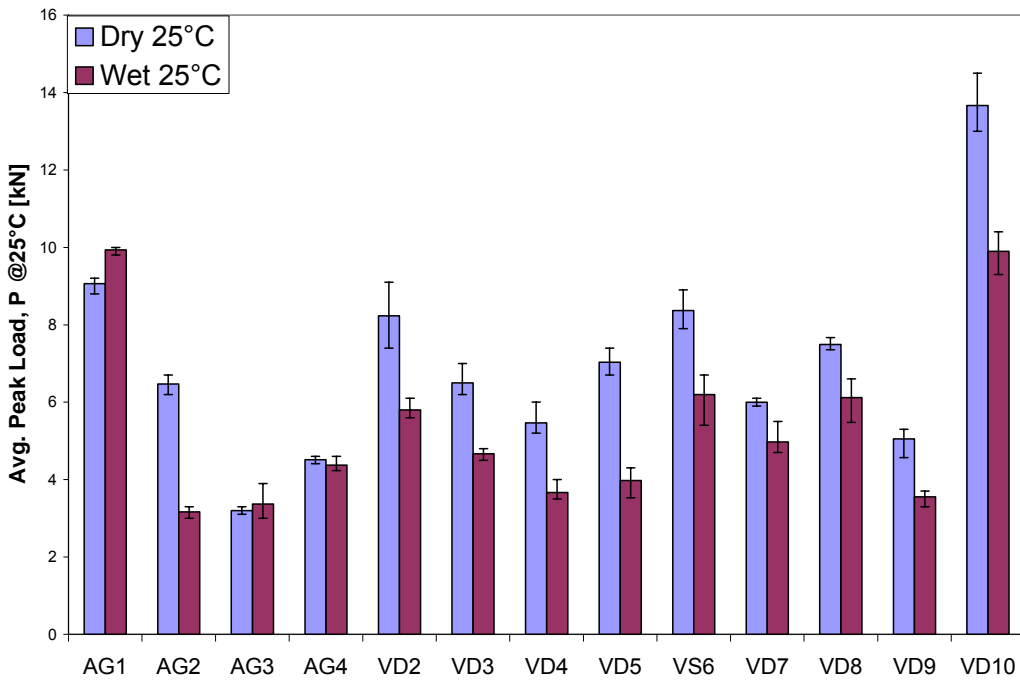


Figure 10. 21: Peak load to failure at 25

D: Maximle Bruchkraft bei 25°C

F: Charge maximale de rupture à 25°C

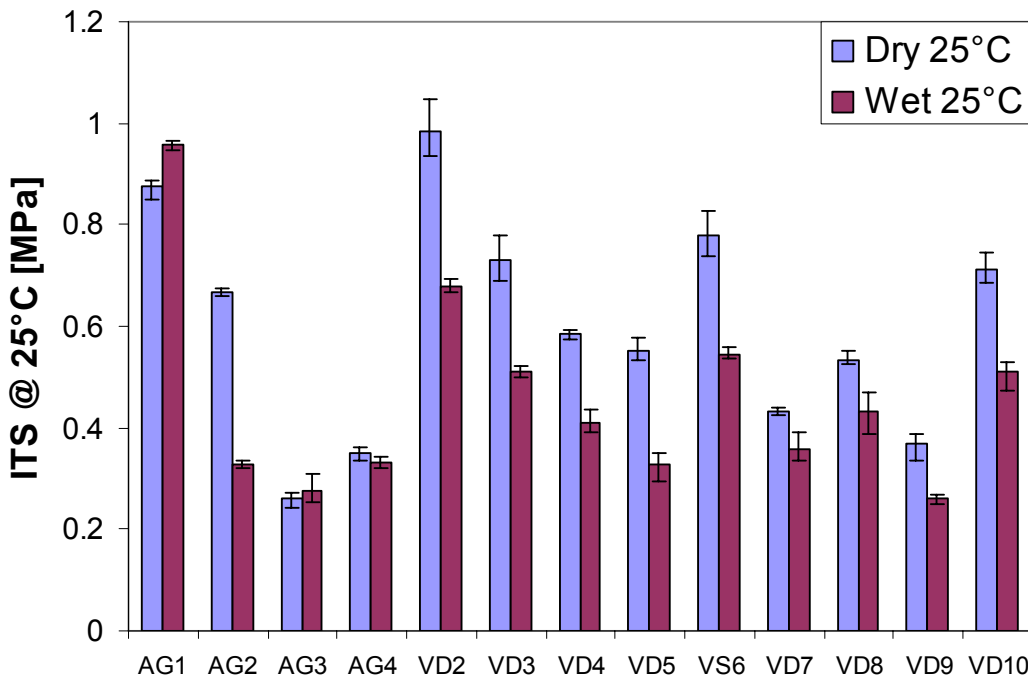
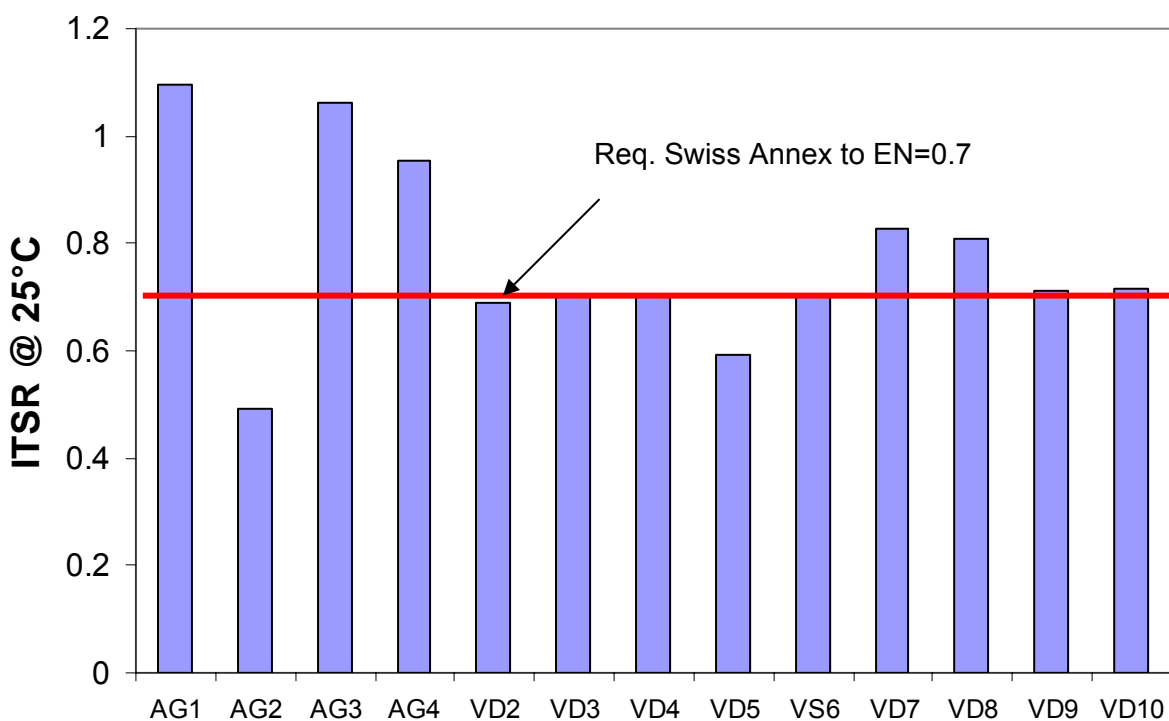


Figure 10. 22 : Indirect tensile strength (ITS) at 25°C with error bars indicating maximum and minimum values.

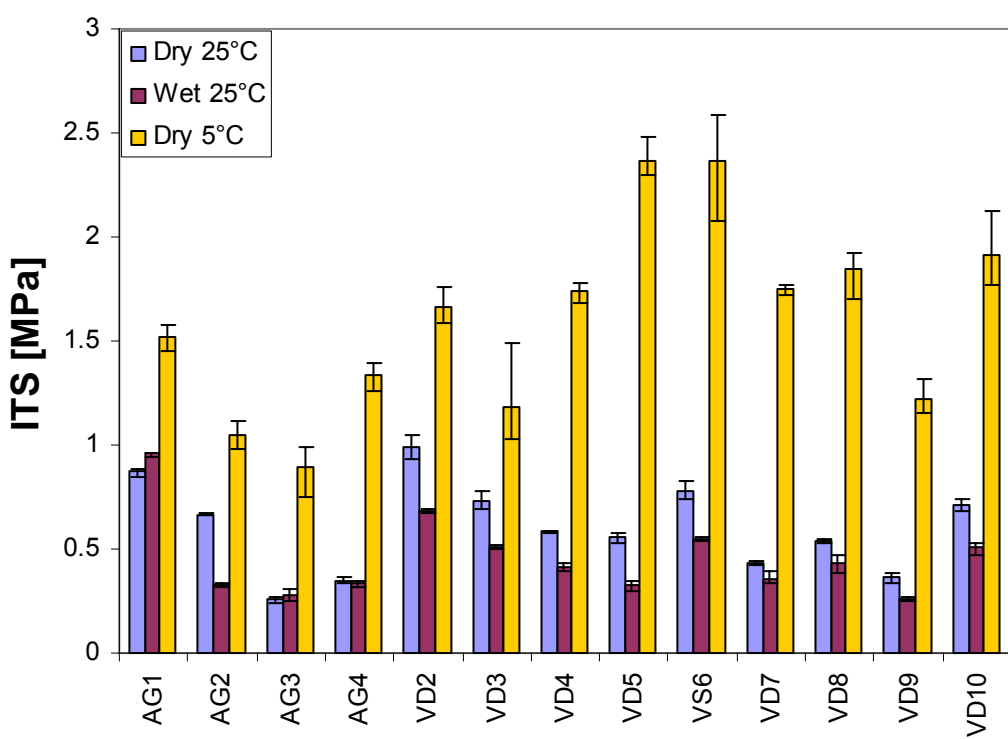
D: Indirekter Zugfestigkeits (ITS) bei 25°C mit Angabe des Wertebereichs

F: Résistance à la traction indirecte (ITS) à 25°C avec domaine de dispersion maximum et minimum

**Figure 10. 23 : Indirect Tensile Strength Ratio (ITSR) at 25°C**

D : Wasserempfindlichkeit (ITSR) bei 25°C

F : Sensibilité à l'eau (Ratio ITSР) à 25°C

**Figure 10. 24 : Indirect Tensile Strength at 5°C and 25°C**

D : Indirekter Zuversuch bei 5°C und 25°C

F : Résistance à la traction indirecte à 5°C et 25°C

Effect of compaction mode

In order to investigate the effect of compaction mode and resulting compaction energy on the ITSR, specimen of VD9 and AG1 were compacted using the gyratory compactor with 40 gyrations, the Marshall hammer with 2x25 blows and 2x50 blows. Figure 10. 25 shows the ITSR with respect to compaction mode and total air void content. Using 2x50 blows, the ITSR of VD9 has fallen about 17% and AG1 by about 9% in comparison to the values for 2x25 blows. The results obtained by the gyratory compaction method lie in between the values obtained by the other two compaction methods. It is shown that the 2x50 blows results in a reduction in air void content as well as ITSR. This can be a result of micro cracks forming within the material during the 2x50 blows compaction, leading to elevated water sensitivity. It is also possible that the petrography and mechanical properties of the material contribute to these results.

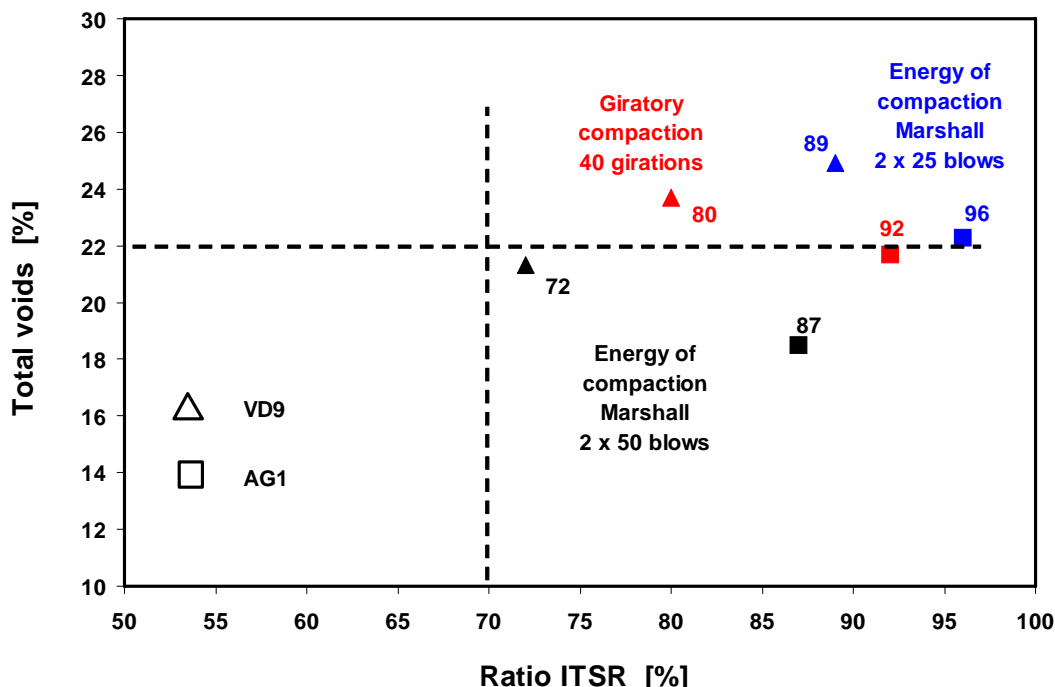


Figure 10. 25: Indirect Tensile Strength Ratio (ITSR) at 25°C - Effect of compaction mode

D: Verhältnis indirekter Zugfestigkeiten (ITSR) bei 25°C- Effekt der Verdichtungsmethode

F: Rapport de résistance en traction indirecte (ITSR) à 25°C - Effet du mode de compactage

Effect of aging on the indirect tensile strength

The effect of aging of the Aargau material can be seen in Figure 10. 26 and Figure 10. 27. AG 1 is the original mix from the job site and AG2 is the core before the renewal of the pavement. As shown in the figure on the average, a reduction of the ITS by 31% is obtained. The resistance to damage due to water has also been reduced by 55%.as seen in Figure 10. 23.

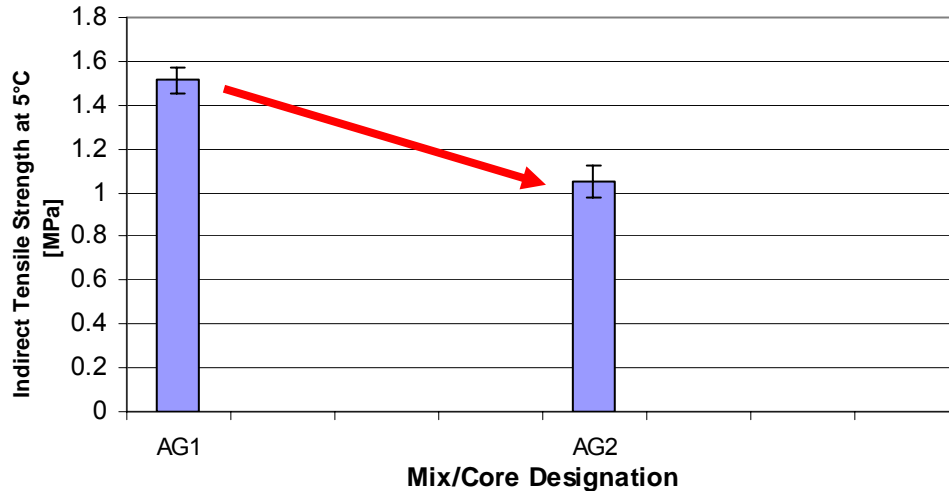


Figure 10. 26: Effect of aging as characterized by the indirect tensile strength (ITS)

D: Wirkung der Alterung, charakterisiert durch den indirekten Festigkeit

F: Effet du vieillissement sur les caractéristiques de résistance à la traction indirecte (ITS)

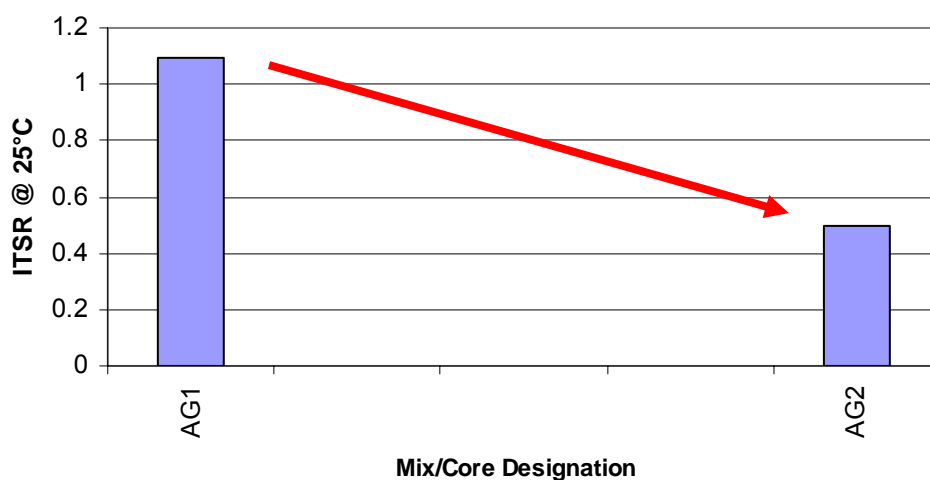


Figure 10. 27: Effect of aging as characterized by the indirect tensile strength ratio (ITSR)

D: Wirkung der Alterung auf die Wasserempfindlichkeit (ITSR)

F: Effet du vieillissement sur les caractéristiques de sensibilité à l'eau (ratio ISTR)

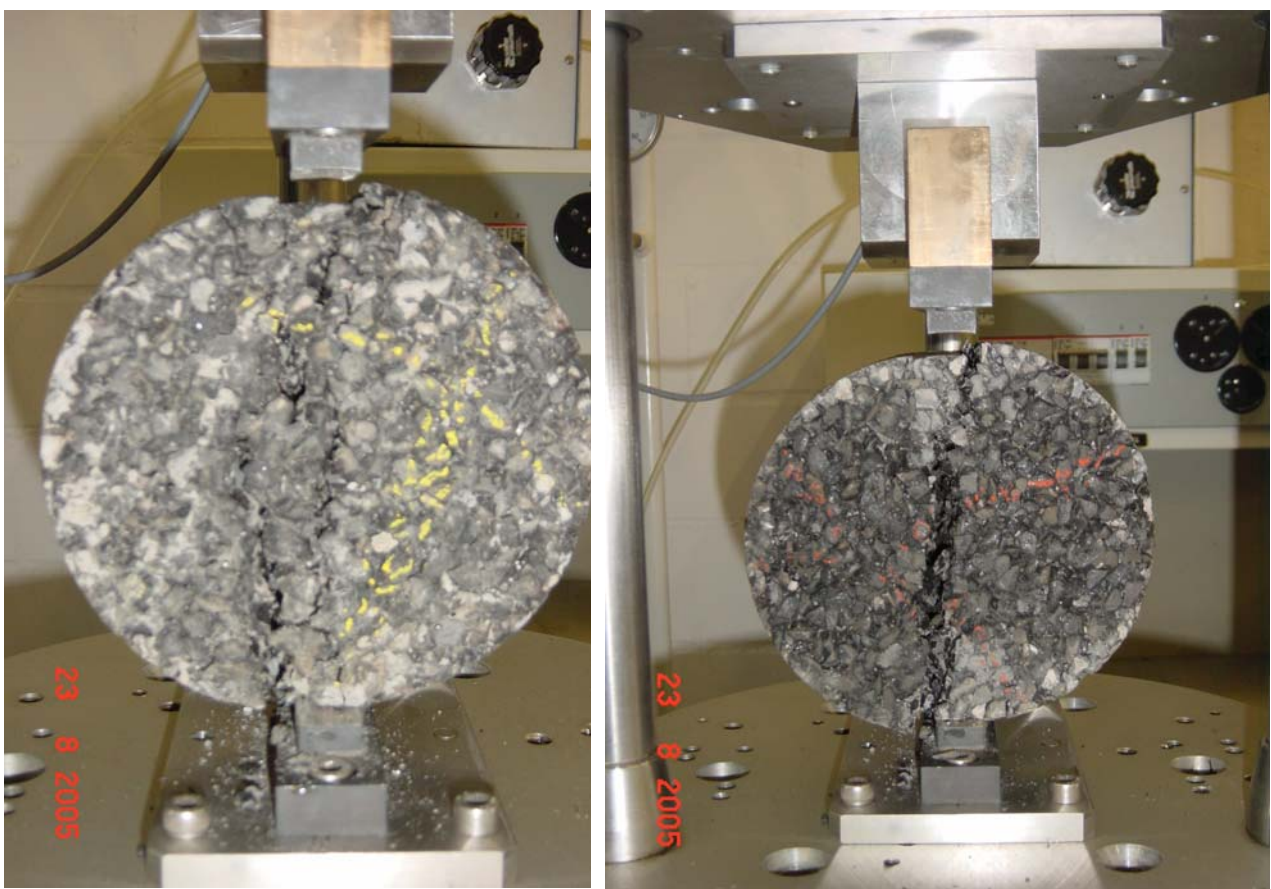


Figure 10. 28: Failure of the twinlayer system at 25°C left and example of brittle fracture at 5°C right

D:Bruch des zweischichtigen PA bei 25°C (links) und Beispiel eines Sprödbruches (rechts)
F: Rupture ductile à 25°C sur PA bicouches (gauche) et rupture fragile à 5°C (droite)



Figure 10. 29 : Conditioning of the specimen in a water bath (left) and fracture surface of the twinlayer after ITS test at 5°C.

D:Konditionieren der Prüfkörper im Wasser (links) und Bruchfläche des zweischichtigen PA nach dem indirekten Zugfestigkeit bei 5°C rechts
F: Conditionnement d'un échantillon dans bain thermostatique (gauche) et plan de rupture sur PA bicouches après essai ITS à 5°C

10.8. Rheology of the Binder Using the Dynamic Shear Rheometer DSR

The DSR test was performed on recovered binder. As seen in the results in Figure 10. 30, all curves show moduli along a curved characteristic line of a polymer modified binder except the binder for AG1 which is not polymer modified. The scatter of the results between the binder types is an indication of different aging states of the binders. For example VD2 and VD3 are 13 and 12 years old respectively at the time the cores were removed and as a result are the stiffest. Comparing DSR results and those from CAST (Figure 10. 32) shows a correlation between the binder strength and the mix strength. In most cases choosing a high performance binder resulted in a high performance mix.

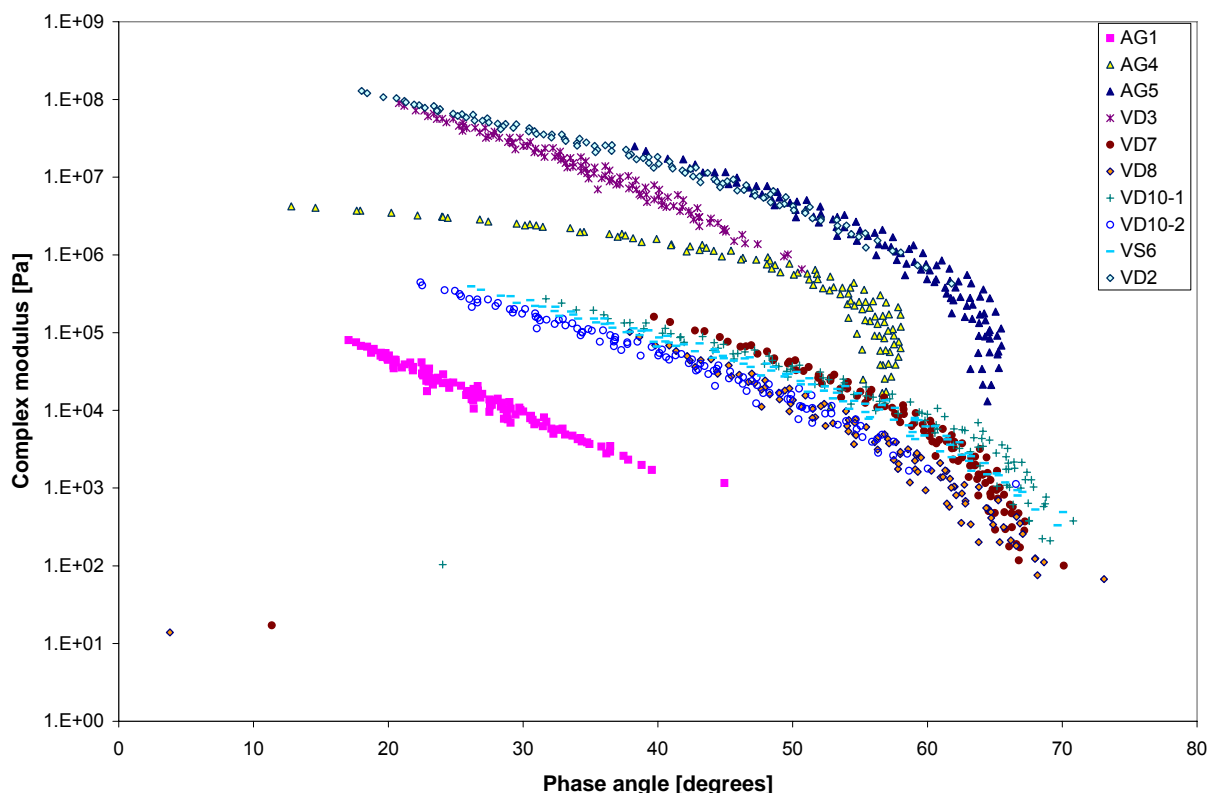


Figure 10. 30 : Black diagrams for the recovered binders

D: *Black Diagramm für die rückgewonnenen Bindemittel*

F: *Diagramme de Black - Liants récupérés*

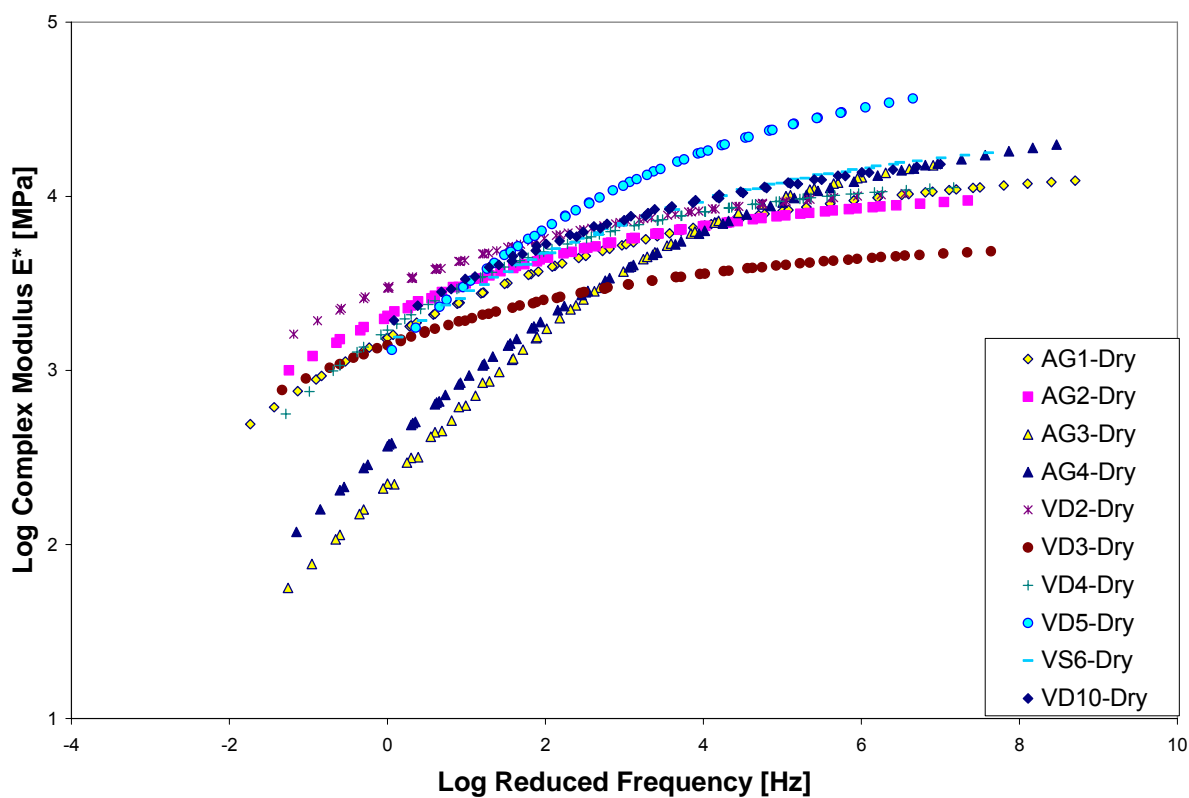
10.9. Stiffness

Coaxial Shear Test (CAST)

Cast results part 1- Modulus

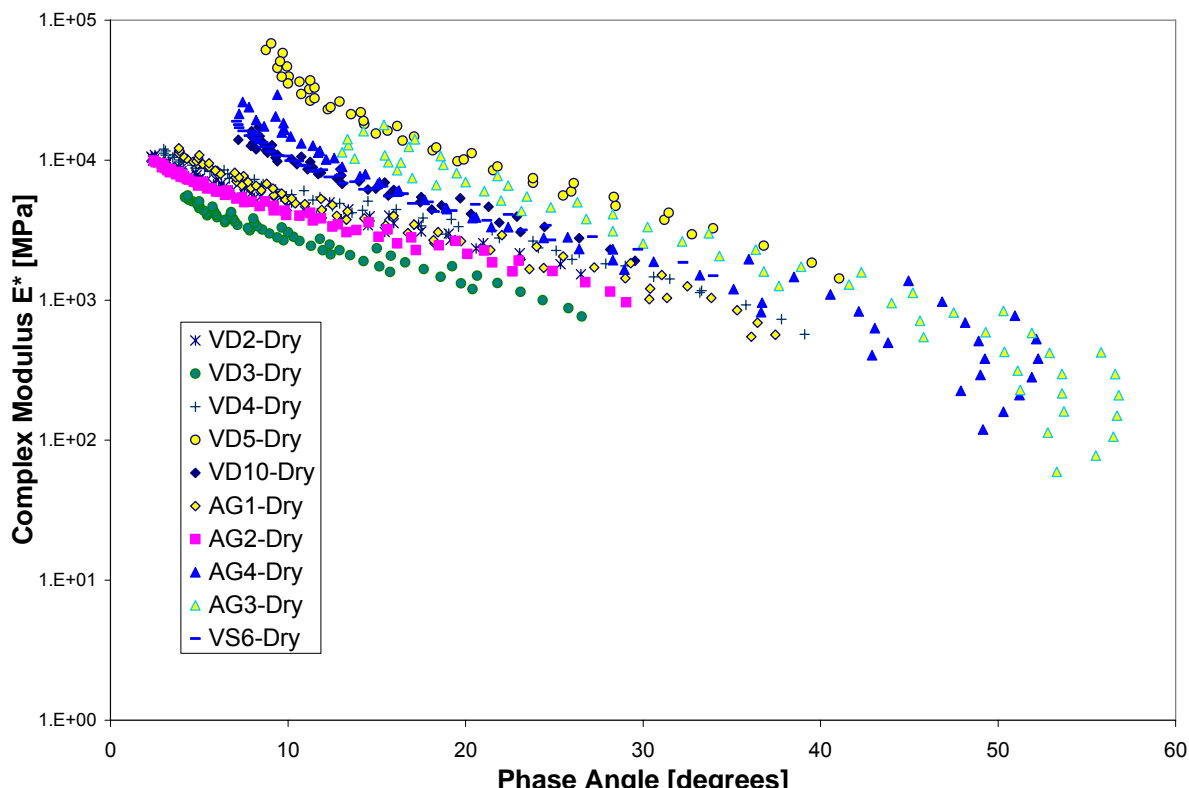
As indicated in section 9.9 the specimens were tested at -10, -5, 0, 5, 10, 15 and 20°C. The values presented are the average results for two specimens.

Comparison of AG1 and AG2 as well as AG3 and AG4 demonstrate that the field cores were well reproducible in the laboratory. Most materials fall within a band as seen in Figure 10. 31. At higher frequencies VD3 falls below this band and VD5 falls above this band. Similar to the results of other tests in this research project, the behavior of AG3 and AG4 is considerably different with the other materials in this case especially with lower values of modulus at lower frequencies. VD10 that is the twin-lay was tested as a system consisting of the two layers. It can be seen from the Figure that the modulus is within the band indicating the average performance of the materials tested.

**Figure 10. 31: Master curves from CAST, at reference temperature of 25°C**

D: Master-Kurven für 25°C, KAST Modulbestimmungen

F: Essai de rigidité CAST - Courbe maîtresse à la température de référence de 25°C

**Figure 10. 32: Results of CAST ; Black diagrams**

D: Blackdiagramme, KAST Modulbestimmungen

F: Essai de rigidité CAST - Diagramme de Black

The Black diagrams shown in Figure 10. 32 display the complex modulus vs. phase angle. All materials again fall into a band defined by VD3 as the lower limit and VD5 as the upper limit. The curve characteristic of a polymer modified binder is most defined in case of AG3 and AG4.

For standardization purposes; at average frequencies (ca 4Hz) and 25°C temperature, a modulus between 3000 MPa and 7000MPa is recommended.

CAST results Part 2-water sensitivity

In order to determine the sensitivity of the materials in the presence of water, CAST tests were performed in a dry state and under water. In order to simulate field conditions the development of the mechanical properties of specimens under combination of repeated loading, water immersion and temperature cycles was studied. For example, it can be seen that the wet AG1 specimen is already displaying a reduction in modulus after the third cycle of loading in comparison to the dry specimen. This sensitivity is more exaggerated in case of AG2 which is the core that was already in an aged state (Figure 10. 34). However the new pavement AG3 shows very little sensitivity to water (Figure 10. 35) as was also seen in the ITS.

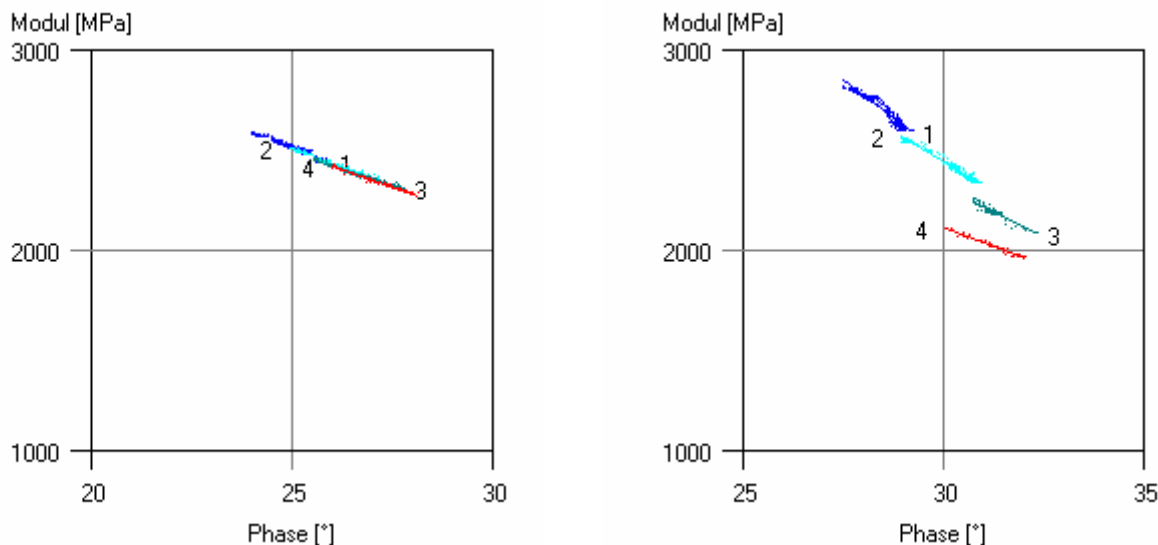


Figure 10. 33: Water sensitivity of AG1 dry specimen under repeated loading left, and wet specimen under repeated loading right

D: Wasserempfindlichkeit der AG1 unter wiederholter Belastung im trockenen Zustand links und nassen Zustand rechts

F: Incidence de la répétition de charges sur le module de rigidité d'éprouvettes AG1, à sec (gauche) et après essai de sensibilité à l'eau (droite)

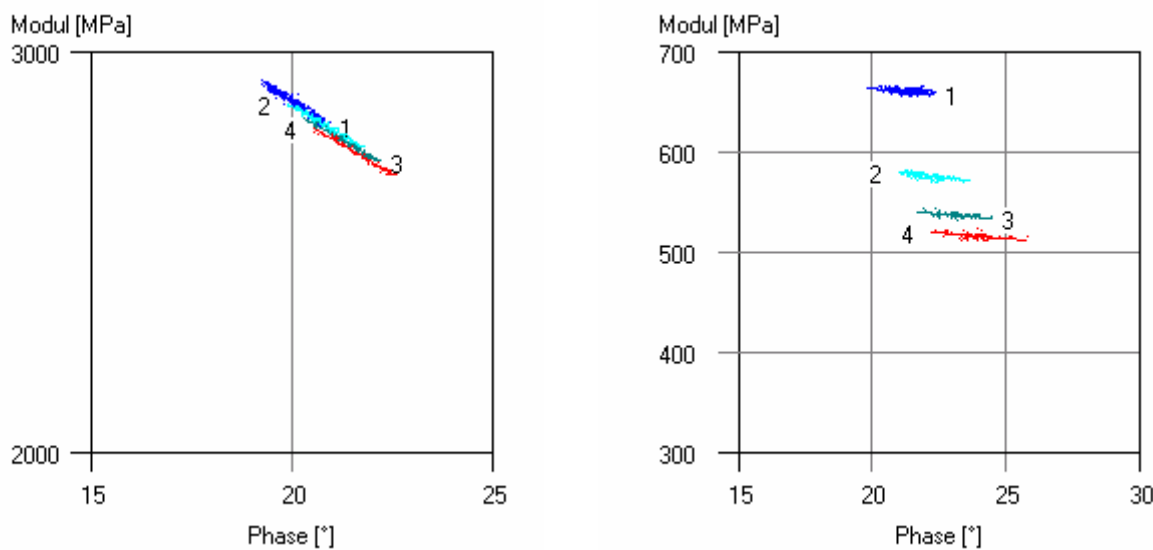


Figure 10. 34: Water sensitivity of AG2 dry specimen under repeated loading left, and wet specimen under repeated loading right

D: Wasserempfindlichkeit der AG2 unter wiederholter Belastung im trockenen Zustand links und nassen Zustand rechts

F: Incidence de la répétition de charges sur le module de rigidité d'éprouvettes AG2, à sec (gauche) et après essai de sensibilité à l'eau (droite)

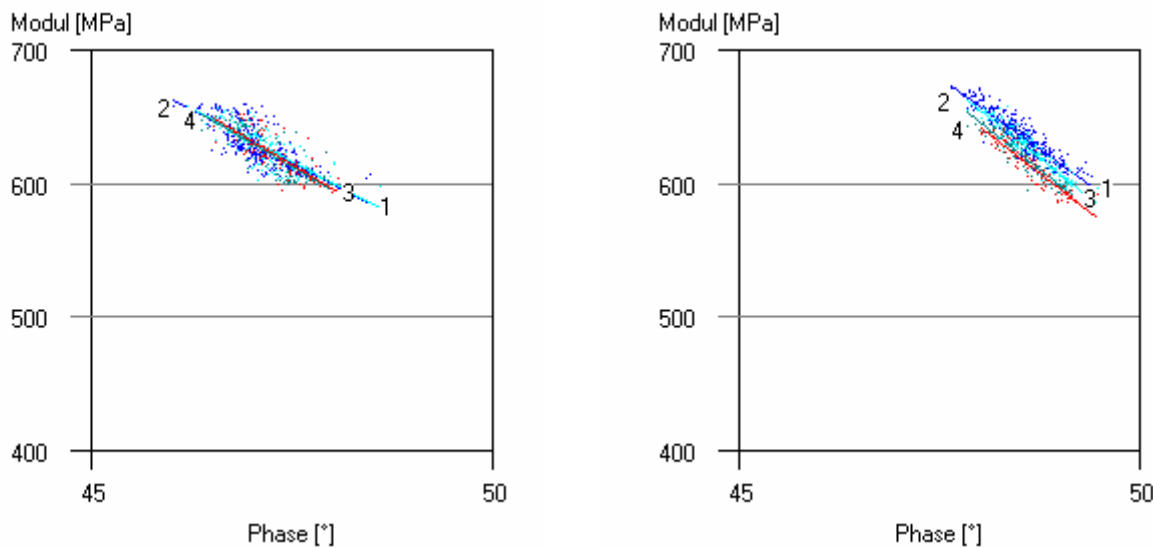


Figure 10. 35: Water sensitivity of AG3 dry specimen under repeated loading left, and wet specimen under repeated loading right

D: Wasserempfindlichkeit der AG3 unter wiederholter Belastung im trockenen Zustand links und nassen Zustand rechts

F: Incidence de la répétition de charges sur le module de rigidité d'éprouvettes AG3, à sec (gauche) et après essai de sensibilité à l'eau (droite)

Two Point Bending Test

As explained earlier complex modulus E * of mixes AG1, VD7, VD8 and VD9 was determined in the temperature range of -10°C - 30°C for frequencies of 1, 3, 10, 25 and 40 Hz as well as the representation of the master curve at reference temperature 15°C gives some information on material rigidity. The AG1 mix differs clearly from the three other materials as seen from Figure 10. 36. It is relatively flat that reveals a lower thermal susceptibility mainly for low "reduced

frequencies" (high temperatures) as compared to the other mixes. In the range of the high frequencies (low temperatures), it is known that level of compactness plays a significant role on the modulus E^* . One notices for mixes VD8 and VD9 (same binder), that the reduction in the voids content leads to an increase in the modulus E^* . In addition, a lower values of modulus is noticed at high frequencies for the VD9 mix as compared to the VD7 one (same porosity and binder BmP). This is an indication of the mechanical behavior at low temperatures which augurs limited brittleness behavior.

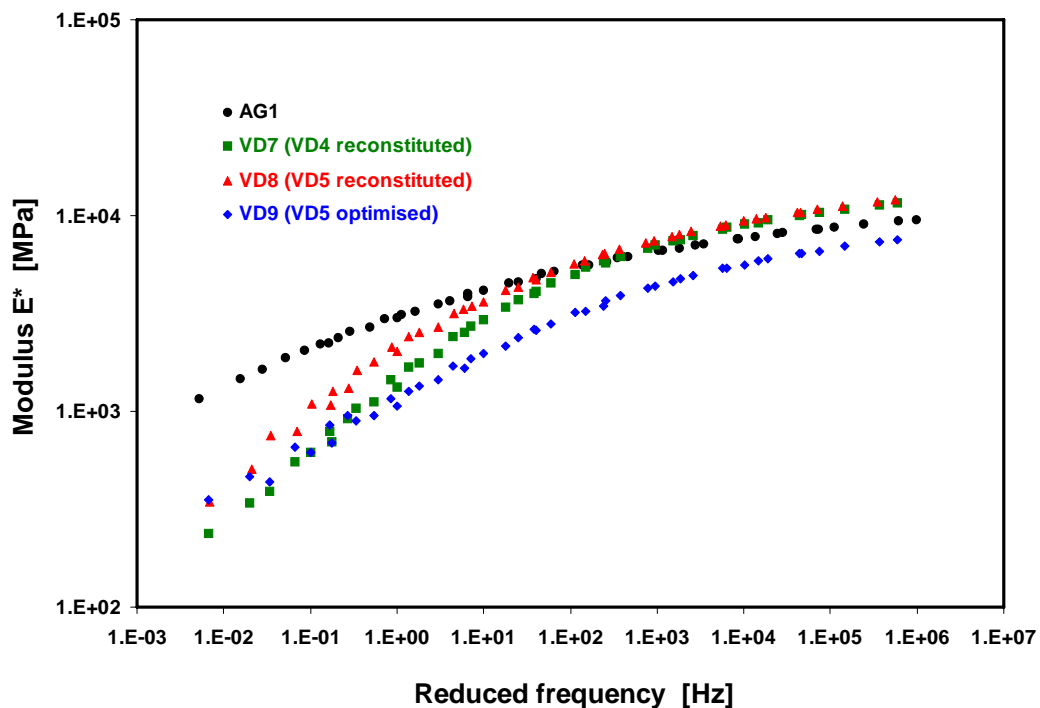


Figure 10. 36 : Master curves from Two Point Bending Test, at ref. temperature of 15°C

D: Master-Kurven für 15°C, Modulbestimmungen mit der Zweipunktbiegung

F: Essai en flexion 2 points - Courbe maîtresse à la température de référence de 15°C

Direct Tension

The test was successfully applied to dense asphalt mixes; showing an excellent indication as to the mechanical behavior at low temperatures of the bituminous mixes. However, limited data is available for the mechanical characterization of porous asphalt. The direct tensile test carried out at low temperatures and with low speed of $2000 \cdot 10^{-6}$ m/m.h gives relevant information with regard to the resistance and the strain of asphalt concrete. It should be specified that compared to the procedure for dense graded mixes used by Pucci [46], in this case the strain rate was increased by a factor 10 (from 200 to $2000 \cdot 10^{-6}$ m/m.h); it has been shown that in this range, strain rate had a weak influence on the results.

One sample has been tested for each temperature. Results are presented in Figure 10. 37, Figure 10. 38 and Figure 10. 39 as stress strain curves. As function of temperature, the rupture occurs either by brittle cracking or by a plastic flow the threshold of which is indicated in the figures. The thermal sensitivity of the materials appears clearly on these curves. The AG1 mix is characterized by a low mechanical resistance confirmed by the behavior observed in situ (aggregate loss). For the test carried out for a temperature of -15°C, the maximum stress recorded is lower than 1 MPa and the rupture strain is of about $250 \cdot 10^{-6}$ m/m. Bituminous mix VD7 and VD9 characterized by a higher mechanical resistance (Cantabro test) exhibit a higher stress level for a temperature of -15°C (higher than 2 MPa) with a maximum strain of about $750 \cdot 10^{-6}$ m/m for the VD7 mix and $600 \cdot 10^{-6}$ m/m for VD9 mix.

The results recorded here constitute a first step in order to adjust the Direct Tensile Test to the study of porous asphalt. The recorded results show that a limit of 1 MPa could be adopted for the

characterization of the PA mix. This empirical value is consistent with a microstructural approach of the material. The decrease in the density of the inter-granular contacts for porous asphalt mix results in an increase in the load on the binder. Therefore the 4 MPa limit used for dense asphalt mix must be reduced to 1.5MPa in the case of the porous bituminous mix.

A more detailed study must be carried out in order to validate or adjust this limiting value. However, the preliminary results show that the test appears well adapted for the characterization of this kind of material.

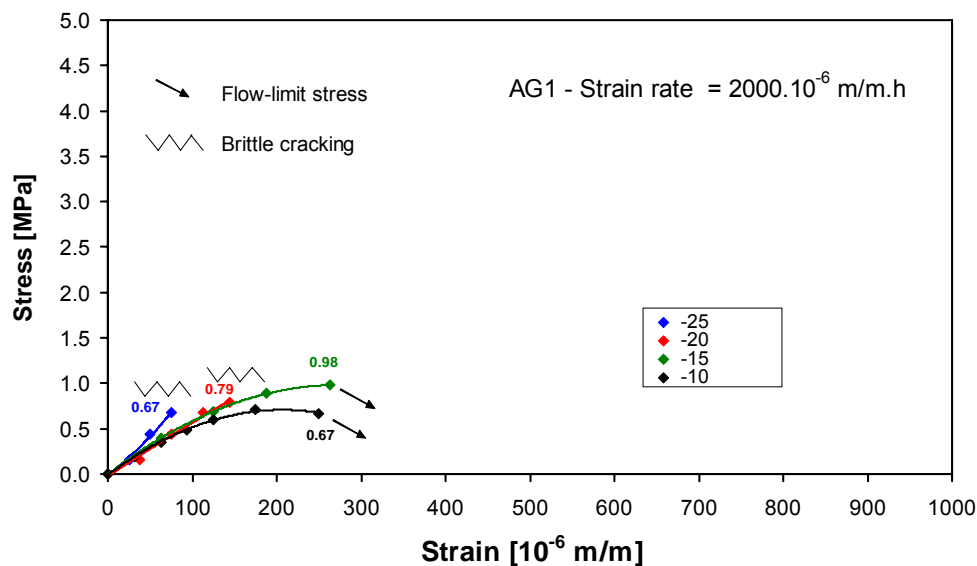


Figure 10.37 : Results of the Direct Tensile Test for AG1

D: Ergebnisse des direkten Zugversuchs für AG1

F: Résultats de l'essai de traction directe sur PA AG1

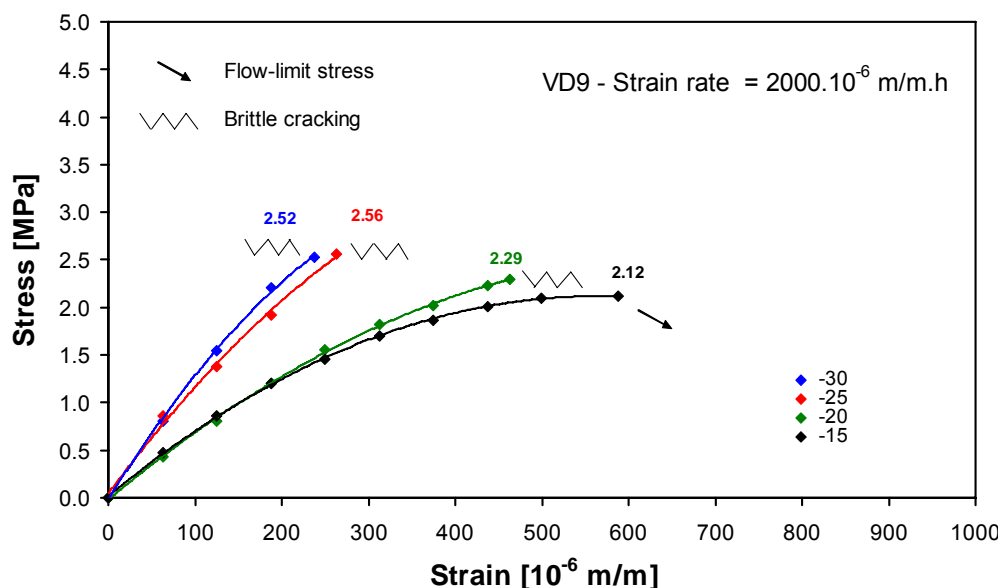


Figure 10.38: Results of the Direct Tensile Test for VD9

D: Ergebnisse des direkten Zugversuchs für VD9

F: Résultats de l'essai de traction directe sur PA

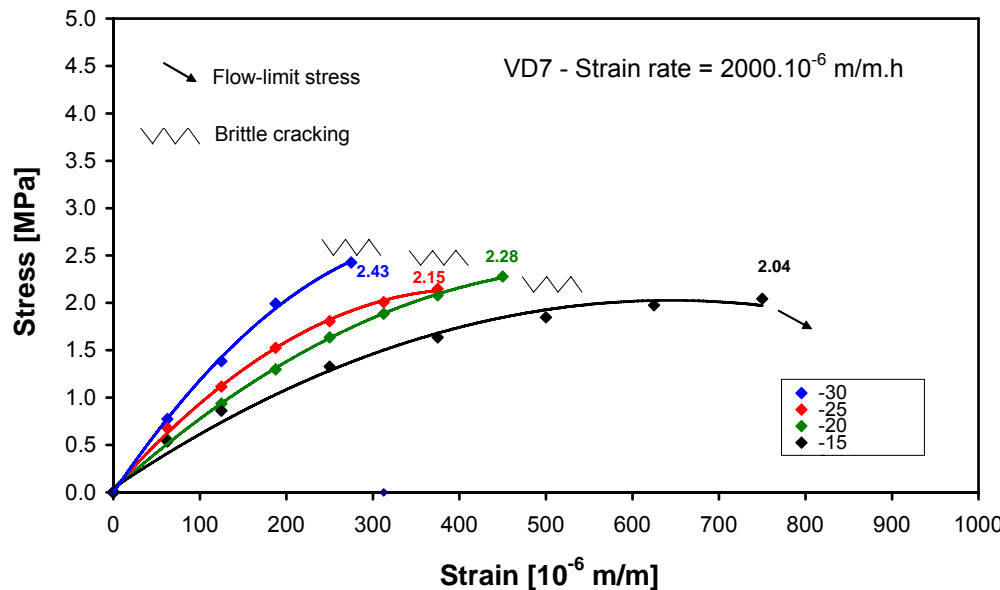


Figure 10.39: Results of the Direct Tensile Test for VD7

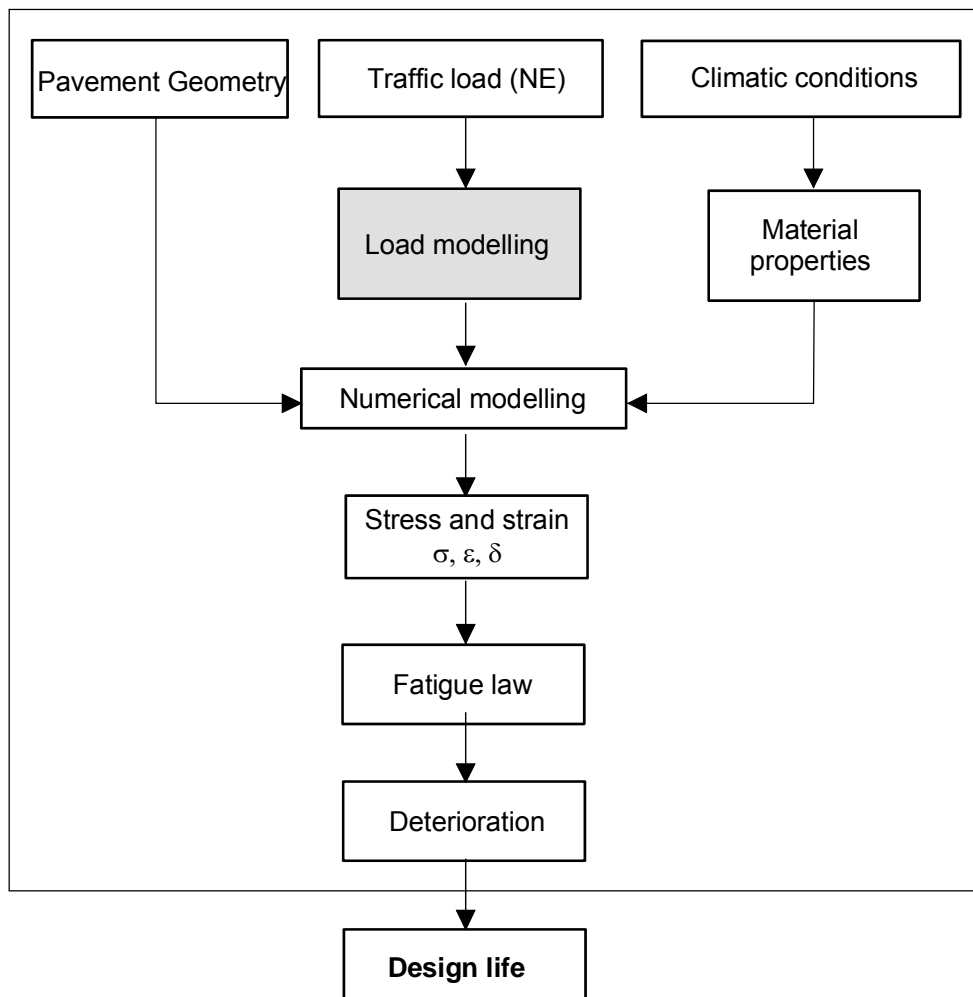
D: Ergebnisse des direkten Zugversuchs für VD7

F: Résultats de l'essai de traction directe sur PA VD7

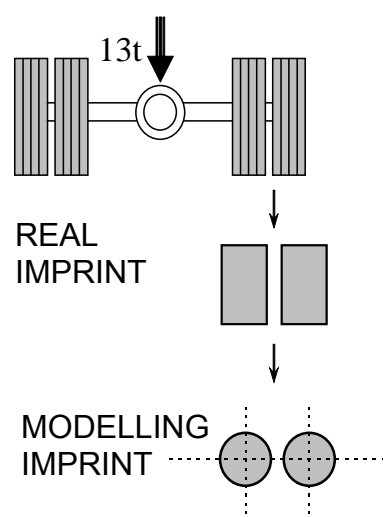
11. MODELING

Appropriate modeling techniques can provide the pavement designer with appropriate tools to predict the behavior of a potential pavement before construction leading to substantial economic benefits.

The design life calculation procedure of a pavement can be summarized as shown in Figure 11. 1, with the following load modeled as shown in Figure 11. 2:

**Figure 11. 1: Design life of a pavement**

D: Nutzungsdauer des Belages
F: Dimensionnement du revêtement

**Figure 11. 2 : Modeling of the load**

D : Modellierung der Last
F: Modélisation de la charge

Pavement fatigue life is well defined in the literature see for example Shahin et al [38] and is controlled by one of three strains located in the pavement structure:

1. Vertical compressive strain on the top of the subgrade.
2. The horizontal tensile strain at the bottom of the overlay,
3. The horizontal tensile strain at the bottom of the original asphalt surface.

Strains at these locations can be used to determine the fatigue life of the subgrade, overlay, and original asphalt surface respectively. A comparison of the fatigue lives at these locations leads to the critical location or control of the structural life of the entire pavement. Based on the French standards [36] the first two conditions are used in this report. The model used assumes no layer slippage has occurred. If the top layer is allowed to slip over the original asphalt surface, the effective stiffness of the two layers decreases, surface loads are less distributed at the subgrade, and vertical compressive strains on the subgrade increase [38].

Numerical modeling

The numerical model used here is a rational method based on the Burmister model [34,35]. Various parameters are considered in this linear elastic model such as layer thickness (h), mechanical properties (E , μ) and number of layers (n) are shown in Figure 11. 3

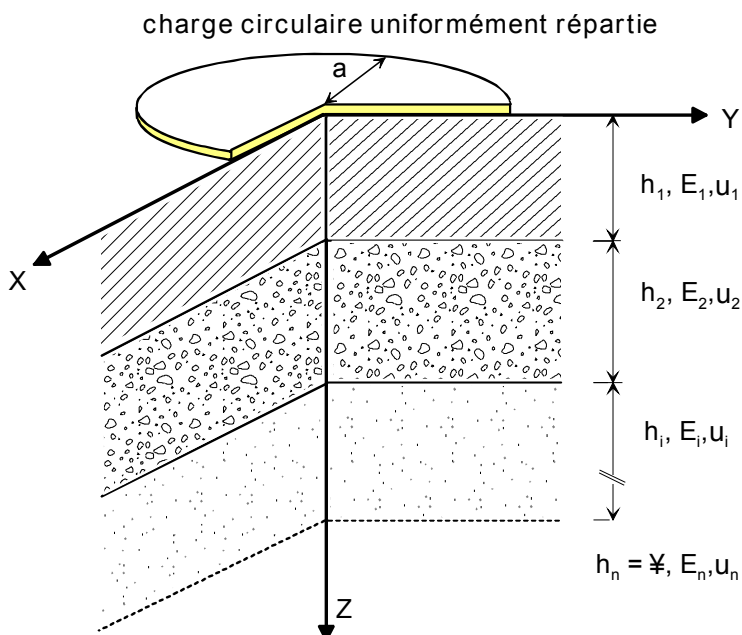


Figure 11. 3: Geometrical scheme of the pavement indicating modeled parameters.

D: Schematische Darstellung des Belags mit modellierten Parametern

F : Schéma de la structure avec indications des paramètres du modèle

The program used at LAVOC is **NOAH** [35]. The structure is represented by several elastic layers bonded (i.e. no slippage) one to the next allowing continuity of displacement at interfaces. The modulus at 15°C and 10 Hz is used as the mechanical properties of the materials. However, according to the French standards [36], for the fatigue law evaluation, the modulus at 10°C and 25 Hz is calculated.

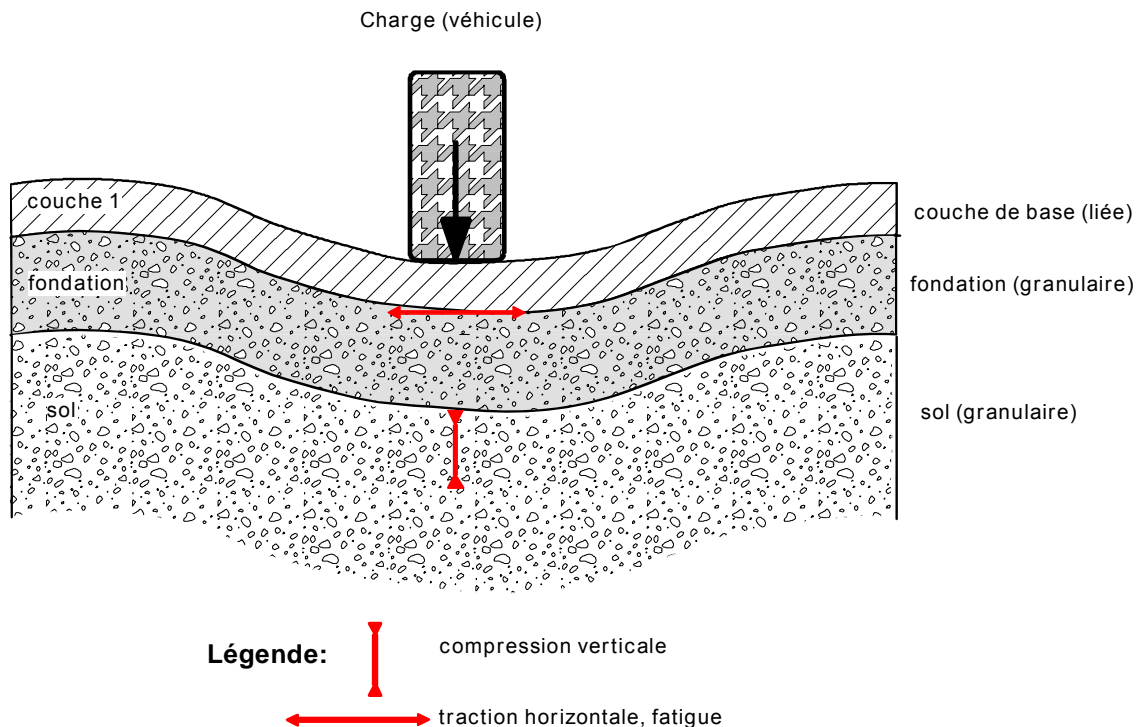
The following results will be presented:

- Horizontal tensile strain at the bottom of the base layer overlay (representing fatigue behavior)
- Vertical compressive strain at the top of the sub-base layer (representing rutting behavior)

Performance modeling, Fatigue Law

The fatigue law is based on the French standards for design life calculation. According to these standards two criteria must be verified:

1. the elongation (maximum horizontal tensile strain) ε_t at the base of the asphalt layer must remain less than a working value (equation 11.1)
2. the vertical strain ε_z (maximum vertical tensile strain) at the surface of the untreated layers and the subgrade must be less than a limiting value



D: Verhalten der Struktur unter Last

F: Comportement de la structure sous chargement

The value of the working strain according to the French standards is given by the equation

$$\varepsilon_{t,ad}(\theta, f) = \varepsilon_6(10^\circ\text{C}, 25\text{Hz}) \sqrt{\frac{E(10^\circ\text{C})}{E(\theta_{eq})}} \cdot \frac{NE}{10^6}^b k_c k_r k_s \quad [11.1]$$

E: complex modulus

f: frequency (Hz)

θ: temperature (°C)

ad: admissible

θ_{eq} : equivalent temperature (15°C)

ε_6 : fatigue strain data obtained with the fatigue law

b: slope of the linear regression for the fatigue law (for bituminous materials b=-0.2)

$$\sqrt{\left(\frac{E(15^\circ\text{C})}{E(10^\circ\text{C})}\right)} : \text{temperature adjustment factor}$$

NE: number of equivalent axle loads

k_r : risk coefficient chosen according to factors of a confidence interval around thickness and around fatigue tests' results (depends on risk percentage, if 5% $k_r=0.787$)

k_s : coefficient of reduction to take into account the effect of a lack of uniformity in the bearing capacity of a soft soil layer underneath treated layers (usually $k_s=1$)

k_c : coefficient which adjusts the results of the calculation with the numerical model in line with the behavior observed on actual pavements (normally $k_c=1.3$)

Since the pavement structure is already known, equation 11.1 can be transformed in order to obtain the number of maximum equivalent axle loads or design life of the pavement by calculating the working strain. The equation is as follows:

$$NE^b = \frac{\varepsilon_{t,calc}(15^\circ\text{C})}{\varepsilon_6(10^\circ\text{C})} \sqrt{\frac{E(15^\circ\text{C})}{E(10^\circ\text{C})}} \frac{10^6}{k_c k_r k_s} \quad [11.2]$$

With two different structures, two different working strains are obtained. This difference is then translated into maximum number of axles NE using (11.2) (i.e. design life). This procedure will help to compare the pavements with high stiffness porous asphalt and low stiffness porous asphalt.

Additionally, the different pavement structures are checked for rutting of the subgrade (i.e. sub-base) to ensure that it will remain under the value considered acceptable. This verification is based on the French standards and is done by selecting a vertical strain criterion ε_z of shape in the form

$$\varepsilon_{z,ad} = f(NE) \quad [11.3]$$

$$\varepsilon_{z,ad} = 0.012 \cdot (NE)^{-0.222} \quad [11.4]$$

It should be verified that even in the case of porous asphalt with lower modulus the second criterion is still verified.

Table 11. 1: Summary of modeling results*D : Zusammenfassung der Ergebnisse**F : Résumé des résultats*

Material code	AG 1	AG 2	AG 3																																				
Structure	<table border="1"> <tr><td>PA 11</td><td>(4 cm)</td></tr> <tr><td>HMT 22</td><td>(8 cm)</td></tr> <tr><td>HMT 32</td><td>(10 cm)</td></tr> <tr><td>HMF 22</td><td>(10 cm)</td></tr> <tr><td>Gravel bed</td><td>(58 cm)</td></tr> <tr><td>Soil</td><td></td></tr> </table>	PA 11	(4 cm)	HMT 22	(8 cm)	HMT 32	(10 cm)	HMF 22	(10 cm)	Gravel bed	(58 cm)	Soil																											
PA 11	(4 cm)																																						
HMT 22	(8 cm)																																						
HMT 32	(10 cm)																																						
HMF 22	(10 cm)																																						
Gravel bed	(58 cm)																																						
Soil																																							
Materials	<table border="1"> <tr><td>Mat.</td><td>G* [MPa]</td></tr> <tr><td>PA</td><td>4000</td></tr> <tr><td>HMT</td><td>7700</td></tr> <tr><td>HMF</td><td>1000</td></tr> <tr><td>Gravel</td><td>200</td></tr> <tr><td>Soil</td><td>50</td></tr> </table>	Mat.	G* [MPa]	PA	4000	HMT	7700	HMF	1000	Gravel	200	Soil	50	<table border="1"> <tr><td>Mat.</td><td>G* [MPa]</td></tr> <tr><td>PA</td><td>3000</td></tr> <tr><td>HMT</td><td>7700</td></tr> <tr><td>HMF</td><td>1000</td></tr> <tr><td>Gravel</td><td>200</td></tr> <tr><td>Soil</td><td>50</td></tr> </table>	Mat.	G* [MPa]	PA	3000	HMT	7700	HMF	1000	Gravel	200	Soil	50	<table border="1"> <tr><td>Mat.</td><td>G* [MPa]</td></tr> <tr><td>PA</td><td>700</td></tr> <tr><td>HMT</td><td>7700</td></tr> <tr><td>HMF</td><td>1000</td></tr> <tr><td>Gravel</td><td>200</td></tr> <tr><td>Soil</td><td>50</td></tr> </table>	Mat.	G* [MPa]	PA	700	HMT	7700	HMF	1000	Gravel	200	Soil	50
Mat.	G* [MPa]																																						
PA	4000																																						
HMT	7700																																						
HMF	1000																																						
Gravel	200																																						
Soil	50																																						
Mat.	G* [MPa]																																						
PA	3000																																						
HMT	7700																																						
HMF	1000																																						
Gravel	200																																						
Soil	50																																						
Mat.	G* [MPa]																																						
PA	700																																						
HMT	7700																																						
HMF	1000																																						
Gravel	200																																						
Soil	50																																						
Horizontal strain at point A	76.4 [10 ⁻⁶]	77.6 [10 ⁻⁶]	81.7 [10 ⁻⁶]																																				
Horizontal stress at point A (MPa)	0.67	0.68	0.71																																				
Design life (NE) (axle load 13 t)	5'060'000	4'680'000	3'619'000																																				
Design life (axle load 8.16 t)	32'586'400	30'139'200	23'306'360																																				
Axle load per day (8.16 to.) (20 year period)	4'463	4'128	3'192																																				
Traffic class (SN 640 324a)	T6	T6	T6																																				
Vertical strain at point B	-66.5 [10 ⁻⁶]	-72.8 [10 ⁻⁶]	-92.5 [10 ⁻⁶]																																				
Admissible vertical strain at point B	-389.9 [10 ⁻⁶]	-396.6 [10 ⁻⁶]	-419.9 [10 ⁻⁶]																																				

Effect of asphalt stiffness on fatigue life

The relationship between design life vs. modulus value of wearing course indicate that modulus value for the PA wearing courses has a relatively small influence on the design life of the structure (Figure 11. 4).

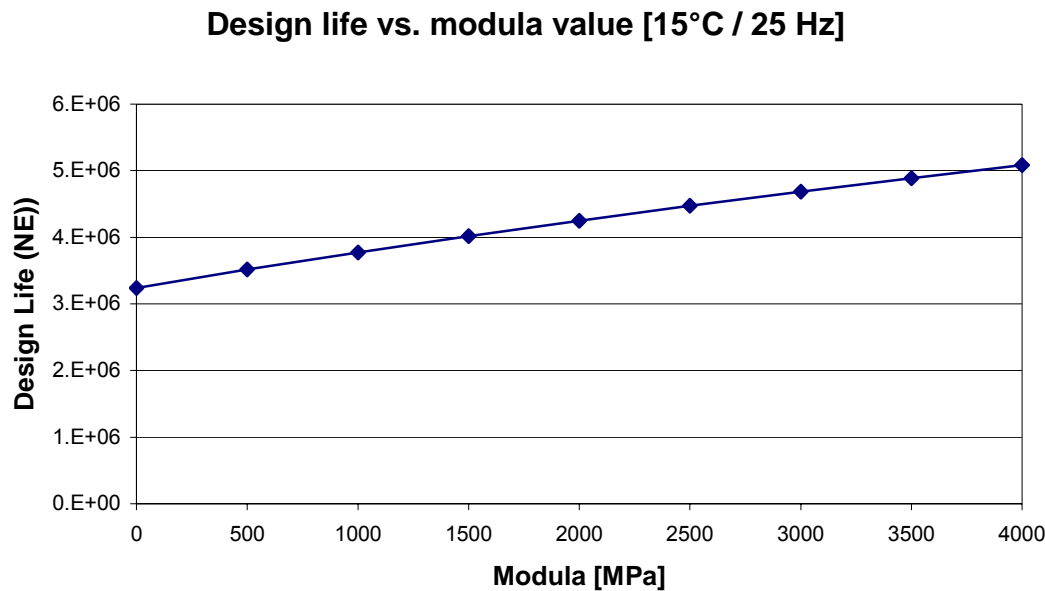


Figure 11. 4: Design life vs. modulus of the wearing course

D: Lebensdauer als Funktion des Moduls der Deckschicht
F: Dimensionnement en fonction du module de la couche de roulement

Reduction of 35% of the modulus value leads to a reduction of only 7.5% of the design life (Porous asphalt from AG 1 to AG2) and a reduction of 85% of the modulus value leads to a reduction of only 29.5% of the design life (Porous asphalt from AG1 to AG3). These results are obtained without compromising the pavement structure regarding rutting (as shown in Figure 11. 3 and Table 11.1).

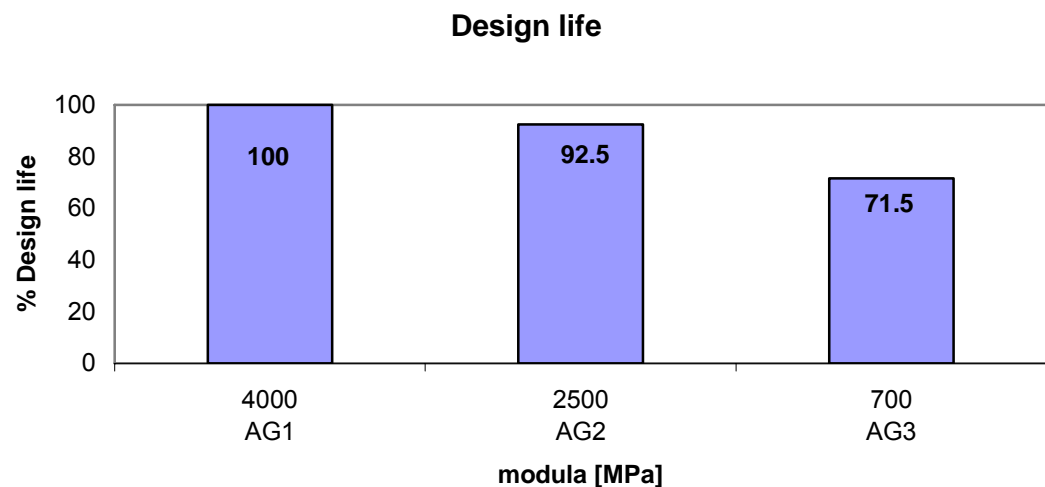


Figure 11. 5: Design life in comparison with modulus

D: Lebensdauer als Funktion des Moduls der Tragschicht
F: Dimensionnement comparatif en fonction du module

Table 11. 2: Summary of modeling results of VD5*D: Zusammenfassung der VD5 Modellierung-Ergebnisse**F: Résumé des résultats de modélisation de VD5*

Material code	-	VD9	VD5																																				
Structure		<table border="1"> <tr><td>PA 11</td><td>(4.5 cm)</td></tr> <tr><td>HMT 32</td><td>(6.0 cm)</td></tr> <tr><td>HMF 32</td><td>(7.0 cm)</td></tr> <tr><td>Gravel bed</td><td>(60 cm)</td></tr> <tr><td>Soil</td><td></td></tr> </table>	PA 11	(4.5 cm)	HMT 32	(6.0 cm)	HMF 32	(7.0 cm)	Gravel bed	(60 cm)	Soil																												
PA 11	(4.5 cm)																																						
HMT 32	(6.0 cm)																																						
HMF 32	(7.0 cm)																																						
Gravel bed	(60 cm)																																						
Soil																																							
Materials	<table border="1"> <tr><td>Mat.</td><td>G* [MPa]</td></tr> <tr><td>PA</td><td>1000</td></tr> <tr><td>HMT</td><td>7700</td></tr> <tr><td>HMF</td><td>1000</td></tr> <tr><td>Gravel</td><td>200</td></tr> <tr><td>Soil</td><td>50</td></tr> </table>	Mat.	G* [MPa]	PA	1000	HMT	7700	HMF	1000	Gravel	200	Soil	50	<table border="1"> <tr><td>Mat.</td><td>G* [MPa]</td></tr> <tr><td>PA</td><td>1996</td></tr> <tr><td>HMT</td><td>7700</td></tr> <tr><td>HMF</td><td>1000</td></tr> <tr><td>Gravel</td><td>200</td></tr> <tr><td>Soil</td><td>50</td></tr> </table>	Mat.	G* [MPa]	PA	1996	HMT	7700	HMF	1000	Gravel	200	Soil	50	<table border="1"> <tr><td>Mat.</td><td>G* [MPa]</td></tr> <tr><td>PA</td><td>2500</td></tr> <tr><td>HMT</td><td>7700</td></tr> <tr><td>HMF</td><td>1000</td></tr> <tr><td>Gravel</td><td>200</td></tr> <tr><td>Soil</td><td>50</td></tr> </table>	Mat.	G* [MPa]	PA	2500	HMT	7700	HMF	1000	Gravel	200	Soil	50
Mat.	G* [MPa]																																						
PA	1000																																						
HMT	7700																																						
HMF	1000																																						
Gravel	200																																						
Soil	50																																						
Mat.	G* [MPa]																																						
PA	1996																																						
HMT	7700																																						
HMF	1000																																						
Gravel	200																																						
Soil	50																																						
Mat.	G* [MPa]																																						
PA	2500																																						
HMT	7700																																						
HMF	1000																																						
Gravel	200																																						
Soil	50																																						
Horizontal strain at point A	123.3 [10 ⁻⁶]	122.0 [10 ⁻⁶]	120.1 [10 ⁻⁶]																																				
Horizontal stress at point A (MPa)	0.90	0.88	0.84																																				
Design life (NE) (axle load 13 t)	451'681	485'411	519'160																																				
Design life (axle load 8.16 t)	2'908'825	3'126'046	3'343'390																																				
Axle load per day (20 year period)	399	428	458																																				
Traffic class (SN 640 324a)	T4	T4	T4																																				
Vertical strain at point B	-391.2 [10 ⁻⁶]	-397.3 [10 ⁻⁶]	-411.5 [10 ⁻⁶]																																				
Admissible vertical strain at point B	-666.5 [10 ⁻⁶]	-655.9 [10 ⁻⁶]	-646.2 [10 ⁻⁶]																																				

The modeling results show that if the stiffness of the porous layer increases the design life decreases. This can be due to the relatively small thickness of the bituminous layers. The graphic below shows the strain vs the depth in the base bituminous layer (HMT 22).

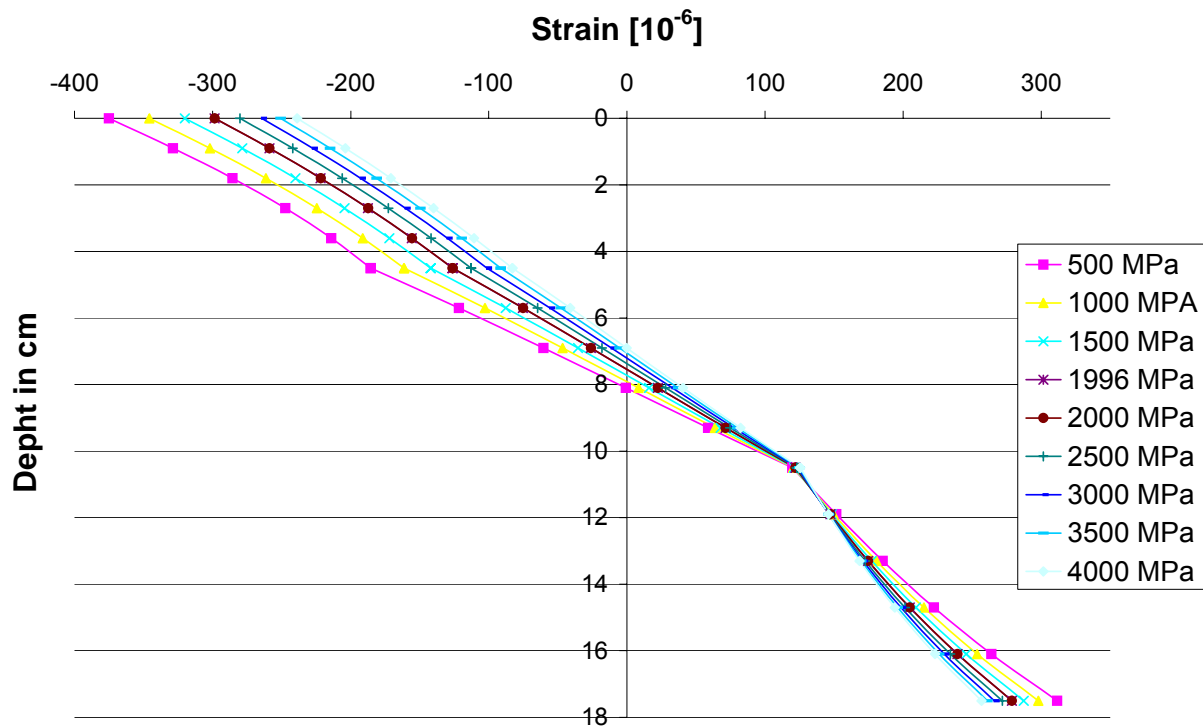


Figure 11.6 : Strain [10^{-6}] distribution as a function of depth

D: Verteilung der Dehnung [10^{-6}] als Funktion der Belagstiefe
F: Distribution des déformations [10^{-6}] en fonction de la profondeur

One can observe that the difference in the horizontal strain at point A in VD5 and VD9 is less than 1.5% for a decrease of 20% of the modulus value. To evaluate the effect of the modulus value, the calculation with a modulus value of 1000 MPa was done (this is not an existing structure; a new one with these characteristics was simulated). Regarding VD5 a modulus value that is 60% less was used. However the calculated horizontal strain is only 2.5% less.

In conclusion the modulus value of the porous asphalt does not have a strong effect on the horizontal strain at the bottom of the asphalt layer and hence does not have a strong influence on the design life of the structure. Nevertheless it is important that the asphalt layer under the porous asphalt layer has a reasonable thickness in order to distribute the load on the subgrade layer.

12. MAINTENANCE AND REHABILITATION

Because of the lower thermal conductivity of porous asphalt in winter, this surface may be about one degree celcius colder than dense asphalt [6, 54]. Therefore, on the porous asphalt surface, snow tends to settle earlier and remain longer; also ice forms earlier when the roads are wet. The winter maintenance of porous asphalt is different than that of dense asphalt. It is necessary to adjust the practices for winter maintenance often and to react quickly to the actual weather conditions. Winter maintenance practices in canton Vaud indicate that timing of the application of salt is very important as when the snow depth increases it is harder to solve the freezing problem. Furthermore, more salt should be applied in the first application of the season and salt application

should be repeated regularly to maintain the permeability of the wearing course. The road agency of canton Vaud notes a significant decrease in the number of accidents occurring on PA under snowy conditions as compared to dense courses.

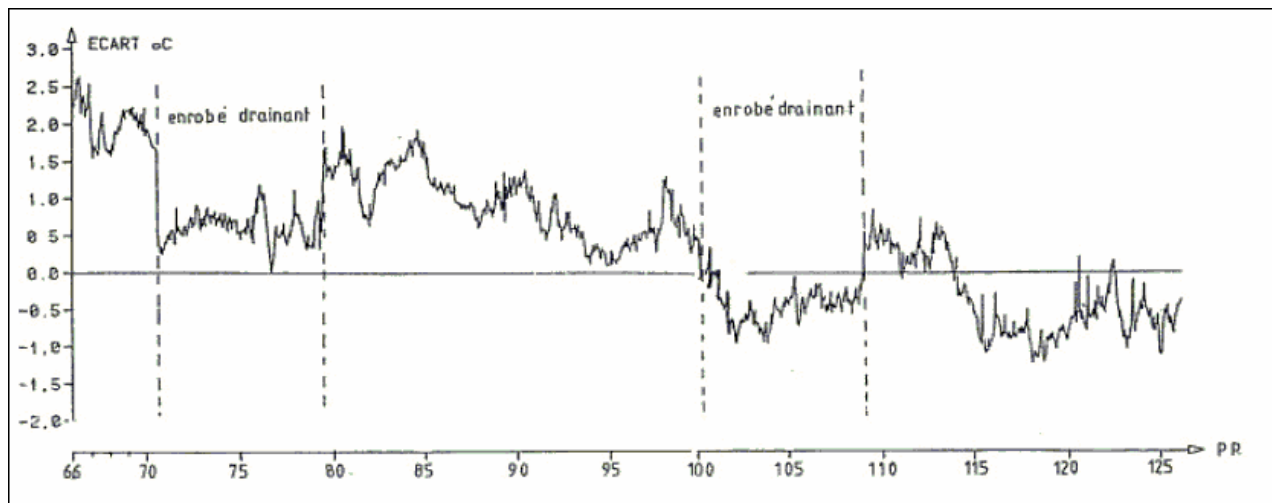


Figure 12. 2 : Change of surface temperature of two sections of porous asphalt (enrobé drainant) between sections of dense graded asphalt. The position is indicated by the x-axis. [54]

D: Änderung der Oberflächentemperatur von zwei Abschnitten mit offenporigem Asphalt zwischen Abschnitten aus Asphaltbeton. Die X-Achse zeigt die Kilometrierung.

F: Changement de la température de surface entre deux sections avec asphalte poreux (enrobé drainant) et enrobé dense. La position est indiquée par l'axe des abscisses.

For the road network manager the two most important factors are the long term permeability and acoustic performance of porous asphalt. In situ permeability tests in canton Vaud as measured by the standard method (SN 640-430a, 2003) indicate that permeability decreased by half after 2 to 3 years and then has continued to decrease at a slower pace. However, in situ observation does not indicate a reduction of functionality in this sense and an increase in aquaplaning. Currently, it is expected that a porous asphalt pavement would have to be rehabilitated after 15 years due to loss of permeability.

In situ noise reduction properties have been shown to be closely related to raveling. Higher raveling has resulted in increased noise emissions. For example, the oldest porous asphalt section (installed in 1991 and renewed in 2005 with porous asphalt) had still after 14 years a sufficient permeability for a "normal" rainfall. However, the noise emissions were significantly increased due to extensive raveling caused by the use of snow chains by trucks in winter. In the absence of such problems, current experience shows that the rehabilitation period for noise can also be as much as 15 years.

13. CONCLUSIONS AND RECOMMENDATIONS

In the framework of this research program and based on the results of an inquiry of 26 Cantons, a wide range of Swiss PA mixes with heterogeneous composition and performance have been studied. Furthermore, an overview on long term in situ performance as well as some specific technical aspects of winter maintenance and rehabilitation is discussed. This research project did not evaluate noise reduction properties of the selected pavements.

After the initial survey of the literature appropriate mechanical tests for porous asphalt were chosen. At the same time a survey of current experience with porous asphalt in Switzerland was conducted. Resulting from the survey taken porous asphalt used as a drainage course (DRAS) was not included in this project due to its limited use. Tests were performed on laboratory prepared specimens (AG1, AG4, AG5, VD7, VD8, VD9) and cores (VD2, VD3, VD4, VD5, VS6, AG2, AG3, VD10) taken from selected pavements chosen based on the feedback from various cantons. The behavior of the selected materials was also assessed using an analytical model.

Laboratory tests allowed the comparison of core performance with that of laboratory prepared specimen as well as comparison with field performance. Based on the results two mixes were optimized and recommendations for mechanical tests appropriate for porous asphalt were made.

Porous asphalt is characterized by high porosity and strong water permeability. Hence, it generally has a high macro roughness, a lower thermal conductivity and less contact points between the stones in comparison to the traditional dense graded mixes. The choice of a binder of excellent durability and mechanical resistance, high quality hard aggregates and additives adapted to the conditions of traffic and to the situation of the road is imperative in the design of high performing mixtures. The key point is to ensure cohesion and adhesion of the surface particles subjected to the mechanical loads. To this end, polymer modified binders have been shown to improve the performance of PA. The results in this research program indicate that in most cases standard laboratory tests corroborated field performances. With design and maintenance adapted, the current Swiss experience shows that good long term behavior (mechanical, permeability, acoustical) of up to 15 years can be obtained.

Moreover, national and local road agencies have observed that with this kind of wearing course there is a need to introduce some changes in practice in particular with regard to winter viability. A significant improvement in terms of driving comfort (drainage of rain water, surface properties in particular) is observed. In addition, a significant decrease of the accidents on snowy roads covered with PA has been recorded. However, use of PA has not been free of disadvantages such as: frost-deicing, excessive use of salt, reduced durability, clogging, cleaning, mechanical resistance against snow chains, other mechanical abrasion, repairing, and patch-working.

Laboratory tests on the selected cores showed that air void content is not enough as a parameter to assess the permeability, the quality of the voids as well as dimensions of the capillaries and amount of interconnected voids should be considered.

It is apparent from the results of this research project that by identifying and properly using the correct mechanical tests significant economic gains can be made. As seen from the field results the PA from canton Aargau (AG1) had to be rehabilitated due to extensive raveling. The lab performance of this material in comparison to others could have signaled the pavement designer of the susceptibility of this material to raveling before the construction.

In summary, the following observations were made:

1. The Cantabro test showed consistent results with field experience and can be recommended as an important test method for the characterization of adhesion in the mix.
2. With respect to reduction in particle loss the effect of aggregate hardness is minor in comparison to the effect of polymer modified binder.
3. Water sensitivity results at 25°C should be used in conjunction with indirect tensile strength at 5°C to give a broader understanding of material behavior.
4. The modulus of porous asphalt does not have a strong effect on the horizontal strain at the bottom of the asphalt layer and hence does not have a strong influence on the design life of the structure.
5. Polymer modified binders improve the performance of PA as can be seen when AG2 and AG3 are compared.
6. Based on the results, for PA, Marshall compaction with 2X50 blows is recommended for the estimation of maximal voids and Marshall compaction with 2X25 blows is recommended as best match to gyratory compaction with 40 gyrations for estimation of sensitivity to compaction and for the realisation of mechanical tests.
7. Preliminary results show that the direct tension test as adapted for PA delivers important results for the characterization of PA. However, a more detailed study must be carried out in order to validate or adjust this test procedure.

The current European standard for type testing [66] lists the required testing procedures to be carried out as proof that the formulation meets the relevant requirements in the product standard.

These required tests are listed in Table 13. 1. The corresponding Swiss standard [75] however does not include all the tests in this Table as indicated. As a result of this research project some adjustments to the values in EN is recommended as listed in Table 13. 1. Furthermore Table 13.2 lists additional mechanical tests and desired values that are recommended in order to predict mechanical properties of porous asphalt. These properties could be introduced into the European standards.

Table 13. 1 : Summary of recommendations for mechanical tests for PA standardization

D: Zusammenfassung der Empfehlungen für die Normierung von PA

F: Résumé des recommandations pour la normalisation des PA

Property	Existing value	Existing standard	Recommendations+Comments
Air void content	PA8: $\geq 20\%$ PA11: $\geq 22\%$	pr EN13108-7 SN 640 431-7NA (L)	(1), Marshall compaction 2X50 blows for estimation of maximal voids and Marshall compaction to 2X25 blows for estimation of sensitivity to compaction and realisation of mechanical tests
Binder content	PA8: $\geq 5\%$ PA11: $\geq 4\%$	pr EN13108-7 SN 640 431-7NA (L)	(1)
Vertical water permeability (Initial+Lab)	$\geq 0.1\text{-}4.0 \text{ (}10^{-3}\text{m/s)}$	pr EN13108-7	(1); ≥ 1
Horizontal water permeability	$\geq 0.1\text{-}4.0 \text{ (}10^{-3}\text{m/s)}$	pr EN13108-7	(1); ≥ 1
Particle loss (Cantabro)	10%-50% (300 rev.)	pr EN13108-7 EN 12697-17 (P)	$\leq 20\%$ (25°C , 300 rev.) $\leq 50\%$ (-10°C , 300 rev.) Water cond. and freeze thaw effects not significant (2) Marshall compaction to 2X25 blows
Water sensitivity (ITSR)	$\geq 70\%$	EN 12697-12 (P) SN 640 431-7NA (L)	(1) Marshall compaction to 2X25 blows

(1) Current standard is acceptable (2) currently not in SN [75], P=test procedure, L=limiting values

Table 13. 2 : Summary of recommendations for mechanical tests to be introduced for PA standardization

*D: Zusammenfassung der Empfehlungen für die Einführung mechanischer Prüfverfahren für PA
F: Résumé des recommandations retenues pour la normalisation des essais mécaniques des PA*

Property	Recommended value	Existing standard	Comments
Interconnected air voids/Total air voids	≥ 70%	SN 640 433b (L) NF P 98-254-2 (P)	
In situ vertical water permeability	≥ 15 l/min (initial) ≥ 10 l/min	SN 640-430a	15 l/min initial could not be maintained after 2 years
Particle loss (Cantabro) Colder regions	≤ 50% (300 rev.)	None	Water cond and freeze thaw effects not significant
Stiffness	≥3500 MPa (at 15°C, 10 Hz)	None	Higher modulus has slight influence on Fatigue life
Indirect Tensile Strength (ITS)	ITS=1.5MPa(5°C) ITS=0.5MPa(25°C)	EN 12697-23 (P) No L	
Direct tensile test	DTT = 1.5MPa Temperature flow-limit stress	None	

P=test procedure, L=limiting values

14. ACKNOWLEDGEMENTS

This project has been possible by the financial support of the Swiss Federal Roads Authority (FEDRO, ASTRA) and cooperation of the local cantonal authorities in providing vital data as well as specimens. The authors would like to acknowledge the laboratory staff at both laboratories for performing most of the numerous mechanical tests.

15. LITERATURE

1. Maupin G W, Virginia's Experience with Open-Graded Surface Mix, Transportation research Record 595, pp. 48-51, 1976.
2. Tesoriere G, Canale S and Ventura F, Analysis of Draining Pavements from a Point of View of Phono-Absorption, Proc. 4th European Symp., Madrid, pp.878-881, 1989.
3. Nicholls J.C, Review of UK porous asphalt trials, TRL Report 264, Transport Research Laboratory, Crowthorne, 1996.
4. Junker, J.P. „Entwicklungen zur Bestimmung mechanischer Materialkennwerte an bituminösen Baustoffen, insbesondere an Asphalt“, Empa report no. 215, 1987.
5. Nicholls J.C, Review of UK porous asphalt trials, TRL Report 264, Transport Research Laboratory, Crowthorne, 1996.
6. Köster, H. Drainasphalt Beobachtungen des Verhaltens von hohlraumreichen Verschliessschichten unter Verkehr, Obsevation of the behavior of porous asphalt under raf-fic, 1991 VSS report Nr. 218.
7. Bochové G.G., Twinlay, a New Concept for Porous Apshalt, Proc. Eurasphalt & Eurobitume Congress, 1996, pp. E&E.7.187.
8. Japan Highway Research Institute, Staticstic data of Porous Asphalt on Japanese High-ways. (Unpublished).
9. Moore, L.M., Hicks, R.G., Rogge, D.F., Design, Construction, and Maintenance Guidelines for Porous Asphalt Pavements, Transportation Research Record 1778, Paper No. 01-0422, 2001.
10. Daines M.E., Trials of porous asphalt and rolled asphalt on the A38 at Burton, Department of transport TRRL Report RR323, Transport and Road research Laboratory, Crowthorne, 1992.
11. Express Highway Research Foundation of Japan, Report of Study and Research for Porous Asphalt; Haisuisei-hosou ni kansuru Chousa Kenkyu Houkokusho, Tokyo, 1993.
12. Hoban T W S, Liversedge F and Searby R, Recent Developments in Pervious Macadam Surfaces, Proc. 3rd Eurobitumen Symp., The Hague, pp 635-640, 1985.
13. Van Heystraeten G and Moraux C, Ten Years' Experience of porous Asphalt in Belgium, Transportation Research Record 1265, pp. 34-40, 1990.
14. Pérez Jiménez, F.E., Calzada Pérez, M.A., "Analysis and Evaluation of the Performance of Porous Asphalt: The Spanish Experience", Surface Characteristics of Roadways: International research and technologies, ASTM STP 1031, Meyers and Reichert, Eds. American Society for Testing and materials, Philadelphia, 1990, pp. 512-527.
15. Huber, G., „Performance Survey on Open-Graded Friction Course Mixes“. National Co-operative Highway Research Program (NCHRP) Synthesis 284, 2000.
16. Japan Highway Public Corporation, Design and Execution Manual for Porous Asphalt; Haisuisei-hosou Sekkei Sekou Manual, Tokyo, 1994.
17. Potter J F and Halliday A R, The Contribution of Pervious Macadam Surfacing to the Structural Performance of Roads, TRRL Laboratory Report 1022, 1981.
18. Graf, B., Simond, E., 2005, Erfahrungen mit Drainasphaltbelägen im Kanton Waadt“ (experience with porous asphalt in canton Vaud), VSS Publikation Strasse und Verkehr, Route et Trafic, 4/2005, (in German and French).
19. Takahashi, S., Poulikakos, L., Partl, M.N.: "Evaluation of Improved Porous Asphalt by Various Test Methods". Proceedings of 6th Int. RILEM Symposium on Performance Testing and Evaluation of Bituminous Materials PTEBM03, Zürich, Switzerland, 14-16April, edited by M.N. Partl, RILEM Publications S.A.R.L., ISBN 2-912143-35-7, pp230-236 (2003)

20. Poulikakos, L., Takahashi, S., Partl, M.N.: "Evaluation of Improved Porous Asphalt by Various Test Methods". Empa Report No. 113/13 Empa No 860076, 2006.
21. Losa, M. Bonomo,G., Licitra,G., Cerhiai,M., "Performance Degradation of Porous Asphalt Pavements". MAIREPAV'03, 2003.
22. Poulikakos,L. Partl,M., "bestimmung des Wassersättigungssrades von Walzaspalhlt", Vorschungsauftrag 26/98 VSS, Empa Nr. 201465, 2004.
23. AASHTO design guide, 2000.
24. Angst, C., Bosshart, D., Clavien, C., Grolimund, H-J., Pestalozzi, H., 2004 "Lärmarme Strassenbeläge innerorts"(Quiet pavements in urban areas), Progress report. www.astra.ch, www.buwalshop.ch.
25. Sojaati, M., Blötz, A., Horat, M., Caprez, M., 2000, Lärmverhalten verschiedener Belags-oberflächen, , (study on noise emission of various pavements) in German.
26. Zoorob S.E., Cabrera J.G. and Takahashi S., 'Effect of Aggregate Gradation and Binder Type on the Properties of Porous Asphalt', Proc. 3rd European Symp. Performance and Durability of Bituminous Materials and Hydraulic Stabilised Composites, University of Leeds, April 1999, pp 145-162.
27. Younger, K.D., Partl, M.N., Fritz H.W., Gubler, R., „asphalt concrete shear testing with the co-axial shear tester at Empa, Mechanical tests for bituminous materials, DiBenedetto & Franken (eds) 1997 RILEM.
28. Gubler, R., Partl, M.N., Canestrari, F., Grilli, A., June 2005, Influence of water and temperature on mechanical properties of selected asphalt pavements, Materials and Structures, v. 38.
29. J.E.Kiewer, C.A.Bell and D.D.Sosovske, `*Investigation of the Relationship Between Field Performance and Laboratory Aging Properties of Asphalt Mixtures*`. ASTM Symposium on Engineering Properties of Asphalt Mixtures and the Relationship to their Performance, Phoenix, AZ, December 6th 1994.
30. Standard Conditioning Practice for Hot Mix Asphalt (HMA), AASHTO Provisional Standards, 2001 edition.
31. Gubler R., Methode d'essai par oscillation axiale pour la détermination des caractéristiques mécaniques et du comportement à la fatigue des asphalte. In Mechanical tests for bituminous mixes. Fourth int. symposium by RILEM, Budapest, 24-26 October 1990, Rilem proceeding. pp432-444,(1990)23, 1931, pp. 1052-1058.
32. Sokolov, K., Gubler, R., Partl, M.N.: Extended Numerical Modeling and Application of the Coaxial Shear Test for Asphalt Pavements, J. of Materials & Structures Nr 279, June, pp 515...522 (2005)
33. Grolimund, H-J., Attinger, R., Meister, A., „Lärmarme bituminöse Strassenbeläge inner- und ausserorts“, Cooperative research of BUWAI, ASTRA, 2002
34. Eckmann, B.(1997) New tools for Rational Pavement Design. 8th International Conference on Asphalt Pavements, Washington, pp 25-42.
35. Van Cauwelaert,(1995) F. Stresses and displacements in multi-layered orthotropic systems – Theoretical background to the stress/strain calculation program used within the NOAH software.]
36. French standards, French design manual for pavement structures – guide technique, LCPC-SETRA, may 1997.
37. Fonseca, O. A., Witczak, M. W. (1996). A Prediction Methodology for the Dynamic Modulus of In-Placed Aged Asphalt Mixtures, Journal of the Association of Asphalt Pavement Technologists, Vol. 65

38. Shahin, M. Blackmon, E., Van Dam, T. Kircher, K. "Consequence of layer Separation on Pavement Performance" US Army Department of Transportation Federal Aviation Administration. April 1987
39. AMERICAN ASSOCIATION OF STATE HIGHWAY AND TRANSPORTATION OFFICIALS (AASHTO), Standart test method for thermal stress restrained specimen tensile Strength, AASHTO designation:TP10-93, first edition, may 1993
40. ISACSSON U., ZENG H., Cracking of asphalt at low temperature as related to bitumen rheology, Journal of materials science n°33, 1998
41. Pucci T., Approche prévisionnelle de la fissuration par sollicitation thermique des revêtements bitumineux, thèse de doctorat, Ecole Polytechnique Fédérale de Lausanne, Suisse, octobre 2001
42. Publication RGRA HDB
43. Dumont A.-G, Pittet M., Vieillissement thermique des enrobés – Incidence sur les caractéristiques rhéologiques et mécaniques lors de fabrication et/ou du réchauffage en laboratoire, LAVOC Ecole Polytechnique Fédérale de Lausanne, research in progress.
44. Perret J., Ould-Henia M., Dumont A.-G., High modulus pavement design using accelerated loading testing (ALT), 3rd Eurasphalt & Eurobitume Congress, Vienne, 2004
45. Perret J., Strain and stress distribution in flexible pavements under moving loads, Hermes: Int. Journal of Road Materials and Pavement Design, 2004
46. Pucci T., Dumont A.-G., Di Benedetto H., Thermomechanical and mechanical behaviour of asphalt mixes at cold temperature: road and laboratory, Hermes: Int. Journal of Road Materials and Pavement Design, 2002
47. Pittet M., Mise au point et application d'une formule d'enrobé DRA 11 au liant bitume-caoutchouc, LAVOC Ecole Polytechnique Fédérale de Lausanne, 2005
48. Dumont A-G., Turtschy J-C., Pucci TH., Autoroute N9, planches comparatives avec bitumes modifiés et ajouts, étude économique, rapport final. Mai 2000.
49. Dumont A.-G., Huet M., Turtschy J.-C. Méthodes de mesure de la drainabilité des enrobés drainants. LAVOC Ecole Polytechnique Fédérale de Lausanne. Novembre 1995.
50. Pittet M. A1-autoroute Yverdon-Berne – revêtements Payerne-Avenches, lot 1816. Couche de roulement DRA 11 et DRA 8 au liant Styrelf 13/80 Spécial. Caractérisation des liants et des enrobés. LAVOC Ecole Polytechnique Fédérale de Lausanne, octobre 1999.
51. Simond E., L'expérience vaudoise des drainants sur autoroute. Journée technique LAVOC, septembre 2000.
52. Bhaskar A. Noise measurement for isolated vehicle under acceleration/deceleration and constant speed A5- Autoroute Yverdon- Neuchâtel, juin 2006
53. Ferry, J. "Viscoelastic properties of polymers" second edition. 1970
54. Nancy, LR "Le Comportement Hivernal Particulier de Certaines Surfaces Routières" Note D'Information 67 SETRA-CSTR.

European Standards

55. EN12697-5, Bituminous mixtures- test method for hot mix asphalt-Part 5: Determination of maximum density.
56. EN12697-6, Bituminous mixtures- test method for hot mix asphalt-Part 6: Determination of bulk density of bituminous specimen.

57. EN12697-8, Bituminous mixtures- test method for hot mix asphalt-Part 8: Determination of void characteristics of bituminous specimens, March 2003.
58. EN12697-10, Bituminous mixtures- test method for hot mix asphalt-Part10: Compactability, November 2001.
59. EN 12697-12, Bituminous mixtures- Test Method for hot mix asphalt- Part 12: Determination of the water sensitivity of bituminous specimens, Draft European Standard Dec 2003.
60. EN 12697-17: Bituminous mixtures- Test methods for hot mix asphalt- Part 17: Particle Loss of porous asphalt specimen, 2004.
61. prEN 12697-19: Bituminous mixtures- Test method for hot mix asphalt-Part 19: Permeability of specimen. 2003.
62. EN 12697-23, Bituminous mixtures- Test Method for hot mix asphalt- Part 23: Determination of indirect tensile strength of bituminous specimens, July 2003.
63. EN13108-7- provisional European Standard, Bituminous mixtures material specifications Part 7- porous asphalt (PA), May 2006.
64. ISO/CD 13472-1 Norm Acoustics- Procedure for measuring Sound Absorption Properties of Road Surfaces in situ-Part 1:Extended Surface Method.
65. EN-ISO 10534-1 Norm Acoustics-Determination of Sound Absorption Coefficient and Impedance in Impedance Tubes-Part 1: Method using Standong Wave Ratio.
66. EN 13108-20: Bituminous mixtures- Material specification- Part 20: Type Testing, January 2006.

Swiss Standards "Verein Schweizerischer Strassenfachleute" (VSS)

67. SN 640 452c: Heissmischfundationsschichten HMF Anforderungen, Ausführung
68. SN 671 965a: "Bituminöses Mischgut: Dichte", 1981
69. SN 640 433b:, Drainasphaltsschichten, Konzeption Anforderung, Ausführung, Januar 2001. Swiss Standards for porous asphalt Original in German and French.
70. SN 671 967a: "Bituminöses Mischgut: Rohdichte, Berechnen des Hohlraumgehaltes"
71. SN 640 431-7NA: Asphalt- Offenporiger Asphalt, National Annex to the prEN13108-7, August 2001.
72. SN 670 130: Sand, Kies, Splitt und Schotter für Beläge; Qualitätsvorschriften. Quality control guidelines for minerals (sand, gravel) to be used in pavements.
73. SN 640 430a : Walzaspalt – Konzeption, Ausführung, Anforderungen an die aingebauten Beläge – Anhang 2 – Messung der Wasserdurchlässigkeit (1. Janunar 2005).
74. SN 640 925b, 2003, Swiss Standards, Erhaltungsmanagement der Fahrbahnen (EMF), Anleitung zur visuellen Zustanderhebung und Indexbewertung mit dem Schadenkatalog. August. (Guidelines for surface inspection), in German and French.
75. SN 640 431-20, Swiss Standards, Asphaltmischgut- Mischgutanforderungen Teil 20: Erstprüfung, Januar 2005.

APPENDIX1: SUMMARY OF LITERATURE SURVEY ON TEST METHODS

Table A. 1 : Summary of results of the tests evaluated

Property	Test	Adv.	Disadv.	Specimen Type	who
Stiffness	4 point bending	repeatability	Specimen production	Prismatic	
	2 point bending	repeatability	Specimen production		
	CAST (Dry)	Specimen production Simulates road well	Complex test	Gyratory	
Water sensitivity	Cantabro (wet)[16]	simple	100 Ø Marshall specimen Not in EN anymore	100 Ø Marshall compaction	
	CAST (wet)	Specimen production Simulates road well	Complex test	Gyratory	
	Indirect tension	Simple Per EN	Not sufficiently sensitive to variations of components in the mix like binder [1]. Not suited for open graded mixes [1] High dispersion of results [1].	Marshall (w/ Gyr)	
Particle Loss Cohesion, Bonding	Cantabro (Dry)	sensitive to variations of components in the mix like binder [1]. Good repeatability[1].	Marshall compaction specimen	100 Ø Marshall (w/ Gyr)	
Low Temp Behavior	CAST (Freeze-thaw cycles))	Specimen production Simulates road well G^* after ea. cycle	Complex test	Gyratory	
Wheel Tracking		Represents the road	Not sufficiently sensitive to variations of components in the mix like binder [1]. High dispersion of results [1].	Wheel tracking	
Permanents deformation	Druckschwell Versuch (50°C)	repeatability	uniaxial	100mm Gyr	
Permeability (Lab)	Durchflussmesser	Per Standards			
Permeability (In situ)	Per standards				
	Thermographie				
Binder Drain-down evaluation					
compaction	Marshall	Use only when req'd by Standards.	Does not represent compaction on the road		
	Gyratory	reproducible	Does not represent compaction on the road		
	Wheeltracking	reproducible	Best represent compaction on the road		
Void content	geometric		repeatability		
	vacuum	repeatability			
Fatigue, Shear Stress resistance	CAST	Specimen production Simulates road well	Complex test	Gyratory	
Aging	unaged		Not representative		
	STOA	AASHTO			
	LTOA Age specimen	AASHTO	Binder drain down observed		
	LTOA Age mix	Homogeneously aged	No experience Maybe hard to compact		
Noise reduction	Lab, initial	Important property			Empa, acous.
	Lab, aged				
	In situ, aged				

APPENDIX 2: SUMMARY OF RESULTS OF THE SURVEY FROM VARIOUS SWISS CANTONS

N°	Material Designation Project	Material Designation Project	Material Designation Project	Material Designation Project	Material Designation Project	Material Designation Project	Material Designation Project	Material Designation Project	Material Designation Project	Material Designation Project	Material Designation Project
N°	Material Designation Project	Material Designation Project	Material Designation Project	Material Designation Project	Material Designation Project	Material Designation Project	Material Designation Project	Material Designation Project	Material Designation Project	Material Designation Project	Material Designation Project
1	AG2-AG3	Argau	N1 / 01-03	Offringen-Gränichen;	km 62,34-76,17		13,830	2x2	7/98 – 10/99	DRA 11	B 55/70 + Trinidad + CTS
2		Freiburg	A1	Séreaz-Payerne	km 114.620 - 117.120		2'500m	2x2	July 2000	DRA 11	PmB ¹
3		Geneva	A1	Descente lac			1'700 m	2 x 2 + Em ²	May 2003	DRA 11	PmB II (Olexobit SMA)
4		Geneva	A1	Airport zone -Palexpo			600 m	2 x 2 + Em	Oct 2001	DRA 11	PmB II (Colflex N55 and Olexobit SMA)
5		Jura	H18	Soyhières			365 m	2	Sept 2001	DRA 11	Practiplast PmB
6		Neuchâtel	N5	Vaumarcus-Bevaux	km 19.700-27.000		3'000 m	2x2	Apr 2002	DRA 11	Styrelf 13/80
7		Uri	A2	Gotthard Tunnel			9'900 m	2	Apl 1980	drainage 0/16mm	B 80/100 + Haftmittel
8		Valais	RN9	Vernayaz	(PR 700)		700 m	2x2 + Em	Fall 1991	DRA 11	Colflex S
9		Valais	RN9	St-Maurice	(PR 620)		500 m	3 + 2 + Em	octobre 1993	DRA 11	Vec-traphalt EL 80
10		Valais	RN9	Granges	(PR 1090 to PR 1100)	1400 m	2x2 + Em	mai 1996	DRA 11	Practiplast M 40 DR	
11		Valais	RN9	Saxon	(PR 820 to PR 830)	1400 m	2x2 + Em	octobre 1997	DRA 11	PmB	
12		Valais	RN9	Evionnaz	(PR 640 to PR 660)	600 m	+ 1 2 0 0 m	2x2 + Em	Sep 1998	DRA 11	PmB
13	VS6	Valais	RN9	Riddes	(PR 830 to PR 870)	4100 m	2x2 + Em	Sept 1999	DRA 11	Styrelf 13/80	
14		Valais	RN9	Saxon (PR 770 à PR 820)			4700 m	2 + 1 Em	oct.00	DRA 11	PmB
N°	Project Material Designation	Material Designation Project	Material Designation Project	Material Designation Project	Material Designation Project	Material Designation Project	Material Designation Project	Material Designation Project	Material Designation Project	Material Designation Project	Material Designation Project
15		Valais	RN9	Sion-Ouest (PR 990)			700 m	2x2 + Em	oct.01	DRA 11	PmB
16		Valais	RN9	Riddes-Vétroz (PR 870 à PR 940)			6900 m	2x2 + Em	Sept./Oct. 2002 May/Jun 2003	DRA 11	PmB
17		Valais	A21	Tunnel of Mont-Chemin à Martigny (PR 0 à PR 20)			2000 m	2x2	Jun 2003	DRA 11	PmB
18		Valais	RN9	St-Maurice à Evionnaz (PR600 à PR 640)			150 m + 600 m + 1800 m	2x2 + Em	Sep 2003	DRA 11	PmB

19		Vaud	N9		4500 m	4 + 2 Em	Summer 2000	DRA 11	Styrelf 13/80	4
20	VD5	Vaud	N9	Autoroute du Léman Aigle-Bex km 48.400 à km 58.700	10'300 m 400 m	4 + 2 Em	Summer 1998	DRA 11	Styrelf 13/80 – CTS Rubber additive	4
21	VD2	Vaud	N9	Ponts des Vuarennnes à Baye de Montreux km 32.750 à km 33.600	850 m	2 + Em	Summer 1991	DRA 11	Colflex N	4
22	VD3	Vaud	N1 GL	Tolochenaz-Lonay km 62.000 à 54.700	6300 m	4 + 2 Em	Summer 1993	DRA 11	Practiplast M-40 DR	4
23		Vaud	N9		7700 m	4 + 2 Em	July to september 1994	DRA 11	Colflex N	4
24		Vaud	N1 GL Lake		2700 m	2 + 1 Em	été 1997	DRA 11	Practiplast M-40 DR	4
25		Vaud	N1		10'000 m.	2 + Em	été 1999	DRA 11 + DRA 8	Styrelf 13/80 spécial	4
26		Vaud	N1		7000 m	2 + Em	août.98	DRA 11	Colflex N 55	4
27		Vaud	N1		2400 m	4 + 2 Em	été 1998	DRA 11	Colflex N 55	4
28	VD4	Vaud	N9	Contournement de Lausanne	7700 m	6 + 2 Em	avril à septembre 1997	DRA 11	Colflex N 55 + Styrelf 13/80	4
29		Vaud	N1 GL		2600 m	4 + 2 Em	été 1999	DRA 11	Colflex S	4
30		Vaud	N1 GL		7700 m	2 + 1 Em	sept.95	DRA 11	BP Practiplast M40 DR	4
31	VD10	Vaud	N9	Autoroute du Léman Vevey-Pertit Km 33.010 à km 32.760	250 m	2 + 1 Em	Sept. 2000	Bi-couche DRA 8/22S	Styrelf 13/80	2.5 + 5